

We would like to thank Anonymous Referee #1 for the valuable comments. Below are our responses in blue:

Modelling of chemical composition of the troposphere has been challenging in particular for the short-lived species, such as the hydroxyl (OH) and its feedback with the green- house gases (e.g., methane) and other air pollutants (e.g., CO). The authors show a simplified approach to get reasonable answers to these questions, which are welcoming news for the community. The CH₄-CO-OH system has now been implemented in the NASA GEOS-5 Atmospheric Global Circulation Model for chemistry-climate feed- back related studies. However, the challenges remain on the validity of this simplified CH₄-CO-OH approach as that is the case for the state-of-the-art full chemistry model. The manuscript is generally well prepared, and can be published after minor revisions. My specific comments are listed below.

p.9453, line 24-26: Agree, but the system is so non-linear that this simplification may bias the results in different ways! So I am not sure whether you can claim that CH₄-CO- OH will be any better.

We do not claim that ECCOH is “simplified”, but rather “computationally efficient” - the main advantage of our code. To address this concern, we have considerably “beefed up” our description of the ECCOH module in Section 2.1.

p.9454, line 19-21: Can you be a bit more specific here - are you talking about the global mean OH or also about the inter-hemispheric distribution or regional differences? If all, it would be useful for the readers to get some of your opinions on each of the issues. Also relevant for the paper for discussions later on.

We modified the sentence from:

“Furthermore, simulated OH from full chemistry mechanisms in global models is still highly uncertain because of incomplete knowledge and representation of OH sources, sinks and recycling (e.g., Elshorbany et al., 2010, 2012a, b, 2014; Stone et al., 2012).”

To:

“Furthermore, simulated OH from full chemistry mechanisms in global models is still highly uncertain because of incomplete knowledge and representation of OH sources, sinks and recycling (e.g., Elshorbany et al., 2010, 2012a, b, 2014; Stone et al., 2012). For example, 1) nitrous acid (HONO) is typically underestimated in models by an order of magnitude (Elshorbany et al., 2012b), which can lead to a significant underestimation of OH, especially in urban high-NO_x regions; 2) in unpolluted, forested environments, significant discrepancies exist between models and measurements (Stone et al., 2012); and 3) Patra et al. (2014) indicate that the inter-hemispheric OH ratio (northern to southern hemisphere) is near unity, while a recent model inter-comparison had a multi-model average of about 1.3.”

We would like to thank Anonymous Referee #2 for valuable comments. We have worked to amend the manuscript so as to more clearly explain our method. Please see our responses to specific reviewer comments below in blue.

An efficient representation of tropospheric OH as described here can facilitate multi-decadal simulations that need to represent the long lifetime of methane and its interactions with OH, and might be useful for future studies of paleo or future atmospheres. Below I suggest some additional information to help guide future adopters of this approach, as well as some additional evidence, if available, to strengthen the paper

General comments.

If possible, it would be stronger to show in the main text the differences in results using archived, annually-varying OH fields versus the parameterized approach as a demonstration of the utility of the parameterization relative to the currently favored computationally efficient approach. For example, is there a scenario with archived OH that could be compared with Base?

Yes, we did such a scenario using annually-repeating archived OH fields from a full chemistry simulation of the NASA GMI CTM (*Base_GMI* scenario). The OH in this simulation falls within the multi-model mean of MIPs, but is generally on the low side. Consequently, it leads to too high methane as shown in the figure below. We didn't adjust the OH field upward to account for this, such as was done in the TransCom MIP – the climatology of Spivakovsky et al. (2000) was adjusted down by 8%. That is, if we were to compare a simulation using the ECCOH module and one using archived OH, the comparison will be dependent on the archived OH used (i.e., seasonally-repeating vs seasonally-varying, the overall magnitude, etc.). Therefore, we decided not to include the comparison.

To address this concern, we added the underlined text to a paragraph in the Introduction:

“Limitations of using archived, monthly OH fields for studies of methane’s and CO’s evolution are that feedbacks of the CH₄-CO-OH system on methane, CO and OH are not captured as the losses of methane and CO by reaction with OH are assumed to be linearly proportional to the OH fields. For methane, this assumption is not desirable, particularly on multi-decadal time-scales (e.g., Prather, 1996). Chen and Prinn (2006) found that using an archived, annual cycle of OH may mask or bias the interannual changes of methane. For relatively short-lived CO (~1-2 months), this assumption is not valid given the strong feedback between CO and OH (e.g., Duncan and Logan, 2008; Voulgarakis et al., 2015). If a multi-decadal simulation of methane or CO using archived and annually-repeating OH reproduces observations, then there must be some compensating factor, for example a bias in emissions. That is, the simulation reproduces observations, but for the wrong reason. The models in the TranCom MIP adjusted down (by 8%) the archived OH

climatology of Spivakovsky et al. (2000) so that the simulated decline in the global atmospheric methylchloroform (MCF) concentration since 2000 better matched that observed (Patra et al, 2011). Adjusting archived OH to improve a simulation of MCF, methane and/or CO makes the specious assumption that emissions inventories, model dynamics, etc. used in the simulation are correct. If using archived and annually-repeating OH, whether adjusted or not, inverse modeling studies of methane and CO will incorrectly determine a posteriori fluxes as the impact of nonlinear feedback of the CH₄-CO-OH system on concentrations will be erroneously folded into the flux estimates. Therefore, there is a need for a computationally-efficient solution to simulate credible temporal and spatial distributions of OH over several decades, while capturing the nonlinear feedbacks of the CH₄-CO-OH system.

And we added an introductory paragraph to Section 4.2:

“Any model simulation using annually-repeating and archived OH will not accurately capture regional and interannual variations in the loss rates of methane and CO. A simulation using zonally-averaged archived OH (e.g., Spivakovsky et al., 2000), such as was done in the TransCom MIP, will not capture any regional and interannual variations. For example, Fig. S 7 and Fig. S 12 reproduce Fig. 4a and Fig. 5, respectively, but includes methane from a simulation using archived and annually-repeating OH of the NASA Global Modeling Initiative model (Duncan et al., 2007b; Strahan et al., 2007). The simulated longer methane lifetime (Fig. S 7), using archived OH, leads to an accumulation of methane over the multi-decadal simulation.”

And we added the following paragraph to the end of Section 4.3:

“Accurate quantification of the magnitude of the combined nonlinear feedbacks is ultimately dependent on the uncertainties and errors of emissions, such as those discussed in Sect. 3, and independent variables, each of which have their own uncertainties, used in the parameterization of OH. With our sensitivity simulations, we discussed instances when changes to emissions and/or the input to the parameterization of OH improved or worsened the simulated methane and CO. In some instances, simulated methane and/or CO from the least complex *Base* scenario more favorably agreed with observations than the other more complex scenarios, including methane in the most complex *AllVary* scenario (e.g., Table 4, Fig. 4). However, in these instances, better correlation does not necessarily imply that a simpler scenario, such as the *Base* scenario or a scenario that uses archived and annually-repeating OH, is inherently better. The best scenario is one that accurately simulates the complex interactions of the factors that influence the CH₄-CO-OH system, which will give confidence in the response of the system to perturbations, such as from large interannual variations in wetland fluxes, biomass burning, ENSO, and volcanic eruptions. The next steps for our research include quantifying the 1) sensitivity of the simulated CH₄-CO-OH system to uncertainties in the factors (e.g., water vapor, clouds, trace gases) that control tropospheric OH so as to improve simulated methane and CO with observations, and 2) the influence of potential large atmospheric carbon perturbations in a warming world, such as may occur from permafrost thaw, methane hydrate release, and enhanced biomass burning.”

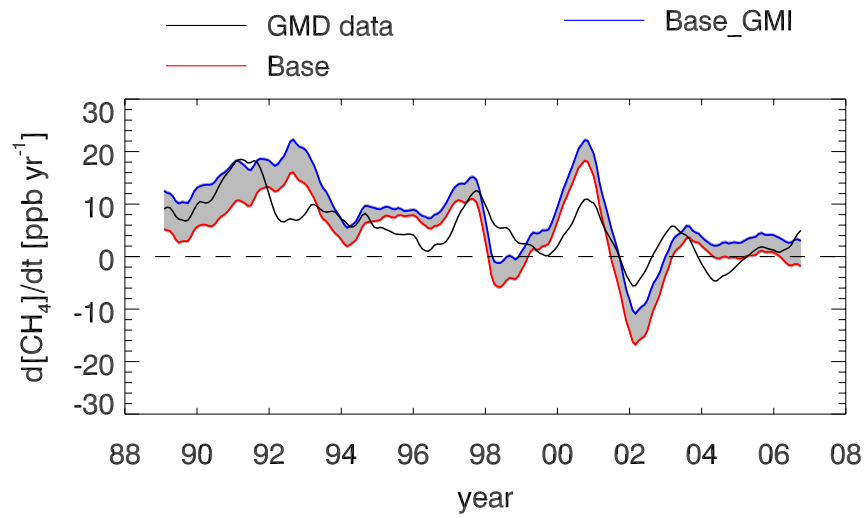


Figure 1: Same as Fig. 4 (Manuscript) but the shaded area is the difference between the *Base_GMI* and *Base* scenarios. *Base_GMI* scenario is similar to the *Base* scenario except that OH is archived 3D fields (i.e., not interactively simulated).

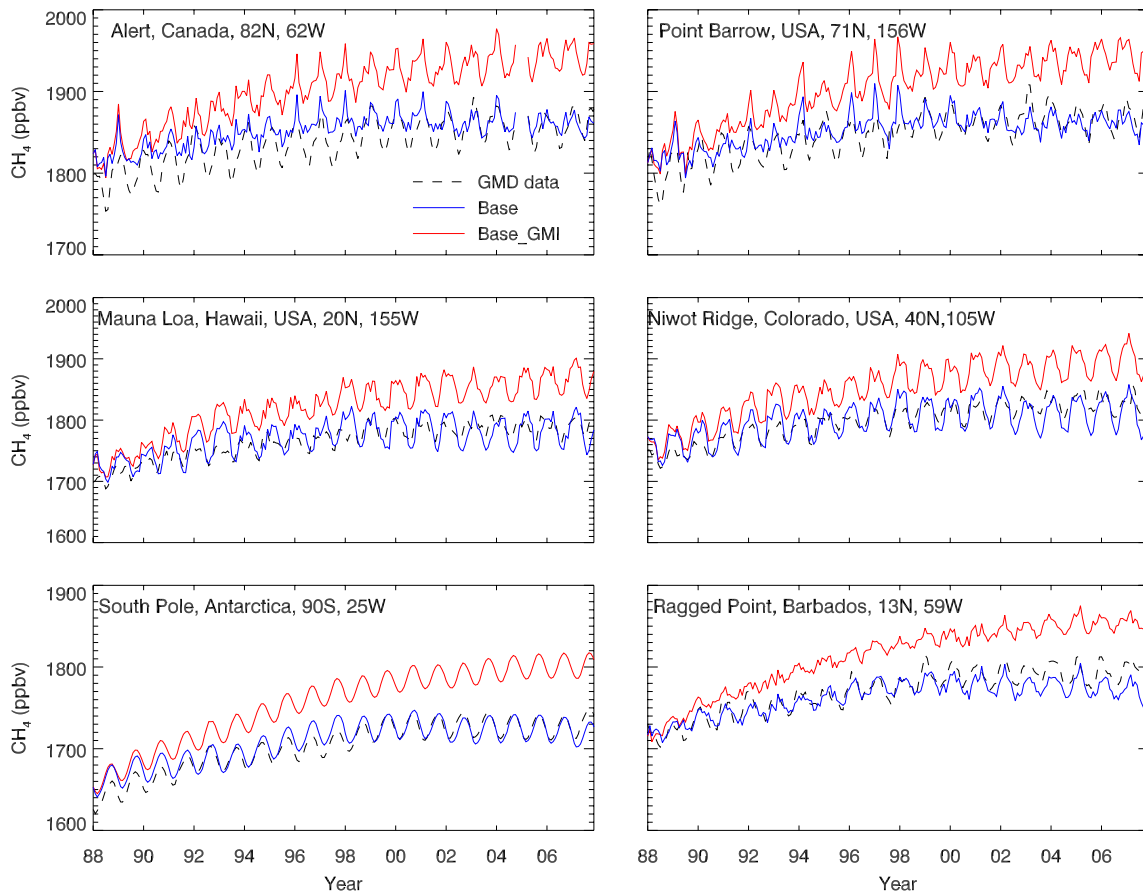


Figure 2: Monthly methane (ppbv) from the *Base* and *Base_GMI* scenarios and observations from six GMD stations. *Base_GMI* scenario is similar to the *Base* scenario except that OH is archived 3D fields (i.e., not interactively simulated).

Comparison with a full chemistry model would also be useful.

That has been done and is discussed in Sect. 3.1, Page 9459, lines 15-27 and in Section S 3 of the Supp. Mat.

Does the parameterization require having a companion full chemistry simulation to provide the driving parameters? If so, then the value here must be that the parameterized version allows for cheaper sensitivity simulations relative to that single full chemistry simulation. If this is correct, it would help to state this more clearly.

To address this suggestion, we added the underlined text to the second paragraph of Section 2.1:

“The parameterization of OH accurately represents OH predicted by a full chemical mechanism as a set of high-order polynomials that describe the functional relationship between the concentration of OH and meteorological variables (i.e., pressure, temperature, cloud albedo), solar irradiance variables (i.e., ozone column, surface albedo, declination angle, latitude) and chemical variables, including CO and methane as well as nitrogen oxides (as a family), ozone, water vapor, and various VOCs. That is, the 24h average OH is calculated interactively in the model and responds to changes in the concentrations of trace gases and meteorology. Input variables to the parameterization of OH may be taken from archived fields from, for instance, an observational climatology or archived fields from a model simulation with a full representation of trace gas and aerosol atmospheric chemistry, and may be annually-repeating or annually-varying. Some variables (e.g., water vapor, clouds) may be taken from the host model as the simulation progresses. Ideally, all input variables should be annually-varying so as to best capture the nonlinear feedbacks of the CH₄-CO-OH system. If one chooses to use output from a single computationally-expensive full chemistry model simulation as input to the parameterization of OH, subsequent sensitivity simulations using the ECCOH chemistry module will be far less computationally-expensive relative to that single expensive simulation, which is the primary strength of using the parameterization of OH. In Section 2.2, we discuss the setup of the simulations presented in this study.

Is the factor of 500 a result from this work or is that number based on the 2000 paper (P 9455 L9-11)? It would be useful to provide a brief description of what the parameterization involves, including that it is tailored to regional chemical and meteorological conditions.

The factor of 500 is from the 2000 paper as cited.

To address the reviewer’s concern, we modified the following sentence from:

“It was designed to be applicable to preindustrial, present day and possible future conditions (Duncan et al., 2000) and has been used in several studies of CO and OH (Duncan et al., 2007a; Duncan and Logan, 2008; Strode et al., 2015).”

To:

“It is based on the method described by Spivakovsky et al. (1990a), who developed an earlier version of the parameterization of OH used in several studies, including Spivakovsky et al. (1990b) and Prather and Spivakovsky (1990). The parameterization of OH of Duncan et al. (2000) is designed to simulate OH over the range of photochemical environments found throughout the troposphere, including a wide enough range so as to be applicable to preindustrial, present day and possible future conditions (Duncan et al., 2000). It has been implemented into two host atmospheric models and has been used in several studies of the nonlinear feedbacks of CO and OH (Duncan et al., 2007a; Duncan and Logan, 2008; Strode et al., 2015).”

Consider reducing the number of figures in the supplemental material and possibly in the main text.

We deleted Figures S11, S12, S17, S18 - S24 from the Supplemental Material.

Specific comments follow.

P9453 L23. How large is this bias from using archived OH?

We added an introductory paragraph to Section 4.2:

“Any model simulation using annually-repeating and archived OH will not accurately capture regional and interannual variations in the loss rates of methane and CO. A simulation using zonally-averaged archived OH (e.g., Spivakovsky et al., 2000), such as was done in the TransCom MIP, will not capture any regional and interannual variations. For example, Fig. S7 and Fig. S12 reproduce Fig. 4a and Fig. 5, respectively, but includes methane from a simulation using archived and annually-repeating OH of the NASA Global Modeling Initiative (GMI) model (Duncan et al., 2007b; Strahan et al., 2007). The simulated longer methane lifetime (Fig. S7), using archived OH, leads to an accumulation of methane over the multi-decadal simulation. In this situation, the archived OH would need to be adjusted higher to improve the simulation of methane as compared to observations.”

P9454 L19-22. Does the parameterization avoid this uncertainty somehow? Is it updated to include more recent isoprene-NO_x-OH relationships?

In this paragraph, we simply make the point that the large uncertainty in OH occurs because there are very few observations of OH and they often disagree with model output that include state-of-the-art chemical mechanisms, including in non-polluted,

forested environments where isoprene is the dominant VOC. That is, there is large uncertainty in current OH chemistry because of incomplete knowledge of OH sources and recycling mechanisms. Therefore, the parameterization of OH is not immune to the uncertainties in OH chemistry. We do not imply this in the paragraph in question.

We added the following sentence to the end of the paragraph in question to address the reviewer's concern:

"Recent updates in isoprene chemistry are not reflected in the parameterization of OH, so OH near the surface in clean, forested environments (e.g., Amazon and Congo basins) is too low relative to current knowledge (e.g., Fuchs et al., 2013). However, the contribution of these regions to global methane and CO loss is small (i.e., < 1%) and the current knowledge of isoprene photochemistry is still highly uncertain (Fuchs et al., 2013). Ultimately, the parameterization of OH reflects uncertainties in the chemistry upon which it is based, as do the photochemical mechanisms in all atmospheric chemistry models (e.g., Stone et al., 2012; Fuchs et al., 2013)."

P9455-9456 Is this the only update from the parameterization described in the 2000 paper?

Yes. Upon comparison of the mechanism used to generate the parameterization with current photochemistry, we found that the quenching reactions of O¹D are by far the most important update, especially as they globally determine the primary production of OH.

Are total ozone columns and stratospheric OH, Cl, and O¹D varying interannually?

As mentioned in Tables 1 and 2, ozone columns are annually-repeating in all simulations, except they are annually-varying in the *OH_{input}Vary* and *AllVary* scenarios. Year-to-year variations in the ozone column are very important in the simulation of tropospheric OH and CO (Duncan et al., 2008).

The stratospheric OH, Cl, and O¹D archived monthly fields are annually-repeating and from an AGCM simulation. Stratospheric loss processes for CO and methane are non-negligible, though their typical year-to-year variations have an unimportant impact on tropospheric OH, CO, and methane.

Are photolysis rates calculated explicitly in ECCOH (P9456 L4)?

No. There are no photochemical rates used as independent variables in the parameterization of OH. The parameterization was designed to be grounded in observations of chemical concentrations, solar irradiance variables and meteorological variables. The independent variables are explicitly listed in the second paragraph of Section 2.1.

P9457 L18. Where does Table 2 describe the input variables?

The input variables are the same in all scenarios as in the *Base* scenario (Table 1), except in the *OH_{input}Vary* and *AllVary* scenarios – the last two rows of Table 2.

We added to the sentence (underlined text) in question to clarify this:

“These causal factors include annually-varying methane and CO emissions (i.e., Scenarios 2-4 in Table 2; natural methane emissions, and anthropogenic and natural CO emissions, Figs. S1 and S2 in the Supplement) and annually-varying input variables to the parameterization of OH (i.e., Scenario 5 in Table 2).”

P9458 L11-13 seems to require the reader to know what these distributions look like. L18-19 consider showing this comparison.

For clarity, we modified the sentence with the underlined text:

“Despite the challenges concerning OH, we show in this section that the spatial and vertical distributions of simulated global mean OH (Figs. 2 and 3) from the *Base* scenario are reasonable relative to the MCF proxy for OH as well as to simulated OH from other models.”

The last sentence of the paragraph is now:

“The seasonal and vertical distributions of the zonal mean OH in the *Base* scenario are quite comparable to the OH climatology of Spivakovsky et al. (2000; see Figure 6 of Spivakovsky et al.), despite the different inputs given to the parameterization of OH in the two studies.”

P9459 L3-15 Are these values all for lifetimes with respect to tropospheric OH loss only?

Yes, as also mentioned in the text (P9459, L4).

The method for calculating lifetime of methane/MCF is similar in all mentioned studies, which is by dividing the global atmospheric burden of methane or MCF by its tropospheric OH oxidation flux, except in the study of Naik et al., 2015, where MCF lifetime was calculated by scaling the methane lifetime with the ratio of the rate coefficient of the reactions of methane and MCF with OH integrated from the surface to the tropopause (see Naik et al., 2015 for more details). In Shindell et al., (2006), the lifetime calculation method is not stated explicitly.

P9459 L26. Are these models for the same period as the ECCOH simulations?

For the ACCMIP simulations (Voulgarakis et al., 2013)), the model experiments are the present day (2000 time slice) and future simulations (representative for the

conditions of 2030 and 2050). The mentioned ACCMIP results are for the 2000 time slice. Our simulations are also from 1988-2007, and using the same CO annually-repeating emissions, as mentioned in the text and in Table 1.

For clarity, we updated the last sentence with the underlined text as follows:

“The global, mean tropospheric OH in the *Base* scenario of 10.9×10^5 molecules cm^{-3} also compares well with that of 11.4×10^5 molecules cm^{-3} from the ACCMIP simulation (the 2000 time slice) as well as within the range of means from other models (e.g., 6.5 – 13.4×10^5 molecules cm^{-3} (Voulgarakis et al., 2013)).”

P9460 L3 Table 3 should be Table 4 ?

We removed the incorrect table reference.

L4 “reasonably well” would be stronger if supported by a more objective measure like a correlation coefficient or bias estimate.

Done. $R^2=0.44$ for the base scenario is now included in the text.

L20. What is the evidence for regional high biases in natural emissions; are there isotopic measurements?

The *Base* scenario (based on the CTL TransCom emissions scenario) has annually-varying anthropogenic emissions but annually-repeating natural emissions (Fig. S1). In the *E_{CH4}Vary* scenario, (based on the EXTRA TransCom emissions scenario) anthropogenic and natural emissions are annually-varying. The regional high bias improves significantly in the *E_{CH4}Vary* scenario, indicating that the reason for the high bias in the *Base* scenario is a high bias in the natural emissions. Saito et al. (2013) mentioned that the CTL and EXTRA emissions differ by more than 100% over some of the regions.

P9466 L26. How large is the vertical gradient in CH4?

We added the underlined text to the sentence in question:

“In addition, most loss occurs near the surface despite higher OH in the mid-troposphere (Fig. 2) because of higher methane mole fractions near the surface (e.g., ~3 % over Alaska, and typically higher over surface source regions), the altitude dependence of air density, and the temperature dependence of the loss rate (Fig. 18). Methane’s loss rates in the *AllVary* scenario are relatively higher, especially over biomass burning regions (Fig. 17) and have much higher spatial variability than in the *Base* scenario (Fig. 19).”

P9467 L12-16. Consider adding a statement to explain why this can’t be equally well studied with sensitivity simulations using archived offline OH fields.

We incorporated the reviewer's suggestion with the underlined text in the paragraph in question:

"The differences in global abundances of CO and OH between our least complex (*Base*, Table 1) and most complex (*AllVary*, Table 2) scenarios are substantial and their impact on methane's evolution is nontrivial as discussed in Sects. 4.1 and 4.2. Therefore, model studies of methane and/or CO, which use archived fields of OH distributions, will not capture these important nonlinear feedbacks of the CH₄-CO-OH system (e.g., Fig. 4). Here, we discuss the contribution of various factors to the observed spatial distributions and temporal evolution of observed methane, CO, and OH to demonstrate the utility of the ECCOH chemistry module for studying the nonlinear CH₄-CO-OH system. We provide a brief summary of our conclusions from the scenarios at the end of this section."

P9468 L25-26. Are overhead ozone columns and lightning NO_x varying in ECCOH online?

Monthly archived fields of overhead zone column and lightning NO_x are annually-varying in the *OH_{input}Vary* and *AllVary* scenarios, but annually-repeating in the other scenarios as shown in Table 2.

For clarity, we modified the sentence in question with the underlined text:

"For example, both variations in the overhead ozone column and NO emissions from lightning are known to cause variations in global OH (e.g., Duncan and Logan, 2008; Murray et al., 2013)."

P9469 L11. Are these numbers for the *Base* or *AllVary* or both?

AllVary scenario. The statement is now rearranged to be clearer:

"Despite large spatial differences in OH, the global, mean MCF lifetime for the *AllVary* scenario, which range from 6.01 (± 0.51) to 6.67 (± 0.61) years over the simulation period, is not significantly different from that of the *Base* scenario."

P9469 L21. How important is this compared to uncertainty in emissions?

We added the following paragraph (with underlined new text) to the end of Section 4.3 to address this concern:

"Accurate quantification of the magnitude of the combined nonlinear feedbacks is ultimately dependent on the uncertainties and errors of emissions, such as those discussed in Sect. 3, and independent variables, each of which have their own uncertainties, used in the parameterization of OH. With our sensitivity simulations, we discussed instances when changes to emissions and/or the input to the parameterization of OH improved or

worsened the simulated methane and CO. In some instances, simulated methane and/or CO from the least complex *Base* scenario more favorably agreed with observations than the other more complex scenarios, including methane in the most complex *AllVary* scenario (e.g., Table 4, Fig. 4). However, in these instances, better correlation does not necessarily imply that a simpler scenario, such as the *Base* scenario or a scenario that uses archived and annually-repeating OH, is inherently better. The best scenario is one that accurately simulates the complex interactions of the factors that influence the CH₄-CO-OH system, which will give confidence in the response of the system to perturbations, such as from large interannual variations in wetland fluxes, biomass burning, ENSO, and volcanic eruptions. The next steps for our research include quantifying the 1) sensitivity of the simulated CH₄-CO-OH system to uncertainties in the factors (e.g., water vapor, clouds, trace gases) that control tropospheric OH so as to improve simulated methane and CO with observations, and 2) the influence of potential large atmospheric carbon perturbations in a warming world, such as may occur from permafrost thaw, methane hydrate release, and enhanced biomass burning.”

We added the following figures to the Supplemental Material.

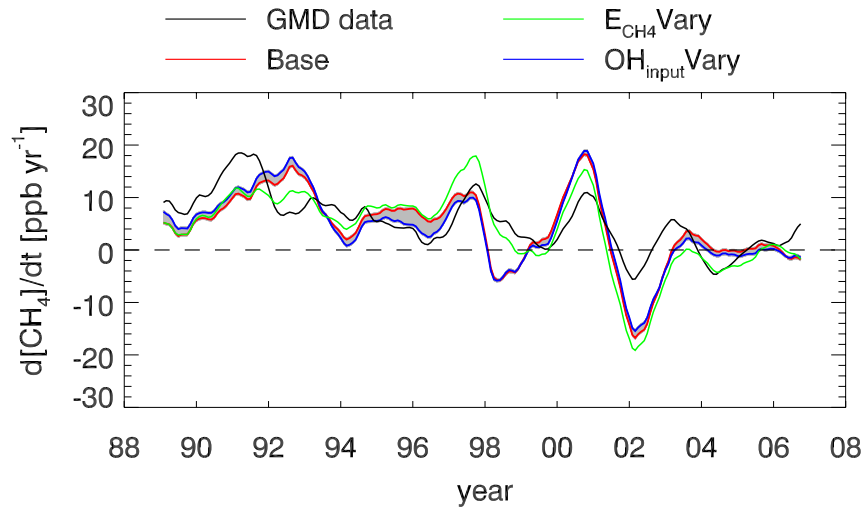


Fig. 1: Atmospheric methane growth rate (ppbv/yr, average of 92 GMD stations) from several scenarios. The shaded area is the difference between the *Base* and *OH_{input}Vary* scenarios.

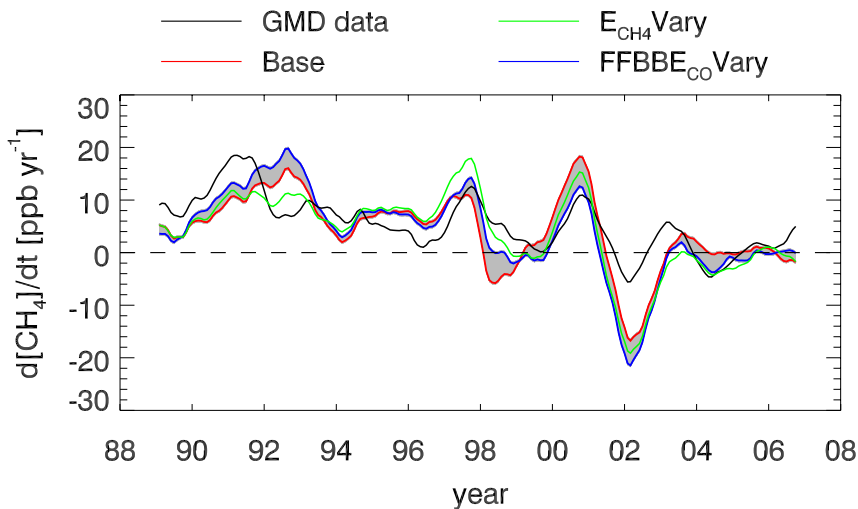


Fig. 2: Atmospheric methane growth rate (ppbv/yr, average of 92 GMD stations) from several scenarios. The shaded area is the difference between the *Base* and *FFBBE_{CO}Vary* scenarios.

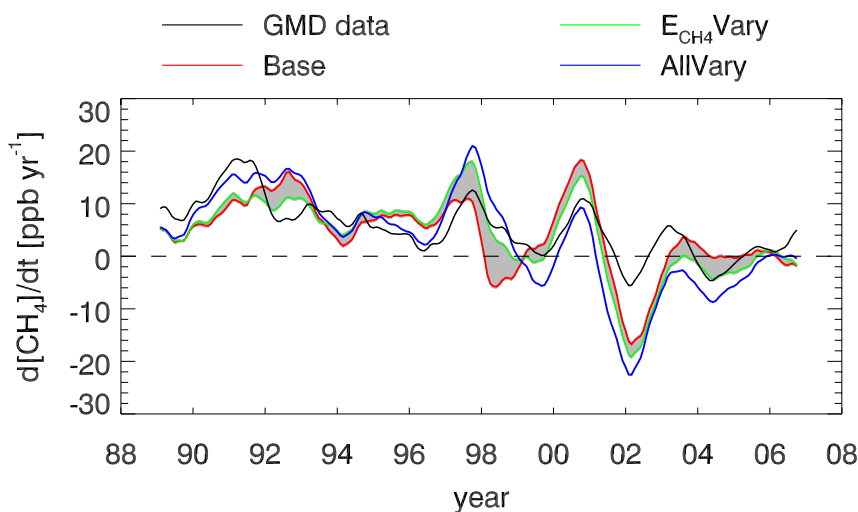


Fig. 3: Atmospheric methane growth rate (ppbv/yr, average of 92 GMD stations) from several scenarios. The shaded area is the difference between the *Base* and *E_{CH4}Vary* scenarios.

P9470 L4-6. It would help to point to the evidence supporting this statement.

We added a new sentence (underlined) to the end of the summary:

“Through our simulations, we show the importance of using an interactive CH₄-CO-OH system as opposed to using static, archived OH fields, as nonlinear feedbacks on methane, CO, and OH are non-trivial. For example, nonlinear feedbacks modulate the global methane growth rate over our study period ($\pm 20 \text{ ppbv yr}^{-1}$) by $\pm 4 \text{ ppbv yr}^{-1}$ (Figure 4).”

Table 1. The methane tracer is inactive in radiation, but surely there is a methane abundance set in the radiation code?

Yes, greenhouse gases, including methane, are provided as archived fields to the radiation scheme in the current setup.

We modified (underlined) the sentence in question to:

“The methane tracer is radiatively inactive and archived, annually-varying methane fields are used in the radiation code; our aim is reproduce the same meteorology in all simulations so as to more cleanly isolate the impact of the causal factors on methane, CO, and OH trends and variations.”

It would be good to clarify that the emissions used here are bottom-up estimates if that is the case. Are the anthropogenic emissions based on EDGAR or have they been optimized through prior inversions?

Methane emissions are based on the TransCom CTL (Base scenario) and EXTRA emission scenarios (Patra et al., 2011). As mentioned in Patra et al. (2011), methane anthropogenic emissions in the CTL scenario are bottom up estimates that are based on EDGAR 3.2, being inter-/extra-polated using 1990, 1995, 2000 emission maps to produce the IAV in emissions (i.e., original EDGAR emissions are only from 1990-1995). EXTRA emissions are optimized to include IAV in biomass burning and wetland emissions. In Table 2, other emissions are explicitly mentioned. CO emissions in the *Base* scenario are gridded emissions that were prepared for the CMIP studies (Lamarque et al., 2013 and Lamarque et al., Atmos. Chem. Phys., 10, 7017–7039, 2010).

To address the referee’s comment, we modified (underlined text) the sentence in question:

“Annually-repeating natural (e.g., wetlands, biomass burning) and annually-varying anthropogenic emissions (EDGAR 3.2, TransCom CTL scenario) are described in Patra et al. (2011).”

Table 4. Is there an explanation for why AllVary often performs worse than Base?

To address this concern, we added the following text to the end of Section 4.3:

“Accurate quantification of the magnitude of the combined nonlinear feedbacks is ultimately dependent on the uncertainties and errors of emissions, such as those discussed in Sect. 3, and independent variables, each of which have their own uncertainties, used in the parameterization of OH. With our sensitivity simulations, we discussed instances when changes to emissions and/or the input to the parameterization of OH improved or

worsened the simulated methane and CO. In some instances, simulated methane and/or CO from the least complex *Base* scenario more favorably agreed with observations than the other more complex scenarios, including methane in the most complex *AllVary* scenario (e.g., Table 4, Fig. 4). However, in these instances, better correlation does not necessarily imply that a simpler scenario, such as the *Base* scenario or a scenario that uses archived and annually-repeating OH, is inherently better. The best scenario is one that accurately simulates the complex interactions of the factors that influence the CH₄-CO-OH system, which will give confidence in the response of the system to perturbations, such as from large interannual variations in wetland fluxes, biomass burning, ENSO, and volcanic eruptions. The next steps for our research include quantifying the 1) sensitivity of the simulated CH₄-CO-OH system to uncertainties in the factors (e.g., water vapor, clouds, trace gases) that control tropospheric OH so as to improve simulated methane and CO with observations, and 2) the influence of potential large atmospheric carbon perturbations in a warming world, such as may occur from permafrost thaw, methane hydrate release, and enhanced biomass burning.”

Figure 2. Consider replacing AllVary with a difference plot.

Done.

Figure 4. Please describe how the growth rate is calculated and how to interpret the gray shaded area.

The new figure caption is:

“Figure 4. 12-month running mean atmospheric growth rate of methane (ppbv yr⁻¹) for the average of 92 GMD stations and from model output for several scenarios averaged for those station locations. The shaded area is the difference between the *E_{CH4}Vary* and *AllVary* scenarios, which indicates the total contribution of nonlinear feedbacks (i.e., from variations of CO emissions and variables input to the parameterization of OH) of the CH₄-CO-OH system to methane’s growth rate.”

Figure 7. Why is ECH4_vary closer to observations than AllVary? Does this imply a problem with the parameterization, emissions, or both?

See our response to the specific comment on Table 4 a few comments ago.

Figure 12. Not sure what the vertical line sentence in the caption refers to.

That is a mistake. Deleted.

Figure 14. Caption needs fixing.

Done.

Figure 15. Is there an explanation for why the model is frequently the wrong sign?

In short, our study isn't the only one that cannot reconcile the observations with model output, which may indicate errors in the observations, the models, or a combination of both. However, we don't explicitly say that several researchers question the validity of the observations. Instead, we subtly indicate this in Sect. 4.1:

"We compare simulated, mass-weighted pseudo first order rate constants (k'), a proxy for OH interannual variations, from each of our scenarios to that inferred from MCF measurements (Fig. 15; 1998–2007; Montzka et al., 2011). We find that none of our model scenarios are able to reproduce the inferred interannual OH variability of Montzka et al. (2011), though the simulated variability is of similar magnitude and within observational uncertainty. Our findings are consistent with other modeling studies (Montzka et al., 2011; Holmes et al., 2013; Murray et al., 2013 and references therein). While global interannual variations are informative, there can be considerable OH interannual variations regionally (as discussed in Sects. 4.2 and 4.3) that may not be reflected in the global average (Lelieveld et al., 2002; Wild and Palmer, 2008)."

Figure 16. Consider adding correlation coefficients.

Done. The following sentence is now added to the caption of Fig. 16:

The correlation coefficients (R^2) of the MEI index with the *Base* and *AllVary* scenarios are 0.20 and 0.59, respectively.

And the correlation coefficients are also mentioned in the text (last paragraph of sect. 4.1):

"As shown in Fig. 16, the deviations of mass-weighted OH from various scenarios over Indonesia (100°–150°E; 6°N–6°S) are generally anti-correlated with the Multivariate ENSO Index (MEI, Wolter et al., 2011), a proxy of ENSO. OH variations in the *Base* scenario, which includes meteorological variations that affect OH via variations in water vapor, clouds, etc., are $\pm 4\%$ ($R^2 = 0.20$), but much higher in the scenarios that include variations in biomass burning emissions (i.e., *AllVary* scenario), which better capture the ENSO variability ($R^2 = 0.59$)."

Figure 22. What are the deviations relative to? Is this the standard deviation?

That is the standard deviation. The caption is now corrected.

Patra, P. K., Krol, M. C., Montzka, S. A., Arnold, T., Atlas, E. L., Lintner, B. R., . . . Young, D. (2014). Observational evidence for interhemispheric hydroxyl-radical parity. *Nature*, 513(7517), 219-23.

p9458, line 6-7 : add 'et al.' to Lawrence. Also I think MCF is used as a proxy for OH since the 1990s by many others. Generally agree, but MCF has recently been used at quite good confidence for broad characterization of OH in the two hemispheres because uncertainties MCF emissions are now small compared its atmospheric burden.

We added the following text (underlined) to the paragraph in question:

“There are very few direct observations of OH with which to constrain models (e.g., Stone et al., 2012) and none on regional or global scales. Therefore, the methylchloroform (MCF) lifetime inferred from measurements serves as a widely used, indirect proxy for global OH abundance (e.g., Lawrence, 2001). Though useful, the MCF lifetime gives an incomplete description of the spatial and vertical distributions of OH (e.g., Lawrence et al., 2001) and there are uncertainties concerning MCF emissions and the resulting lifetime estimate (e.g., Wang et al., 2008). Nevertheless, the MCF data have been recently used to infer the ratio of OH in the Northern to the Southern Hemisphere (Patra et al., 2014).”

p9458, line 18 : can you be a bit more quantitative here? what is quite?

We added the following text (underlined) to the sentence in question:

“The seasonal and spatial distributions of the zonal mean OH in the *Base* scenario are quite comparable to the OH climatology of Spivakovsky et al. (2000), despite the different inputs given to the parameterization of OH in the two studies.”

p9460, line 5 : I think very few sites were in place in 1980s, thus this sentence is misleading. Can you not arrive at this conclusion by using only the sites with full data coverage?

To address this concern, we modified Figure 4 and modified (underlined text) the first paragraph of Section 3.2 to:

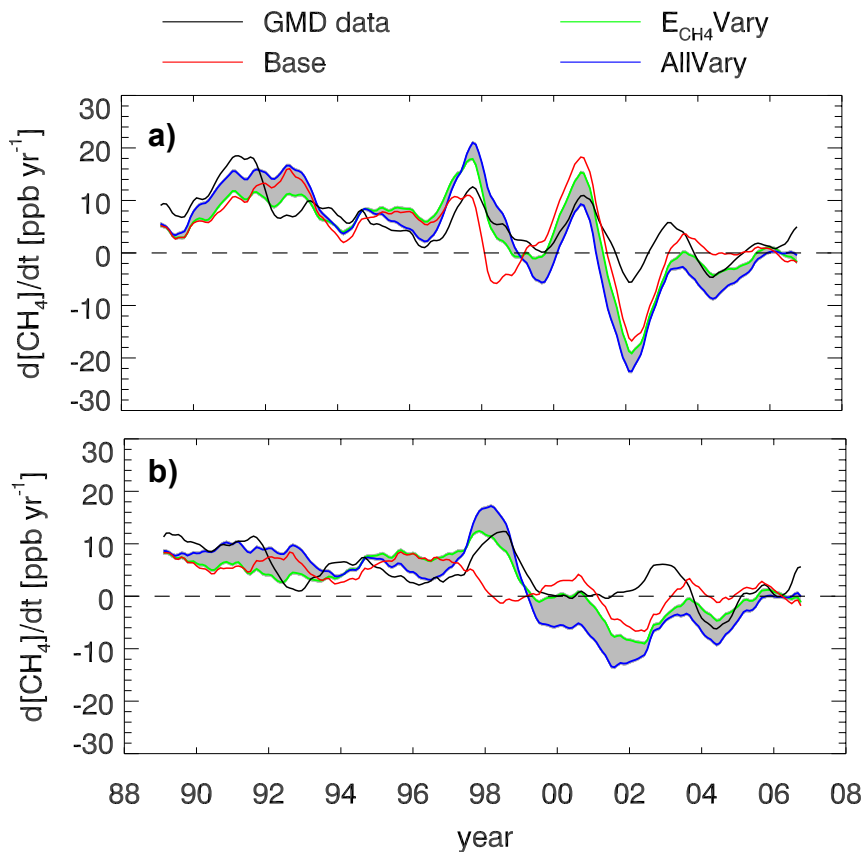


Figure 4: a) 12-month running mean atmospheric growth rate of methane (ppbv yr^{-1}) for the average of 92 GMD stations and from model output for several scenarios averaged for those station locations. The shaded area is the difference between the $E_{\text{CH}_4}\text{Vary}$ and $AllVary$ scenarios, which indicates the total contribution of nonlinear feedbacks (i.e., from variations of CO emissions and variables input to the parameterization of OH) of the $\text{CH}_4\text{-CO-OH}$ system to methane's growth rate. b) Same as a) but for the average of 17 GMD stations, which covers 100% of the simulation period.

“GMD surface data: We evaluate our simulated surface distributions of methane from the *Base* scenario with data from the NOAA Global Monitoring Division (GMD) network. The simulated, interannual variation of methane's global growth rate agrees reasonably well ($R^2 = 0.44$) with that estimated from GMD data, using all available data from 92 stations over the simulation period 1988-2007 (Fig. 4). We decided to include all 92 stations, even those without records that cover the entire simulation period, as we are able to nearly reproduce Fig. 4 using 46 stations that have at least 75% data coverage (Fig. S 4). The agreement of model output with observations is worse ($R^2 = 0.33$) when we only use the 17 stations that have records covering the entire simulation period (Fig. 4). A relatively high correlation coefficient ($R^2 = 0.44$) implies that interannual variations in anthropogenic methane emissions and dynamics explain much of methane's growth rate over the study period, which is consistent with the findings of the TransCom model intercomparison project (Patra et al., 2011).”

p9460, line 14 : Please mention the time period of the data used

Done. The simulation period is 1988-2007.

p9460, line 24 : I thought the base case doing well as seen in Fig. 5, and this problem is more serious in All Vary case

The sentence in question refers to only the *Base* scenario, so the statement is true.

In section 4.3, we compare the *Base* and *AllVary* scenarios to observations, discussing in what regions/time periods the scenarios perform best/worst.

p9462, line 12 : Are those in the tropics or SH?

We added the following text (underlined) to the sentence in question:

“However, the largest biases (Figs. 12 and S14) occur over (1) tropical and subtropical biomass burning regions (~20 %) during boreal winter, indicating that either the CO emissions used in the Base scenario are too high or that simulated OH is too low, and (2) most of the Northern Hemisphere (< -20 %) during the summer season, indicating that either CO emissions are too low or that OH levels are too high, which is consistent with previous studies using similar emissions (e.g., Shindell et al., 2006; Strode et al., 2015).”

p9462, line 21 : But in your model, you see these biases also at the surface stations, in the previous para - right? So the uncertainties in remote sensing products may not be questioned in this context.

The simulated near-surface concentration of CO in the *Base* scenario is underestimated, especially in the northern hemisphere related to using annually repeating CO emissions. Using annually-varying CO emissions (e.g., *FFBBE_{CO}Vary* and *AllVary* scenario) solves this issue.

For MOPITT and TES/MLS, the comparisons reveals higher simulated CO over biomass burning regions during boreal winter and lower simulated CO over the northern hemisphere during summer. The comparison results are consistent with previous model-MOPITT comparisons as mentioned in the text.

p9464, line 10 : The problem is how to say something meaningful out of this comparisons. Can we claim Voulgarakis et al. (2015) is right?

Our results support the conclusions of Voulgarakis et al. (2015) and it also makes sense given that CO interannual variability is a strong function of variations in CO emissions.

p9465, line 12 : I have some concerns when the MCF-inferred OH IAV is marked as "Observation" in Fig. 15. A lot of assumptions has gone in this calculation, so I would recommend to change the legend as 'MCF-inferred" or something like that.

Done.

p9466, line 3 : The fires also emit a lot of ozone precursors. If O₃ increases will there be more OH production under no/less cloudy conditions - how does those feedback works? Any perspective will be appreciated.

It is true that other OH/O₃ precursors are emitted from biomass burning. For example, we know that large amounts of HONO, a primary OH source, are emitted from fires (e.g., Yokelson et al., 2009). However, these fire plumes are characterized by low NO_x conditions and thus OH will not be efficiently recycled (as per current knowledge), which may limit the impact of these precursors on OH and O₃. It has also been shown in other studies that that high boreal fire activity increases O₃ in the free troposphere by up to 10 ppbv with photochemically aged biomass burning influencing tropospheric oxidant chemistry after 1-2 weeks of transport to the region (Parrington et al., 2013 and references therein). However, the extent and the mechanism of these impacts are still not well known. Therefore, it is not possible to test these possible impacts in global models without knowing the actual mechanisms.

Yokelson, R. J., Crouse, J. D., DeCarlo, P. F., Karl, T., Urbanski, S., Atlas, E., Campos, T., Shinozuka, Y., Kapustin, V., Clarke, A. D., Weinheimer, A., Knapp, D. J., Montzka, D. D., Holloway, J., Weibring, P., Flocke, F., Zheng, W., Toohey, D., Wennberg, P. O., Wiedinmyer, C., Mauldin, L., Fried, A., Richter, D., Walega, J., Jimenez, J. L., Adachi, K., Buseck, P. R., Hall, S. R., and Shetter, R.: Emissions from biomass burning in the Yucatan, *Atmos. Chem. Phys.*, 9, 5785-5812, doi:10.5194/acp-9-5785-2009, 2009.

Parrington, M., Palmer, P. I., Lewis, A. C., Lee, J. D., Rickard, A. R., Di Carlo, P., Taylor, J. W., Hopkins, J. R., Punjabi, S., Oram, D. E., Forster, G., Aruffo, E., Moller, S. J., Bauguitte, S. J.-B., Allan, J. D., Coe, H., and Leigh, R. J.: Ozone photochemistry in boreal biomass burning plumes, *Atmos. Chem. Phys.*, 13, 7321-7341, doi:10.5194/acp-13-7321-2013, 2013.

The Description and Validation of a Computationally-Efficient CH₄-CO-OH (ECCOHv1.01) Chemistry Module for 3D Model Applications

Elshorbany, Yasin F.^{1,2*}, Duncan, Bryan N.¹, Strode, Sarah A.^{1,3}, Wang, James S.^{1,3}, Kouatchou, Jules^{1,4}

¹NASA Goddard Space Flight Center, Greenbelt, Maryland, USA,

²Earth System Science Interdisciplinary Center, University of Maryland, College Park, Maryland, USA,

³Universities Space Research Association, Columbia, Maryland, USA

⁴Science Systems and Applications Inc., Lanham, Maryland, USA

*Correspondence to: Y. F. Elshorbany (yasin.f.elshorbany@nasa.gov)

Abstract:

We present the Efficient CH₄-CO-OH chemistry module (ECCOH) that allows for the simulation of the methane, carbon monoxide and hydroxyl radical (CH₄-CO-OH) system, within a chemistry climate model, carbon cycle model, or earth system model. The computational efficiency of the module allows many multi-decadal sensitivity simulations of the CH₄-CO-OH system, which primarily determines the global atmospheric oxidizing capacity. This capability is important for capturing the nonlinear feedbacks of the CH₄-CO-OH system and understanding the perturbations to methane, CO and OH and the concomitant impacts on climate. We implemented the ECCOH chemistry module into the NASA GEOS-5 Atmospheric Global Circulation Model (AGCM), performed multiple sensitivity simulations of the CH₄-CO-OH system over two decades, and evaluated the model output with surface and satellite datasets of methane and CO. The favorable comparison of output from the ECCOH chemistry module (as configured in the GEOS-5 AGCM) with observations demonstrates the fidelity of the module for use in scientific research.

1 Introduction

The coupled methane - carbon monoxide - hydroxyl radical (CH₄-CO-OH) system is nonlinear (e.g., Prather, 1994) and important in determining the atmosphere's oxidizing capacity (e.g., Chameides et al., 1976). Methane is the second most important anthropogenic greenhouse gas (GHG), though its 100-year global warming potential (GWP) is 34 times larger than that for carbon dioxide (CO₂; Myhre et al., 2013). Methane is responsible for about 20% of the warming induced by long-lived GHG's since pre-industrial times (Kirschke et al., 2013). The CH₄-CO-OH system has implications for tropospheric ozone and, subsequently, air quality (e.g., Fiore et al., 2002). A thorough understanding of historical methane, CO and OH trends and variations is necessary to credibly predict future changes and their climate feedback, as well as, to develop strategic national and international emission reduction policies.

The major limitation of forward modeling studies of trends and variability in the CH₄-CO-OH system is the computational expense associated with simulating ozone-nitrogen oxides-volatile organic compounds (O₃-NO_x-VOC) photochemistry for the determination of OH, particularly since perturbations to relatively long-lived methane (~8-10 y) can take several

Yasin Elshorbany, G..., 1/19/2016 1:03 PM

Deleted: .

Yasin Elshorbany, G..., 1/19/2016 1:03 PM

Deleted: .

44 decades to fully evolve (e.g., Prather, 1996). There are few forward modeling studies in the
45 literature that carry a full representation of O₃-NO_x-VOC chemistry, and they necessarily
46 present a limited number of sensitivity simulations (e.g., Fiore et al., 2006; Voulgarakis et
47 al., 2015).

48 To overcome this computational expense, global modeling communities often use archived
49 and annually-repeating monthly OH fields to simulate the oxidation of methane and CO. In
50 the TransCom methane model intercomparison project (MIP), archived and annually-
51 repeating OH fields were used from a climatology (Spivakovsky et al., 2000). Wang et al.
52 (2004) used archived and annually-varying OH fields from Duncan et al. (2007a) to explain
53 the causes of observed interannual variations in methane and the observed slowdown in its
54 growth rate from 1988 to 1997.

55 Limitations of using archived, monthly OH fields for studies of methane's and CO's
56 evolution are that feedbacks of the CH₄-CO-OH system on methane, CO and OH are not
57 captured as the losses of methane and CO by reaction with OH are assumed to be linearly
58 proportional to the OH fields. For methane, this assumption is not desirable, particularly on
59 multi-decadal time-scales (e.g., Prather, 1996). Chen and Prinn (2006) found that using an
60 archived, annual cycle of OH may mask or bias the interannual changes of methane. For
61 relatively short-lived CO (~1-2 months), this assumption is not valid given the strong
62 feedback between CO and OH (e.g., Duncan and Logan, 2008; Voulgarakis et al., 2015). If a
63 multi-decadal simulation of methane or CO using archived and annually-repeating OH
64 reproduces observations, then there must be some compensating factor, for example a bias in
65 emissions. That is, the simulation reproduces observations, but for the wrong reason. The
66 models in the TranCom MIP adjusted down (by 8%) the archived OH climatology of
67 Spivakovsky et al. (2000) so that the simulated decline in the global, atmospheric
68 methylchloroform (MCF) concentration since 2000 better matched that observed (Patra et al.
69 2011). Adjusting archived OH to improve a simulation of MCF, methane and/or CO makes
70 the specious assumption that emissions inventories, model dynamics, etc. used in the
71 simulation are correct. If using archived and annually-repeating OH, whether adjusted or
72 not, inverse modeling studies of methane and CO will incorrectly determine a posteriori
73 fluxes as the impact of nonlinear feedbacks of the CH₄-CO-OH system on concentrations
74 will be erroneously folded into the flux estimates. Therefore, there is a need for a
75 computationally-efficient solution to simulate credible temporal and spatial distributions of
76 OH over several decades, while capturing the nonlinear feedbacks of the CH₄-CO-OH
77 system.

78 In this manuscript, we present and validate the new, computationally-Efficient CH₄-CO-
79 OH (ECCOH; pronounced like "echo") chemistry module to interactively simulate the
80 chemistry of the CH₄-CO-OH system within a chemistry-climate model, carbon cycle model,
81 or Earth System Model. The computational efficiency of the ECCOH chemistry module
82 allows many sensitivity simulations of multiple decades to be performed, which is important
83 for capturing the nonlinear feedbacks of the CH₄-CO-OH system and understanding the
84 perturbations to methane and the concomitant impacts on climate. The ECCOH chemistry
85 module allows one to deconvolve the impacts of various causal factors (e.g., overhead ozone
86 column, NO_x, VOCs, water vapor, etc.) on OH and, subsequently, on methane and CO.
87 Therefore, this capability is valuable in determining these impacts, especially, given that

Yasin Elshorbany, G..., 1/15/2016 1:30 PM

Deleted: that was adjusted so that the methane growth rate matched that observed (Patra et al, 2011)

91 simulated OH varies widely between models (Shindell et al., 2006; Fiore et al., 2009) for a
92 variety of reasons, including differences in the causal factors that influence OH (Shindell et
93 al., 2006). For instance, Voulgarakis et al. (2013) found that simulated tropospheric methane
94 lifetimes of various models ranged from ~7 to ~14 years; this spread is similar to that
95 calculated by Shindell et al. (2006) and Fiore et al. (2009), even when all participating
96 models used identical methane abundances and CO emissions (Shindell et al., 2006).
97 Shindell et al. (2006) related the wide spread of simulated CO between models to the large
98 spread in simulated OH. Furthermore, simulated OH from full chemistry mechanisms in
99 global models is still highly uncertain because of incomplete knowledge and representation
100 of OH sources, sinks and recycling (e.g., Elshorbany et al., 2010, 2012a, 2012b, 2014; Stone
101 et al., 2012). For example, 1) nitrous acid (HONO) is typically underestimated in models by
102 an order of magnitude (Elshorbany et al., 2012b), which can lead to a significant
103 underestimation of OH, especially in urban high-NO_x regions; 2) in unpolluted, forested
104 environments, significant discrepancies exist between models and measurements (Stone et
105 al., 2012); and 3) Patra et al. (2014) indicate that the inter-hemispheric OH ratio (northern to
106 southern hemisphere) is near unity, while a recent model inter-comparison had a multi-model
107 average of about 1.3.

108 The manuscript is organized as follows: In Sect. 2, we 1) describe the ECCOH chemistry
109 module as implemented in the NASA Goddard Earth Observing System, Version 5
110 Atmospheric General Circulation Model (GEOS-5 AGCM), and 2) and describe a series of
111 simulations, which we refer to as “scenarios” hereafter, to illustrate the utility of the ECCOH
112 module for understanding the influence of various factors on the observed spatial
113 distributions and temporal evolution of methane, CO, and OH. In Sect. 3, we show that the
114 simulated trends and variations of methane and CO in our reference scenario agree well with
115 in situ and satellite measurements. In Sect. 4, we demonstrate the ability of the ECCOH
116 chemistry module to capture the nonlinear chemistry of the CH₄-CO-OH system with output
117 from our sensitivity scenarios.

118 **2 Technical Approach and Methodology**

119 **2.1 Description of the ECCOH Chemistry Module and Its Implementation**

120 The ECCOH chemistry module is composed of a parameterization of tropospheric OH and
121 tracers of methane and CO as shown in Fig. 1. The advantage of the ECCOH chemistry
122 module over a full representation of O₃-NO_x-VOC chemistry is computational
123 efficiency. The computational cost of simulating tropospheric OH is reduced by about a
124 factor of 500 when the full O₃-NO_x-VOC chemistry is replaced by the parameterization of
125 OH (Duncan et al., 2000). This computationally-efficient parameterization of OH allows 1)
126 for many multi-decadal model sensitivity simulations to be performed and 2) one to
127 deconvolve the impact of various factors on the observed trends and variability in methane
128 and CO. It is based on the method described by Spivakovsky et al. (1990a), who developed
129 an earlier version of the parameterization of OH used in several studies, including
130 Spivakovsky et al. (1990b) and Prather and Spivakovsky (1990). The parameterization of
131 OH of Duncan et al. (2000) is designed to simulate OH over the range of photochemical
132 environments found throughout the troposphere, including a wide enough range so as to be

133 applicable to preindustrial, present day and possible future conditions (Duncan et al., 2000).
134 It has been implemented into two host atmospheric models and has been used in several
135 studies of the nonlinear feedbacks of CO and OH (Duncan et al., 2007a; Duncan and Logan,
136 2008; Strode et al., 2015).

137 The parameterization of OH accurately represents OH predicted by a full chemical
138 mechanism as a set of high-order polynomials that describe the functional relationship
139 between the concentration of OH and meteorological variables (i.e., pressure, temperature,
140 cloud albedo), solar irradiance variables (i.e., ozone column, surface albedo, declination
141 angle, latitude) and chemical variables, including CO and methane as well as nitrogen oxides
142 (as a family), ozone, water vapor, and various VOCs. That is, the 24-hour average OH is
143 calculated interactively in the model and responds to changes in the concentrations of trace
144 gases and meteorology. Input variables to the parameterization of OH may be taken from
145 archived fields from, for instance, an observational climatology or archived fields from a
146 model simulation with a full representation of trace gas and aerosol atmospheric chemistry,
147 and may be annually-repeating or annually-varying. Some variables (e.g., water vapor,
148 clouds) may be taken from the host model as the simulation progresses. Ideally, all input
149 variables should be annually-varying so as to best capture the nonlinear feedbacks of the
150 CH₄-CO-OH system. If one chooses to use output from a single computationally-expensive
151 full chemistry model simulation as input to the parameterization of OH, subsequent
152 sensitivity simulations using the ECCOH chemistry module will be far less computationally-
153 expensive relative to that single expensive simulation, which is the primary strength of using
154 the parameterization of OH. In Section 2.2, we discuss the setup of the simulations presented
155 in this study.

156 We adjust the OH from the parameterization to account for important updates in kinetic
157 information of O¹D reactions by water vapor, molecular nitrogen, and molecular oxygen
158 (Sander et al., 2011). These reactions are key as the primary production pathway (P) for OH
159 involves the formation of excited O¹D atoms by photolysis of ozone (O₃), followed by their
160 reaction with water vapor in competition with their collisional quenching by molecular
161 nitrogen and oxygen: $P = j[O_3] * 2k_1[H_2O] / (k_1[H_2O] + k_2[N_2] + k_3[O_2])$, where j is the
162 ozone photolysis rate and k_1 , k_2 and k_3 are the rate constants of O¹D reactions with water
163 vapor, nitrogen and oxygen, respectively. Typically, this adjustment decreases OH by 10-
164 30%, depending on altitude and season. Recent updates in isoprene chemistry are not
165 reflected in the parameterization of OH, so OH near the surface in clean, forested
166 environments (e.g., Amazon and Congo basins) is too low relative to current knowledge
167 (e.g., Fuchs et al., 2013). However, the contribution of these regions to global methane and
168 CO loss is small (i.e., < 1%) and the current knowledge of isoprene photochemistry is still
169 highly uncertain (Fuchs et al., 2013). Ultimately, the parameterization of OH reflects
170 uncertainties in the chemistry upon which it is based, as do the photochemical mechanisms
171 in all atmospheric chemistry models (e.g., Stone et al., 2012; Fuchs et al., 2013). The losses
172 of methane and CO in the ECCOH chemistry module are determined by their reaction with
173 tropospheric OH. Additional losses of methane in the stratosphere occur by reactions with
174 OH, Cl and O¹D, whose distributions are simulated using archived and annually-repeating
175 monthly fields.

176 We implemented the ECCOH chemistry module into the Goddard Earth Observing

Yasin Elshorbany, ..., 12/28/2015 2:02 PM

Deleted: It was designed to be applicable to preindustrial, present day and possible future conditions (Duncan et al., 2000) and has been used in several studies of CO and OH (Duncan et al., 2007a; Duncan and Logan, 2008, and Strode et al., 2015).

Yasin Elshorbany, G..., 1/15/2016 1:54 PM

Deleted: in

Yasin Elshorbany, ..., 12/28/2015 1:51 PM

Deleted:

Yasin Elshorbany, G..., 1/20/2016 4:27 PM

Deleted: and photolytic

Yasin Elshorbany, G..., 1/15/2016 1:46 PM

Deleted: ,

187 System, Version 5 Atmospheric General Circulation Model (GEOS-5 AGCM, Fortuna
188 version, Rienecker et al., 2008; Pawson et al., 2008; Ott et al., 2010; Molod et al., 2012).
189 The AGCM combines the finite volume dynamical core described by Lin (2004) with the
190 GEOS-5 column physics package, as summarized by Rienecker et al. (2008). The AGCM
191 domain extends from the surface to 0.01 mb and uses 72 hybrid layers that transition from
192 terrain following near the surface to pure pressure levels above 180 mb. We use a horizontal
193 resolution of 2° latitude × 2.5° longitude and the time step is 30 minutes for physical
194 computations.

195 2.2 Description of the Reference and Sensitivity Scenarios

196 To demonstrate the utility of the ECCOH chemistry module for multi-decadal studies, we
197 performed several model simulations using the module in the GEOS-5 AGCM (Table 1 and
198 Table 2). The model setup (i.e., emissions, input to the parameterization of OH, and
199 dynamics) of the reference scenario, which we refer to as the *Base* scenario, is detailed in
200 Table 1. Compared to the sensitivity scenarios described in Table 2, the *Base* scenario is the
201 least complex. For example, all CO emissions and natural methane emissions are for one
202 year that are repeated for each year of the simulation (1988-2007); therefore, interannual
203 variations in methane and CO levels caused by variations in these emissions will not be
204 captured in the *Base* scenario. However, there are two important sources of variability that
205 are included in the *Base* scenario. First, the dynamics are constrained by varying sea surface
206 temperatures and sea ice concentrations. Therefore, the *Base* scenario will capture variations
207 in methane, CO, and OH resulting from meteorological variations, such as those associated
208 with the El Niño Southern Oscillation (ENSO). In addition, atmospheric temperature,
209 pressure and specific humidity are calculated online by the GEOS-5 AGCM and are fed into
210 the parameterization of OH as the runs progress, so interannual variations in water vapor,
211 temperature, and cloud cover are also included in the *Base* scenario. These factors are known
212 to influence variations in OH and thus CO and methane (e.g., Holmes et al., 2013). Second,
213 interannual variations in anthropogenic methane sources are included in the *Base* scenario. In
214 Sect. 3, we evaluate model output from the *Base* scenario with the observational datasets
215 described in Table 3.

216 We present the results of our sensitivity scenarios in Sect. 4. We explore the influence of
217 several causal factors on the observed spatial distributions and temporal evolutions of
218 methane, CO, and OH. These causal factors include annually-varying methane and CO
219 emissions (i.e., Scenarios 2-4 in Table 2; natural methane emissions, and anthropogenic and
220 natural CO emissions, Figs. S1 and S2 in the Supplement) and annually-varying input
221 variables to the parameterization of OH (i.e., Scenario 5 in Table 2).

222 3 Evaluation of the *Base* Scenario

223 We evaluate the model output of methane and CO from the *Base* scenario with satellite
224 and in situ observations (Table 3). We also compare simulated OH with that from a GEOS-5
225 AGCM simulation (with a full representation of O₃-NO_x-VOC chemistry (Strode et al.,
226 2015)). We highlight where the *Base* scenario's simplicity results in a poor or satisfactory
227 comparison of the model output with the observed temporal and spatial distributions of

Yasin Elshorbany, G..., 1/19/2016 1:09 PM

Deleted: hPa

Yasin Elshorbany, G..., 1/19/2016 1:09 PM

Deleted: hPa

Yasin Elshorbany, ..., 12/28/2015 4:09 PM

Deleted: Table 1

Yasin Elshorbany, ..., 12/28/2015 4:09 PM

Deleted: Table 2

Yasin Elshorbany, ..., 12/28/2015 4:09 PM

Deleted: Table 1

Yasin Elshorbany, ..., 12/28/2015 4:09 PM

Deleted: Table 3

Yasin Elshorbany, ..., 12/28/2015 3:50 PM

Deleted: These causal factors include annually-varying emissions (i.e., natural methane emissions, anthropogenic and natural CO emissions, Fig. S 1 and Fig. S 2) and input variables to the parameterization of OH (

Yasin Elshorbany, ..., 12/28/2015 4:09 PM

Deleted: Table 2

Yasin Elshorbany, ..., 12/28/2015 4:09 PM

Deleted: Table 3

Yasin Elshorbany, G..., 1/19/2016 1:10 PM

Deleted: is

242 methane, CO, and OH. We demonstrate that the ECCOH chemistry module for this scenario
243 reasonably captures the distributions of methane and CO, within the limitations of this
244 scenario, as compared to measurements and other model studies (e.g., Shindell et al. 2006;
245 Patra et al., 2011; Naik et al., 2013).

246 3.1 Tropospheric OH

247 There are very few direct observations of OH with which to constrain models (e.g., Stone
248 et al., 2012) and none on regional or global scales. Therefore, the MCF lifetime inferred
249 from measurements serves as a widely used, indirect proxy for global OH abundance (e.g.,
250 Lawrence et al., 2001). Though useful, the MCF lifetime gives an incomplete description of
251 the spatial and vertical distributions of OH (e.g., Lawrence et al., 2001) and there are
252 uncertainties concerning MCF emissions and the resulting lifetime estimate (e.g., Wang et
253 al., 2008). Nevertheless, the MCF data have been recently used to infer the ratio of OH in the
254 Northern to the Southern Hemisphere (Patra et al., 2014).

255 Despite the challenges concerning OH, we show in this section that the spatial and vertical
256 distributions of simulated global mean OH (Fig. 2 and Fig. 3) from the *Base* scenario are
257 reasonable relative to the MCF proxy for OH as well as to simulated OH from other models.
258 Related to the OH dependency on UV radiation (Rohrer and Berresheim, 2006), the
259 maximum and minimum OH levels at any given location occur in local summer and winter,
260 respectively (Fig. 2). OH maximizes around 600 mb, because of vertical dependencies of the
261 main sources and sinks of OH (Spivakovsky et al., 1990). The seasonal and vertical
262 distributions of the zonal mean OH in the *Base* scenario are quite comparable to the OH
263 climatology of Spivakovsky et al. (2000, see Figure 6 of Spivakovsky et al.), despite the
264 different inputs given to the parameterization of OH in the two studies.

265 The interannual variations in global OH (given by the annual mean standard deviation, not
266 shown) are small (<5%) and mainly related to meteorological variations (e.g., water vapor,
267 clouds, temperature, and transport) as annually-repeating emissions are used in the *Base*
268 scenario, except for anthropogenic methane emissions (Table 1, Fig. S 1, Fig. S 2). This
269 result is consistent with Voulgarakis et al. (2013) who show that OH has the strongest
270 relationship with changes in temperature and humidity when emissions do not vary
271 interannually. As discussed in Sect. 4, we see considerably larger variations in OH in several
272 of our more complex sensitivity simulations, which have interannual variations in methane
273 and CO emissions as well as in factors that affect OH.

274 Over our simulation period, the range of annual mean, atmospheric MCF lifetimes is
275 6.08 ± 0.60 to 6.53 ± 0.65 years with respect to loss by reaction with tropospheric OH for the
276 *Base* scenario, assuming a MCF uniform mixing ratio. Our lifetimes are similar to values
277 reported in the literature (e.g., $6.0^{+0.5}_{-0.4}$ years (Prinn et al., 2005); multi-model mean of
278 5.7 ± 0.9 years (Naik et al., 2013); 6.3 ± 0.9 years (Prather et al., 2012)). The global, annual
279 mean lifetime of methane with respect to tropospheric OH ranges from 10.10 ± 1.06 to
280 10.86 ± 1.15 years. These values are similar to those inferred from measurements (e.g.,
281 $10.2^{+0.9}_{-0.7}$ years (Prinn et al., 2005)) as well as to those reported in previous multi-model
282 comparison studies (e.g., 9.7 ± 1.7 years (Shindell et al., 2006); 10.19 ± 1.72 years (Fiore et al.,
283 2009); 9.7 ± 1.5 years (Naik et al., 2013)). The lifetime of methane is calculated by dividing

Yasin Elshorbany, G..., 1/19/2016 1:10 PM

Deleted: methylchloroform (

Yasin Elshorbany, G..., 1/19/2016 1:10 PM

Deleted:)

Yasin Elshorbany, G..., 12/4/2015 2:44 PM

Deleted: ,

Yasin Elshorbany, G..., 12/4/2015 2:44 PM

Deleted: ,

Yasin Elshorbany, G..., 1/19/2016 1:11 PM

Deleted: hPa

Yasin Elshorbany, ..., 12/28/2015 4:10 PM

Deleted: spatial

Yasin Elshorbany, ..., 12/28/2015 4:14 PM

Deleted: of

Yasin Elshorbany, ..., 12/28/2015 4:15 PM

Formatted: No underline

Yasin Elshorbany, G..., 1/19/2016 1:33 PM

Deleted: overall

Yasin Elshorbany, ..., 12/28/2015 4:09 PM

Deleted: Table 1

Yasin Elshorbany, ..., 12/1/2015 12:38 PM

Deleted: in

Yasin Elshorbany, ..., 12/1/2015 12:37 PM

Deleted: (

295 the total atmospheric burden by the tropospheric methane loss rate (e.g., Fiore et al., 2009).
296 We also compare our simulated OH with that from a GEOS-5 AGCM simulation that
297 carries a full representation of O₃-NO_x-VOC chemistry. This simulation was included in the
298 Atmospheric Chemistry and Climate Model Intercomparison Project (ACCMIP, Lamarque et
299 al., 2013; the model is designated as “GEOSCCM”). Henceforth, we refer to this simulation
300 as the “ACCMIP simulation”. The same CO emissions (annually-repeating emissions for
301 year 2000) are used in both the *Base* and ACCMIP simulations, but there are differences
302 between the simulations (e.g., model dynamics, prescribed methane, etc.). Despite these
303 differences, we find that the spatial and vertical distributions of OH are quite similar with
304 differences generally less than 10% (Fig. S 17). The global, mean tropospheric OH in the
305 *Base* scenario of 10.9x10⁵ molecules cm⁻³ also compares well with that of 11.4x10⁵
306 molecules cm⁻³ from the ACCMIP simulation (the 2000 time slice) as well as within the
307 range of means from other models (e.g., 6.5 – 13.4 x10⁵ molecules cm⁻³ (Voulgarakis et al.,
308 2013)).

309 3.2 Methane

310 *GMD surface data:* We evaluate our simulated surface distributions of methane with data
311 from the NOAA Global Monitoring Division (GMD) network. The simulated, interannual
312 variation of methane’s global growth rate agrees reasonably well ($R^2 = 0.44$) with that
313 estimated from GMD data, using all available data from 92 stations over the simulation
314 period 1988-2007 (Fig. 4a). The agreement of model output with observations is worse (R^2
315 = 0.33) when we only use the 17 stations that cover the entire simulation period (Fig. 4b).
316 We decided to include all 92 stations, even those without records that cover the entire
317 simulation period, as we are able to nearly reproduce Fig. 4a using 46 stations that have at
318 least 75% data coverage (not shown). A relatively high correlation coefficient ($R^2 = 0.44$)
319 implies that interannual variations in anthropogenic methane emissions and dynamics
320 explain much of methane’s growth rate over the study period, which is consistent with the
321 findings of the TransCom MIP (Patra et al., 2011).

322 Overall, the comparison of model output and data at individual GMD stations is favorable.
323 Fig. 5 to Fig. 7 show comparisons for monthly averages, seasonal averages, and annual
324 differences, respectively, at six GMD stations, which were chosen as they have long time
325 records and cover a wide range of latitudes. Over the simulation period (1988-2007), the
326 correlation slope (S) and coefficient (R^2) for these six stations (Table 4) range from 0.56 to
327 0.79 and from 0.58 to 0.91, respectively.

328 There are two important features of the observations that are not simulated in the *Base*
329 scenario. First, the *Base* scenario overestimates methane concentrations by 20-30 ppbv at
330 the northern high latitude stations of Alert and Barrow during the 1980s and 1990s (Fig. 5-
331 Fig. 7). The overestimation of methane in the northern hemisphere during the 1990s occurs
332 because of regional high biases in natural methane emissions (Fig. S 1 and Patra et al., 2011).
333 As shown in Sect. 4.3, simulated methane improves significantly in the northern hemisphere
334 in the *E_{CH4}Vary* scenario, which includes annually-varying natural methane emissions.
335 Second, the *Base* scenario captures the increasing observed methane trend in the 1990s, but
336 under-predicts methane in the 2000’s (Fig. 7). Both of these features (i.e., high bias at high

Yasin Elshorbany, ..., 12/28/2015 4:09 PM
Deleted: Fig. S 23

Yasin Elshorbany, ..., 12/28/2015 6:08 PM
Deleted: (Table 3)

Yasin Elshorbany, G..., 12/8/2015 4:56 PM
Formatted: Superscript

Yasin Elshorbany, ..., 1/11/2016 12:10 PM
Deleted: Fig.

Yasin Elshorbany, ..., 1/14/2016 10:49 AM
Deleted: This result

Yasin Elshorbany, G..., 1/20/2016 4:28 PM
Deleted: model intercomparison project

Yasin Elshorbany, G..., 1/20/2016 4:29 PM
Deleted: T

Yasin Elshorbany, ..., 12/28/2015 4:09 PM
Deleted: Table 4

Yasin Elshorbany, G..., 1/19/2016 2:04 PM
Deleted: and Fig. S 7

345 northern latitudes in the 1990's and low bias in the 2000's) are consistent with the findings
 346 of the TransCom [MIP](#) that used the same methane emissions ([Table 1](#) and Patra et al., 2011).
 347 *SCIAMACHY methane*: We compare the simulated methane dry columns to those from
 348 *SCIAMACHY* ([Table 3](#), [Fig. 8](#)). The data have the best global spatial coverage during boreal
 349 summer because of lower cloud cover during this season (Schneising et al., 2011). The
 350 observed methane dry columns reach their highest levels during boreal summer and fall,
 351 maximizing over Asia (eastern China and northern India) because of high emissions from
 352 wetlands and rice paddies. The *Base* scenario reproduces the spatial distribution of the data
 353 well with a bias of < 2% over most of the globe, except over eastern Asia and western US
 354 during boreal summer where it is biased low, but still within the measurement uncertainties
 355 (~7-10%; Gloude-mans et al., 2008; Houweling et al., 2014). Houweling et al. (2014)
 356 demonstrate that *SCIAMACHY* data have a seasonal bias that ranges from about -50 ppb
 357 during boreal winter to about +50 ppb during boreal summer as compared to the Total
 358 Carbon Column Observing Network (TCCON) measurements, which may also explain the
 359 simulated seasonal biases ([Fig. 8](#)).

360 3.3 CO

361 *GMD surface data*: The *Base* scenario captures the monthly variability of GMD CO data
 362 well with a mean correlations slope (S) and coefficient (R²) of 0.81 and 0.72, respectively
 363 ([Fig. 9](#) to [Fig. 11](#), [Table 4](#)). This result indicates that the seasonal CO cycle is well captured
 364 in the *Base* scenario ([Fig. 11](#)), which includes annually-repeating, but seasonally-varying
 365 biomass burning emissions ([Fig. S 2](#)). As expected, the *Base* scenario does not capture the
 366 significant interannual variations associated with strong variations in emissions ([Fig. 9](#), [Fig.](#)
 367 [10](#)). The low biases reach ~40 ppb in boreal winter and spring at high northern latitudes.
 368 During the 1980's and 1990's, CO levels in the northern hemisphere declined substantially
 369 because of changing patterns of emissions (Duncan et al., 2007a), which is not simulated
 370 with annually-repeating CO emissions. These results are in agreement with the findings of
 371 the multi-model ACCENT study (using annually-repeating CO emissions), in which there
 372 was a low bias of ~50 ppbv at northern hemisphere high latitude stations (Shindell et al.,
 373 2006), as well as with other recent studies (e.g., Monks et al., 2015).

374 *MOPITT and TES/MLS CO*: The primary advantage of satellite data, above ground-based
 375 networks, is spatial coverage, so we compare the spatial and seasonal distributions of
 376 simulated CO with those from the MOPITT and TES/MLS instruments ([Fig. 12](#), [Fig. 13](#)).
 377 The distributions of CO from the *Base* scenario compare well overall with the data. The
 378 mean biases relative to both datasets are within ±10% over most of the globe and in all
 379 seasons. For example, the seasonal correlation slopes (S) range from 0.75 to 0.98 and
 380 coefficients (R²) range from 0.80 to 0.98, respectively, between MOPITT, TES/MLS data
 381 and the *Base* scenario output with the agreement generally highest during boreal winter and
 382 lowest during boreal summer. However, the largest biases ([Fig. 12](#)) occur over 1) **tropical**
 383 **and subtropical** biomass burning regions (~20%) during boreal winter, indicating that either
 384 the CO emissions used in the *Base* scenario are too high or that simulated OH is too low, and
 385 2) most of the northern hemisphere (< -20%) during the summer season, indicating that
 386 either CO emissions are too low or that OH levels are too high, which is consistent with

Yasin Elshorbany, G..., 1/20/2016 4:30 PM
 Deleted: model intercomparison project
 Yasin Elshorbany, ..., 12/28/2015 4:09 PM
 Deleted: Table 1
 Yasin Elshorbany, ..., 12/28/2015 4:09 PM
 Deleted: Table 3
 Yasin Elshorbany, ..., 12/28/2015 4:09 PM
 Deleted: Fig. 8
 Yasin Elshorbany, G..., 1/20/2016 5:35 PM
 Formatted: Font:Times New Roman, Font color: Text 1
 Yasin Elshorbany, G..., 1/20/2016 5:35 PM
 Formatted: Font:Times New Roman
 Yasin Elshorbany, G..., 1/19/2016 2:04 PM
 Deleted: s

Yasin Elshorbany, ..., 12/28/2015 4:09 PM
 Deleted: Table 4

Yasin Elshorbany, G..., 1/19/2016 2:46 PM
 Deleted: (Fig. S 13)

Unknown
 Field Code Changed

Yasin Elshorbany, G..., 1/19/2016 2:52 PM
 Deleted: (Fig. S 15 and Fig. S 17)

Yasin Elshorbany, G..., 1/19/2016 2:53 PM
 Deleted: and

Unknown
 Field Code Changed

Yasin Elshorbany, G..., 1/19/2016 2:53 PM
 Deleted:)

Yasin Elshorbany, GS..., 1/4/2016 1:26 PM
 Formatted: No underline

397 previous studies using similar emissions (e.g., Shindell et al., 2006; Strode et al., 2015). In
398 addition to possible biases associated with emissions, some of the model-observation
399 discrepancies may be associated with uncertainties in the satellite datasets (Ho et al., 2009;
400 Deeter et al., 2012; Amnuaylojaroen et al., 2014). Based on direct comparison with Tall
401 Tower measurements, Deeter et al. (2012) find that a smoothing error, which depends on the
402 retrieval averaging kernels and CO variability in the lower troposphere, exhibits strong
403 geographical and seasonal variability. Amnuaylojaroen et al. (2014) find that simulated CO
404 concentrations are significantly and consistently higher than that of MOPITT V6 data over
405 areas of biomass burning in Southeast Asia, similar to our results.

406 The primary advantage of the TES/MLS joint CO product is that it gives information on
407 vertical distributions (Fig. 13). The simulation captures the tropospheric vertical profiles
408 reasonably well (within $\pm 1\sigma$ of TES/MLS mean) at the selected locations in the northern and
409 southern hemispheres and in all seasons, except over West Africa in boreal winter during the
410 peak of biomass burning. The adjustment of the simulated CO with the TES/MLS averaging
411 kernel (AK) significantly improves the agreement above 300 mb, over all locations and in all
412 seasons while near the surface the effect is geographically varying, in agreement with other
413 studies (e.g., Deeter et al., 2012). Over the eastern US, the adjustment of simulated CO
414 causes a slightly larger positive bias compared to that without adjustment. Though simulated
415 CO is significantly improved near the surface, it is still biased high over West Africa by
416 ~50% during the peak of biomass burning, also consistent with other studies
417 (Amnuaylojaroen et al., 2014).

418 **4 ECCOH as a Tool for Studying the Nonlinear CH₄-CO-OH System**

419 In this section, we 1) present the justification for simulating the nonlinear chemistry of the
420 CH₄-CO-OH system as opposed to using a static climatology of OH distributions, and 2)
421 demonstrate the utility of the ECCOH chemistry module for studying the CH₄-CO-OH
422 system. In Sect. 4.1, we discuss the nontrivial, large-scale interannual variations of methane,
423 CO, and OH in our scenarios. In Sect. 4.2, we discuss the considerable spatial and temporal
424 heterogeneity of OH and methane and CO loss rates, which would not be captured if a static
425 climatology of OH distributions was used. In Sect. 4.3, we present the results of our
426 sensitivity scenarios (Table 2), which demonstrate the utility of the ECCOH chemistry
427 module for studying the CH₄-CO-OH system.

428 **4.1 Large Scale Interannual Variations in Methane, CO, and OH**

429 Even on a global scale, there are large interannual variations in methane, CO, and OH.
430 The deviations of mass-weighted concentrations of methane, CO, and OH for both the *Base*
431 and *AllVary* scenarios are shown in Fig. 14. The magnitudes of the year-to-year deviations in
432 methane are not substantially different between the two scenarios, since the *Base* scenario
433 includes the important source of variation associated with anthropogenic methane emissions
434 and methane's background is large. On the other hand, the deviations for CO and OH are far
435 greater in the *AllVary* scenario. The magnitude of the CO deviations is a factor of ten greater
436 in the *AllVary* scenario than the *Base* scenario, which has annually-repeating CO emissions.
437 The magnitude of the OH deviations increase $\pm 2\%$ to $\pm 5\%$, though as discussed below, there

Yasin Elshorbany, G..., 1/19/2016 2:55 PM

Deleted: hPa

Yasin Elshorbany, G..., 1/20/2016 4:30 PM

Deleted:

Yasin Elshorbany, G..., 1/20/2016 4:30 PM

Deleted: 4.1

Yasin Elshorbany, ..., 12/28/2015 4:09 PM

Deleted: Table 2

442 are much larger variations on regional scales that are masked in the global average. In
443 general, CO and OH deviations are coincident, but of opposite sign as reaction of CO with
444 OH is the primary sink for both gases on a global scale. Similar deviations are seen in the
445 mid-latitudes of both hemispheres, indicating the global extent of some specific events, such
446 as large biomass burning events. These results are also consistent with Voulgarakis et al.
447 (2015) who, using full chemistry simulations, found large deviations ($> 15\%$) in CO using
448 annually-varying CO biomass burning emissions as compared to annually-repeating
449 emissions.

450 The nonlinear effects of the CH₄-CO-OH system on the temporal evolution of global
451 mass-weighted methane are smaller, but significant, as compared to the effects of variations
452 of methane emissions. The *E_{CH₄Vary}* scenario includes variations in anthropogenic and
453 natural methane emissions and also variations in meteorology (e.g., temperature, water
454 vapor) that influence the distributions of methane, CO, and OH. The *AllVary* scenario
455 includes also variations in CO emissions and all the other factors that influence OH, such as
456 the overhead ozone column, NO_x, tropospheric ozone, and VOCs. The influence of the
457 nonlinear effects of the CH₄-CO-OH system is shown in the difference of the *AllVary* and
458 *E_{CH₄Vary}* scenarios. For example, the shaded area between the two scenarios in Fig. 4
459 illustrates the combined effect of nonlinearities of the CH₄-CO-OH system on methane's
460 growth rate. The growth rate in the *AllVary* scenario is about 4 ppb/yr higher than in the
461 *E_{CH₄Vary}* scenario during the early 1990s, a time when stratospheric ozone was impacted by
462 the eruption of Mt. Pinatubo, emissions from the Soviet Union changed as it contracted
463 economically, and there was a prolonged El Niño. While these factors caused changes in
464 methane emissions, they also caused substantial variations in CO and OH (Duncan and
465 Logan, 2008) that influenced methane's growth rate. Briefly in the mid-1990s, the growth
466 rate in the *AllVary* scenario becomes lower than in the *E_{CH₄Vary}* scenario. The decline in
467 methane growth rate in 1994-1997 is primarily related to the variability of the factors that
468 influence OH (Fig. S 4) while the other non-linear feedbacks are primarily related to
469 variability in CO emissions (Fig. S 5). Worldwide, there were record wildfires in 1997 and
470 1998 that were associated with a record El Niño, which began in 1997, that transitioned to a
471 record La Niña in 1998 (Duncan et al., 2003a, 2003b). Consequently, there were large
472 variations in CO (Duncan and Logan, 2008) that causes methane's growth rate to become
473 higher again in the *AllVary* scenario. During the 2000s, a relatively quiet period with few
474 large wildfires or notable ENSO events, the growth rate is lower in the *AllVary* than the
475 *E_{CH₄Vary}* scenario. In summary, the nonlinear effects of the CH₄-CO-OH system cause
476 important fluctuations in methane's growth rate over our study period of ± 4 ppb/yr.

477 We compare simulated, mass-weighted pseudo first order rate constants (k'), a proxy for
478 OH interannual variations, from each of our scenarios to that inferred from MCF
479 measurements (Fig. 15; 1998-2007; Montzka et al., 2011). We find that none of our model
480 scenarios are able to reproduce the inferred interannual OH variability of Montzka et al.
481 (2011), though the simulated variability is of similar magnitude and within observational
482 uncertainty. Our findings are consistent with other modeling studies (Montzka et al., 2011;
483 Holmes et al., 2013; Murray et al., 2013 and references therein). While global interannual
484 variations are informative, there can be considerable OH interannual variations regionally (as
485 discussed in Sections 4.2 and 4.3) that may not be reflected in the global average (Lelieveld

Yasin Elshorbany, G..., 1/19/2016 2:55 PM

Deleted: (not shown)

Yasin Elshorbany, G..., 1/12/2016 1:51 PM

Deleted: and OH

488 et al., 2002; Wild and Palmer, 2008).

489 Despite the lack of agreement between the inferred and simulated OH variations, this
490 comparison exercise allows us to understand the contribution of various factors to the
491 simulated interannual variations of tropospheric OH and, subsequently, the growth rate of
492 methane (Fig. 4). As shown in Fig. 15, the *Base* scenario has $\pm 3\%$ interannual variability.
493 This scenario includes interannual variations in meteorology, such as in clouds, water vapor,
494 temperature and solar radiation, which are known to be important drivers of OH (e.g., Rohrer
495 and Berresheim, 2006; Rohrer et al., 2014). The only large deviation in OH from the *Base*
496 scenario occurs in 1997 and 1998 in the *BBE_{CO}Vary* scenario. There were several major
497 wildfires that account for this deviation, including fires in Indonesia, Mexico, and the boreal
498 forests of Asia and North America (e.g., Duncan et al., 2003a). OH is lower in the *AllVary*
499 scenario than the *Base* scenario because of higher CO emissions from the fires. For instance,
500 Duncan et al. (2003b) used a model to show that the Indonesian wildfires in 1997 depressed
501 OH levels by more than 20% over the Indian Ocean and 5-10% over much of the tropics for
502 several months. Lower OH during 1997 and 1998 in the *AllVary* scenario is consistent with
503 the higher methane growth rate as compared to the *Base* scenario (Fig. 3).

504 ENSO affects the variability of sea surface temperatures, water vapor, deep convection,
505 etc., and, subsequently, OH over large regions of the tropics. As shown in Fig. 16, the
506 deviations of mass-weighted OH from various scenarios over Indonesia (100°-150°E; 6°N-
507 6°S) are generally anti-correlated with the Multivariate ENSO Index (MEI, Wolter et al.,
508 2011), a proxy of ENSO. OH variations in the *Base* scenario, which includes meteorological
509 variations that affect OH via variations in water vapor, clouds, etc., are $\pm 4\%$ ($R_s^2 = 0.20$), but
510 much higher in the scenarios that include variations in biomass burning emissions (e.g.,
511 *AllVary* scenario), which better capture the ENSO variability ($R_s^2 = 0.59$).

512 4.2 Spatial and Temporal Distributions of the Production/Loss Rates of 513 Methane and CO

514 Any model simulation using annually-repeating and archived OH will not accurately
515 capture regional and interannual variations in the loss rates of methane and CO. A
516 simulation using zonally-averaged archived OH (e.g., Spivakovsky et al., 2000), such as was
517 done in the TransCom MIP, will not capture any regional and interannual variations. For
518 example, Fig. S 7 and Fig. S 12 reproduce Fig. 4a and Fig. 5, respectively, but include
519 methane from a simulation using archived and annually-repeating OH of the NASA Global
520 Modeling Initiative (GMI) model (Duncan et al., 2007b; Strahan et al., 2007). The simulated
521 longer methane lifetime (Fig. S 7), using archived OH, leads to an accumulation of methane
522 over the multi-decadal simulation. In this situation, the archived OH would need to be
523 adjusted higher to improve the simulation of methane as compared to observations.

524 Even though methane is relatively well mixed in the troposphere due to its long lifetime,
525 there is important spatial heterogeneity in methane's and CO's loss rates (Fig. 17 to Fig.
526 21), which is associated with the distribution of sources and reaction with OH, and changes
527 in the density of air with altitude. The global methane loss rate maximizes during boreal
528 summer and reaches a minimum during boreal winter (Fig. 17). Most methane loss occurs
529 between 30°S and 30°N (Fig. 17) since OH is most abundant in this region and methane's

Yasin Elshorbany, GS..., 1/4/2016 2:52 PM

Formatted: Superscript

Yasin Elshorbany, GS..., 1/4/2016 2:53 PM

Formatted: Font:Italic

Yasin Elshorbany, GS..., 1/4/2016 2:52 PM

Formatted: Superscript

Yasin Elshorbany, G..., 1/20/2016 8:16 AM

Formatted: Indent: First line: 0.16 cm

530 reaction with OH is temperature dependent (Sander et al., 2011). In addition, most loss
531 occurs near the surface despite higher OH in the mid-troposphere (Fig. 2) because of higher
532 methane mole fractions near the surface (e.g., ~3 % over Alaska, but higher over source
533 regions), the altitude dependence of air density, and the temperature dependence of the loss
534 rate (Fig. 18). Methane's loss rates in the *AllVary* scenario are relatively higher, especially
535 over biomass burning regions (Fig. 17) and have much higher spatial variability than in the
536 *Base* scenario (Fig. 19). In contrast to methane, a higher proportion of CO is lost at
537 northern hemisphere mid-latitudes as the CO loss rate is less temperature dependent than
538 methane's and the lifetime is shorter (Fig. 20). The CO loss rate also varies strongly with
539 altitude (not shown), similar to that of methane. The simulated seasonal mean loss rate of
540 CO from the *AllVary* scenario is also relatively higher over biomass burning regions but
541 lower over Asia (Fig. 20), and has much higher variability that reaches up to ~20%
542 compared to about 5% in the *Base* scenario (Fig. 21).

543 4.3 Factors that Influence the Nonlinear CH₄-CO-OH System

544 The differences in global abundances of CO and OH between our least complex (*Base*,
545 Table 1) and most complex (*AllVary*, Table 2) scenarios are substantial and their impact on
546 methane's evolution is nontrivial as discussed in Sect. 4.1 and 4.2. Therefore, model studies
547 of methane and/or CO, which use archived fields of OH distributions, will not capture these
548 important nonlinear feedbacks of the CH₄-CO-OH system (e.g., Fig. 4). Here, we discuss the
549 contribution of various factors to the observed spatial distributions and temporal evolution of
550 observed methane, CO, and OH to demonstrate the utility of the ECCOH chemistry module
551 for studying the CH₄-CO-OH system. We provide a brief summary of our conclusions from
552 the scenarios at the end of this section.

553 *E_{CH₄}Vary Scenario*: In the *E_{CH₄}Vary* scenario, all methane emissions are annually-varying
554 (Fig. S 1). Variations in emissions from wetlands are the largest single contributor to global
555 interannual variations, with biomass burning being a lesser contributor (e.g., Bousquet et al.,
556 2006). Patra et al. (2011) reported that up to 60% of methane's observed interannual
557 variation can be explained by variations in meteorology as well as interannual variations in
558 wetland and biomass burning emissions. Given the high methane background concentration,
559 the spatial differences of methane columns between the *E_{CH₄}Vary* and *Base* scenarios are
560 rather small (about ±5 ppb (-1 to 1%)) over most of the globe when taken as seasonal
561 averages of 1988-2007 (Fig. S 19). Consistent with the annually-varying natural emissions
562 of methane, the largest differences occur over rice-producing regions of India and
563 Bangladesh (up to ~5%) and the wetlands of South America (down to -5%), including the
564 Pantanal. The simulated methane monthly variations from the *E_{CH₄}Vary* scenario are in better
565 agreement for the northern hemisphere high latitude GMD station observations as compared
566 to the *Base* scenario (Fig. S 8), which is also consistent with the findings of the TransCom
567 MIP (Patra et al., 2011). The impact of annually-varying natural methane emissions has a
568 small effect (-1% to 1%), as expected, on the spatial distributions of CO and OH because of
569 the slow reaction rate of methane with OH (Fig. S 19; Table 4).

570 *BBE_{CO}Vary* and *FFBBE_{CO}Vary Scenarios*: We developed these scenarios to understand the
571 influence of annually-varying CO emissions from biomass burning and fossil fuel

Yasin Elshorbany, ..., 12/28/2015 4:09 PM

Deleted: Table 1

Yasin Elshorbany, ..., 12/28/2015 4:09 PM

Deleted: Table 2

Yasin Elshorbany, G..., 1/19/2016 3:19 PM

Formatted: Font:Italic

Yasin Elshorbany, ..., 12/28/2015 4:09 PM

Deleted: Fig. S 25

Yasin Elshorbany, G..., 1/12/2016 1:04 PM

Deleted: Fig. S 3

Yasin Elshorbany, G..., 1/20/2016 4:34 PM

Deleted: exercises

Yasin Elshorbany, ..., 12/28/2015 4:09 PM

Deleted: Fig. S 25

Yasin Elshorbany, G..., 1/19/2016 3:20 PM

Formatted: Font:Italic

578 combustion (Fig. S 2) on the observed interannual variation of methane, CO and OH.
579 Including annually-varying biomass burning emissions (*BBE_{CO}Vary*) improves the mean
580 agreement of the simulated CO with GMD observations (mean S=0.83, R² = 0.70, Table 4),
581 but not at all individual GMD stations (Table 4). Improvements occur particularly during
582 years with large fires (e.g., 1997, 1998, 2003, 2004; Fig. 9 to Fig. 11). Adding annually-
583 varying anthropogenic CO emissions in addition to annually-varying biomass burning
584 emissions (*FFBBE_{CO}Vary*) further improves the mean comparison (mean S=0.88),
585 particularly in the northern hemisphere during the 1990s (Fig. 10). Overall, annually-varying
586 CO emissions (*FFBBE_{CO}Vary*) have a significant impact on the spatial distributions of
587 tropospheric CO ($\pm 20\%$) and OH ($\pm 10\%$) relative to the *Base* scenario, and influence
588 methane by $\pm 1\%$ (Fig. S 21, Table 4). Simulating annually-varying CO biomass burning
589 emissions (i.e., *BBE_{CO}Vary* scenario) improves simulated methane relative to the *Base*
590 scenario as compared to observations (mean S=0.97, R²= 0.76, Table 4).
591 *OH_{input}Vary* Scenario: In this scenario, we look at the impact of other causal factors that
592 influence OH, including trends in NO_x and VOC emissions and the overhead ozone column
593 (Table 2). For example, both variations in the overhead ozone column and NO emissions
594 from lightning are known to cause variations in global OH (e.g., Duncan and Logan, 2008;
595 Murray et al., 2013). Together, these causal factors have a significant influence on the spatial
596 distributions of OH ($\pm 20\%$) and CO ($\pm 5\%$) relative to the *Base* scenario and a $\pm 1\%$ effect on
597 methane (Fig. S 4, Fig. S 20, Table 4).
598 *AllVary* Scenario: In this scenario, we investigate the combined effect of all variables (Table
599 2) on the simulated distributions of methane, CO, and OH. The seasonal mean spatial (not
600 shown) and zonal (Fig. 2) distributions of OH are quite comparable to that of the *Base*
601 scenario. The interannual variations in the seasonal mean OH (Fig. 22) are significantly
602 higher ($\sim 20\%$) as compared to the *Base* scenario ($< 5\%$, sec. 3.1), which is related to the
603 annually-varying methane and CO emissions as well as OH constraints in this scenario.
604 There are large differences in the spatial distributions of methane ($\pm 5\%$), CO ($\pm 20\%$), and
605 OH ($\pm 20\%$) between the *Base* and *AllVary* scenarios (Fig. S 22, Table 4). Despite large
606 spatial differences in OH, the global, mean MCF lifetime for the *AllVary* scenario, which
607 ranges from 6.01 (± 0.51) to 6.67 (± 0.61) years over the simulation period, is not significantly
608 different from that of the *Base* scenario.
609 *Summary of Key Findings of Sensitivity Studies:* Overall, variations in anthropogenic and
610 natural methane emissions drive the majority of global variations in observed methane and
611 variations in anthropogenic and natural CO emissions drive the majority of global variations
612 in observed CO. These results are consistent with the findings of other literature studies
613 (e.g., Duncan and Logan, 2008; Patra et al., 2011). We find that the influence of variations of
614 CO emissions and factors that influence OH (e.g., overhead ozone column, VOCs, NO_x)
615 have a significant net effect on the distributions and temporal evolution of methane, CO and
616 OH. This result is consistent with the findings of Duncan and Logan (2008) for CO and OH.
617 The significant influence of the combined nonlinear feedbacks on methane is shown in the
618 difference of the *AllVary* and *E_{CH4}Vary* scenarios (e.g., Fig. 4).
619 Accurate quantification of the magnitude of the combined nonlinear feedbacks is
620 ultimately dependent on the uncertainties and errors of emissions, such as those discussed in
621 Sect. 3, and independent variables, each of which have their own uncertainties, used in the

Yasin Elshorbany, ..., 12/28/2015 4:09 PM
Deleted: Table 4

Yasin Elshorbany, ..., 12/28/2015 4:09 PM
Deleted: Fig. S 27

Yasin Elshorbany, ..., 12/28/2015 4:09 PM
Deleted: Table 4

Yasin Elshorbany, ..., 12/28/2015 4:09 PM
Deleted: Table 2

Yasin Elshorbany, ..., 12/29/2015 1:41 PM
Deleted: B

Yasin Elshorbany, ..., 12/28/2015 4:09 PM
Deleted: Fig. S 26

Yasin Elshorbany, G..., 1/20/2016 4:36 PM
Deleted: ;

Yasin Elshorbany, G..., 1/19/2016 3:20 PM
Formatted: Font:Italic

Yasin Elshorbany, ..., 12/28/2015 4:09 PM
Deleted: Table 2

Yasin Elshorbany, ..., 12/28/2015 4:09 PM
Deleted: Fig. S 28

Yasin Elshorbany, G..., 12/8/2015 1:05 PM
Deleted: , ranging from 6.01 (± 0.51) to 6.67 (± 0.61) years over the simulation period

Yasin Elshorbany, G..., 1/19/2016 3:20 PM
Formatted: Font:Italic

Yasin Elshorbany, ..., 12/29/2015 1:45 PM
Deleted: Figure 3

634 [parameterization of OH. With our sensitivity simulations, we discussed instances when](#)
635 [changes to emissions and/or the input to the parameterization of OH improved or worsened](#)
636 [the simulated methane and CO. In some instances, simulated methane and/or CO from the](#)
637 [least complex *Base* scenario more favorably agreed with observations than the other more](#)
638 [complex scenarios, including methane in the most complex *AllVary* scenario \(e.g., Table 4,](#)
639 [Fig. 4\). However, in these instances, better correlation does not necessarily imply that a](#)
640 [simpler scenario, such as the *Base* scenario or a scenario that uses archived and annually-](#)
641 [repeating OH, is inherently better. The best scenario is one that accurately simulates the](#)
642 [complex interactions of the factors that influence the CH₄-CO-OH system, which will give](#)
643 [confidence in the response of the system to perturbations, such as from large interannual](#)
644 [variations in wetland fluxes, biomass burning, ENSO, and volcanic eruptions. The next steps](#)
645 [for our research include quantifying the 1\) sensitivity of the simulated CH₄-CO-OH system](#)
646 [to uncertainties in the factors \(e.g., water vapor, clouds, trace gases\) that control tropospheric](#)
647 [OH so as to improve simulated methane and CO with observations, and 2\) the influence of](#)
648 [potential large atmospheric carbon perturbations in a warming world, such as may occur](#)
649 [from permafrost thaw, methane hydrate release, and enhanced biomass burning.](#)

650 **5 Summary**

651 We present the fully interactive, computationally Efficient CH₄-CO-OH (ECCOH)
652 chemistry module, which we implemented in the NASA GEOS-5 AGCM. To demonstrate
653 the utility of the ECCOH chemistry module, we exercised the module with a set of scenarios
654 to simulate the influence of various causal factors on OH and the observed variations in
655 methane and CO over 1988-2007, which gives confidence in the fidelity of the module for
656 scientific research. Discrepancies between the output and observations are largely explained
657 by known deficiencies (as reported in the literature) in the methane and CO emissions used
658 as input to the ECCOH chemistry module and AGCM. Through our simulations, we show
659 the importance of using an interactive CH₄-CO-OH system as opposed to using static,
660 archived OH fields, as nonlinear feedbacks on methane, CO, and OH are non-trivial. [For](#)
661 [example, nonlinear feedbacks modulate the global methane growth rate over our study](#)
662 [period \(\$\pm 20\$ ppbv yr⁻¹\) by \$\pm 4\$ ppbv yr⁻¹ \(Fig. 4\).”](#)

663

664

665 **Code availability**

666 The GEOS-5 source code is available under the NASA Open-Source Agreement at
667 <http://opensource.gsfc.nasa.gov/projects/GEOS-5/>.

668

669 *Acknowledgements:* This work was supported by the NASA Modeling, Analysis and
670 Prediction and Interdisciplinary Science programs. We would like to thank the
671 SCIAMACHY WFM-DOAS team at the University of Bremen IUP/IFE for using their
672 methane L3 product as well as the TES/MLS Aura team for using their L2 CO product and
673 Stephen Montzka (NOAA) for providing MCF-inferred OH deviations for comparison.
674 MOPITT CO column data were obtained from the NASA Langley Research Center
675 Atmospheric Science Data Center. We would like also to thank Stacey Frith for providing

676 the output of the GEOS-5 CCM full chemistry simulations. Earlier model development of the
677 ECCOH chemistry module by Elena Yegorova is appreciated. Useful discussions with
678 Prabir Patra (RIGC/JAMSTEC), Huisheng Bian, Junhua Liu and Jerald Ziemke (NASA
679 GSFC), as well as, technical support from Michael Manyin, Yasuko Yoshida and Eric
680 Nielsen (NASA GSFC) are gratefully acknowledged.

681 **6 References**

- 682 Amnuaylojaroen, T., Barth, M. C., Emmons, L. K., Carmichael, G. R., Kreasuwun, J.,
683 Prasitwattanaseree, S., and Chantara, S.: Effect of different emission inventories on
684 modeled ozone and carbon monoxide in Southeast Asia, *Atmos. Chem. Phys.*, 14, 12983-
685 13012, doi:10.5194/acp-14-12983-2014, 2014.
- 686 Bousquet, P., Ciais, P., Miller, J. B., Dlugokencky, E. J., Hauglustaine, D. A., Prigent, C.,
687 Van der Werf, G. R., Peylin, P., Brunke, E. G., Carouge, C., Langenfelds, R. L., Lathiere,
688 J., Papa, F., Ramonet, M., Schmidt, M., Steele, L. P., Tyler, S. C., and White, J.:
689 Contribution of anthropogenic and natural sources to atmospheric methane variability,
690 *Nature*, 443, 439–443, 2006.
- 691 Chameides, W., Liu, S. C. and Cicerone, R. J.: Possible variations in atmospheric methane, *J.*
692 *Geophys. Res.*, 81, 4997-5001, 1976.
- 693 Deeter, M. N.: MOPITT (Measurement of Pollution in the Troposphere) Version6 Product
694 User's Guide, available at:
695 http://www2.acd.ucar.edu/sites/default/files/mopitt/v6_users_guide_201309.pdf (last
696 access: May 28th 2015), 2013.
- 697 Deeter, M. N., Worden, H. M., Edwards, D. P., Gille, J. C., and Andrews, A. E.: Evaluation
698 of MOPITT retrievals of lower tropospheric carbon monoxide over the United States, *J.*
699 *Geophys. Res.*, 117, D13306, doi:10.1029/2012JD017553, 2012.
- 700 Dlugokencky, E.J., Lang, P.M., and Masarie, K.A., Atmospheric Methane Dry Air Mole
701 Fractions from the NOAA ESRL Carbon Cycle Cooperative Global Air Sampling
702 Network, 1983-2009, Version: 2010-08-12, Path: [ftp://ftp.cmdl.noaa.gov/ccg/ch4/flask-](ftp://ftp.cmdl.noaa.gov/ccg/ch4/flask-event/)
703 [event/](ftp://ftp.cmdl.noaa.gov/ccg/ch4/flask-event/), 2010.
- 704 Dlugokencky, E.J., Lang, P.M., Crotwell, A.M., Masarie, K.A., and Crotwell, M.J.:
705 Atmospheric Methane Dry Air Mole Fractions from the NOAA ESRL Carbon Cycle
706 Cooperative Global Air Sampling Network, 1983-2013, Version: 2014-06-24, 2014.
- 707 Duncan, B. N., Portman, D., Bey, I., and Spivakovsky, C. M.: Parameterization of OH for
708 efficient computation in chemical tracer models, *J. Geophys. Res.*, 105 (D10), 12259–
709 12262, 2000.
- 710 Duncan, B. N., Martin, R. V., Staudt, A. C., Yevich, R. M., and Logan, J. A.: Interannual and
711 Seasonal Variability of Biomass Burning Emissions Constrained by Satellite Observations,
712 *J. Geophys. Res.*, 108(D2), 4040, doi:10.1029/2002JD002378, 2003a.
- 713 Duncan, B.N., I. Bey, M. Chin, L.J. Mickley, T.D. Fairlie, R.V. Martin, and H. Matsueda,
714 Indonesian Wildfires of 1997: Impact on Tropospheric Chemistry, *J. Geophys. Res.*, 108,
715 [D15, 4458](https://doi.org/10.1029/2002JD003195), doi:10.1029/2002JD003195, 2003b.
- 716 Duncan, B. N., Logan, J. A., Bey, I., Megretskaya, I. A., Yantosca, R. M., Novelli, P. C.,
717 Jones, N. B., and Rinsland, C. P.: Global budget of CO, 1988–1997: Source estimates and

718 validation with a global model, *J. Geophys. Res.*, 112(D22), D22301,
719 doi:10.1029/2007JD008459, 2007a.

720 Duncan, B. N., Strahan, S. E., Yoshida, Y., Steenrod, S. D., and Livesey, N.: Model study of
721 the cross-tropopause transport of biomass burning pollution, *Atmos. Chem. Phys.*, 7,
722 3713–3736, doi:10.5194/acp-7-3713-2007, 2007b.

723 Duncan, B. and Logan, J.: Model analysis of the factors regulating the trends and variability
724 of carbon monoxide between 1988 and 1997, *Atmos. Chem. Phys.*, 8, 7389-7403, 2008.

725 Elshorbany, Y. F., Barnes, I., Becker, K. H., Kleffmann, J., and Wiesen, P.: Sources and
726 Cycling of Tropospheric Hydroxyl Radicals-An Overview, *Zeitschrift für Physikalische*
727 *Chemie*, 224, 967-987, DOI:10.1524/zpch.2010.6136, 2010.

728 Elshorbany, Y. F., Kleffmann, J., Hofzumahaus, A., Kurtenbach, R., Wiesen, P., Dorn, H.-P.,
729 Schlosser, E., Brauers, T., Fuchs, H., Rohrer, F., Wahner, A., Kanaya, Y., Yoshino, A.,
730 Nishida, S., Kajii, Y., Martinez, M., Rudolf, M., Harder, H., Lelieveld, J., Elste, T., Plass-
731 Dülmer, C., Stange, G., and Berresheim, H.: HO_x Budgets during HO_xComp: a Case
732 Study of HO_x Chemistry under NO_x limited Conditions, *J. Geophys. Res.*, 117, D03307,
733 doi: 10.1029/2011JD017008, 2012a.

734 Elshorbany, Y. F., Steil, B., Brühl, C., and Lelieveld, J.: Impact of HONO on global
735 atmospheric chemistry calculated with an empirical parameterization in the EMAC model,
736 *Atmos. Chem. Phys.*, 12, 9977-10000, doi:10.5194/acp-12-9977-2012, 2012b.

737 Elshorbany, Y. F., Crutzen, P. J., Steil, B., Pozzer, A., Tost, H., and Lelieveld, J.: Global and
738 regional impacts of HONO on the chemical composition of clouds and aerosols, *Atmos.*
739 *Chem. Phys.*, 14, 1167-1184, doi:10.5194/acp-14-1167-2014, 2014.

740 Fiore, A. M., Jacob, D. J., Field, B. D., Streets, D. G., Fernandes, S. D., and Jang, C. :
741 Linking air pollution and climate change: The case for controlling methane, *Geophys. Res.*
742 *Lett.*, 29(19), 1919, doi:10.1029/2002GL015601, 2002.

743 Fiore, A. M., Horowitz, L. W., Dlugokencky, E. J. and West, J. J.: Impact of meteorology
744 and emissions on methane trends, 1990-2004, *Geophys. Res. Lett.*, 33, L12809,
745 doi:10.1029/2006GL026199, 2006.

746 [Fiore, A.M., Dentener, F.J., Wild, O., Cuvelier, C., Schultz, M.G., Hess, P., Textor, C.,](#)
747 [Schulz, M., Doherty, R.M., Horowitz, L.W., MacKenzie, I.A., Sanderson, M.G., Shindell,](#)
748 [D.T., Stevenson, D.S., Szopa, S., Van Dingenen, R., Zeng, G., Atherton, C., Bergmann,](#)
749 [D., Bey, I., Carmichael, G., Collins, W.J., Duncan, B.N., Faluvegi, G., Folberth, G.,](#)
750 [Gauss, M., Gong, S., Hauglustaine, D., Holloway, T., Isaksen, I.S.A., Jacob, D.J., Jonson,](#)
751 [J.E., Kaminski, J.W., Keating, T.J., Lupu, A., Marmer, E., Montanaro, V., Park, R.J.,](#)
752 [Pitari, G., Pringle, K.J., Pyle, J.A., Schroeder, S., Vivanco, M.G., Wind, P., Wojcik, G.,](#)
753 [Wu, S., Zuber, A.](#); Multimodel estimates of intercontinental source-receptor relationships
754 for ozone pollution, *J. Geophys. Res.*, 114, D04301, doi:10.1029/2008JD010816, 2009.

755 Fujino J, Nair R, Kainuma M, Masui T, Matsuoka Y, Multigas mitigation analysis on
756 stabilization scenarios using aim global model. *The Energy Journal Special issue #3:343–*
757 *354*, 2006.

758 Frankenberg, C., Aben, I., Bergamaschi, P., Dlugokencky, E. J., van Hees, R., Houweling,
759 S., [van der Meer, P., Snel, R., Tol, P.](#); Global column-averaged methane mixing ratios from
760 2003 to 2009 as derived from SCIAMACHY: Trends and variability, *J. of Geophys. Res.*,
761 [116, D04302](#), doi: 10.1029/2010JD014849, 2011.

Yasin Elshorbany, ..., 10/27/2015 1:33 PM
Deleted: Fiore, A. M., et al.

Yasin Elshorbany, ..., 10/27/2015 1:35 PM
Deleted: et al. (2011).

764 | [Fuchs, H., Hofzumahaus, A., Rohrer, F., Bohn, B., Brauers, T., Dorn, H.-P., Hafseler, R.,](#)
765 | [Holland, F., Kaminski, M., Li, X., Lu, K., Nehr, S., Tillmann, R., Wegener, R., Wahner,](#)
766 | [A.: Experimental evidence for efficient hydroxyl radical regeneration in isoprene](#)
767 | [oxidation. *Nat. Geosci.* 6, 1023-1026, doi:10.1038/ngeo1964, 2013.](#)

768 | Giglio, L., Randerson, J. T., van der Werf, G. R., Kasibhatla, P. S., Collatz, G. J., Morton, D.
769 | C., and DeFries, R. S.: Assess- ing variability and long-term trends in burned area by
770 | merging multiple satellite fire products, *Biogeosciences*, 7, 1171–1186, doi:10.5194/bg-7-
771 | 1171-2010, 2010.

772 | Gloudemans, A. M. S., Schrijver, H., Hasekamp, O. P., and Aben, I.: Error analysis for CO
773 | and CH₄ total column retrievals from SCIAMACHY 2.3 μm spectra, *Atmos. Chem. Phys.*,
774 | 8, 3999-4017, doi:10.5194/acp-8-3999-2008, 2008.

775 | Hijioaka Y, Matsuoka Y, Nishimoto H, Masui T, Kainuma M.: Global GHG emission
776 | scenarios under GHG concentration stabilization targets. *J Glob Environ Eng* 13:97–108,
777 | 2008.

778 | Ho, S.-P., Edwards, D. P., Gille, J. C., Luo, M., Osterman, G. B., Kulawik, S. S., and
779 | Worden, H.: A global comparison of carbon monoxide profiles and column amounts from
780 | Tropospheric Emission Spectrometer (TES) and Measurements of Pollution in the
781 | Troposphere (MOPITT), *J. Geophys. Res.*, 114, D21307, doi:10.1029/2009JD012242,
782 | 2009.

783 | Holmes, C. D., Prather, M. J., Søvde, O. A., and Myhre, G.: Future methane, hydroxyl, and
784 | their uncertainties: key climate and emission parameters for future predictions, *Atmos.*
785 | *Chem. Phys.*, 13, 285-302, doi:10.5194/acp-13-285-2013, 2013.

786 | Houweling, S., Krol, M., Bergamaschi, P., Frankenberg, C., Dlugokencky, E. J., Morino, I.,
787 | Notholt, J., Sherlock, V., Wunch, D., Beck, V., Gerbig, C., Chen, H., Kort, E. A.,
788 | Röckmann, T., and Aben, I.: A multi-year methane inversion using SCIAMACHY,
789 | accounting for systematic errors using TCCON measurements, *Atmos. Chem. Phys.*, 14,
790 | 3991-4012, doi:10.5194/acp-14-3991-2014, 2014.

791 | Lamarque, J.-F., Shindell, D. T., Josse, B., Young, P. J., Cionni, I., Eyring, V., Bergmann,
792 | D., Cameron-Smith, P., Collins, W. J., Doherty, R., Dalsoren, S., Faluvegi, G., Folberth,
793 | G., Ghan, S. J., Horowitz, L. W., Lee, Y. H., MacKenzie, I. A., Nagashima, T., Naik, V.,
794 | Plummer, D., Righi, M., Rumbold, S. T., Schulz, M., Skeie, R. B., Stevenson, D. S.,
795 | Strode, S., Sudo, K., Szopa, S., Voulgarakis, A., and Zeng, G.: The Atmospheric
796 | Chemistry and Climate Model Intercomparison Project (ACCMIP): overview and
797 | description of models, simulations and climate diagnostics, *Geosci. Model Dev.*, 6, 179–
798 | 206, doi:10.5194/gmd-6-179-2013, 2013.

799 | Lawrence, M. G., Jöckel, P., and von Kuhlmann, R.: What does the global mean OH
800 | concentration tell us?, *Atmos. Chem. Phys.*, 1, 37-49, doi:10.5194/acp-1-37-2001, 2001.

801 | Lelieveld, J., Peters, W., Dentener, F. J., and Krol, M. C.: Stability of tropospheric hydroxyl
802 | chemistry, *J. Geophys. Res.*, 107(D23), 4715, doi:10.1029/2002JD002272, 2002.

803 | Lin, S.-J.: A “vertically Lagrangian” finite-volume dynamical core for global models, *Mon.*
804 | *Weather Rev.*, 132(10), 2293–2307, 2004.

805 | Luo, M., Read, W., Kulawik, S., Worden, J., Livesey, N., Bowman, K. and Herman, R.:
806 | Carbon monoxide (CO) vertical profiles derived from joined TES and MLS measurements,
807 | *J. Geophys. Res. Atmos.*, 118, 10601–10613, doi:10.1002/jgrd.50800, 2013.

Yasin Elshorbany, ..., 10/27/2015 1:36 PM
Deleted: , doi:10.1175/1520-0493

809 Molod, A., Takacs, L., Suarez, M., Bacmeister, J., Song, I.-S., and Eichmann, A.: The
810 GEOS-5 Atmospheric General Circulation Model: Mean Climate and Development from
811 MERRA to Fortuna, NASA/TM-2012-104606, Technical Report Series on Global
812 Modeling and Data Assimilation, Vol. 28, edited by: Suarez, M., available at:
813 <http://gmao.gsfc.nasa.gov/pubs/docs/tm28.pdf> (last access: October 27, 2015), 2012.

814 Monks, S. A., Arnold, S. R., Emmons, L. K., Law, K. S., Turquety, S., Duncan, B. N.,
815 Flemming, J., Huijnen, V., Tilmes, S., Langner, J., Mao, J., Long, Y., Thomas, J. L.,
816 Steenrod, S. D., Raut, J. C., Wilson, C., Chipperfield, M. P., Diskin, G. S.,
817 Weinheimer, A., Schlager, H., and Ancellet, G.: Multi-model study of chemical and
818 physical controls on transport of anthropogenic and biomass burning pollution to the
819 Arctic, *Atmos. Chem. Phys.*, 15, 3575-3603, doi:10.5194/acp-15-3575-2015, 2015.

820 Montzka, S. A., Krol, M., Dlugokencky, E., Hall, B., Joeckel, P., and Lelieveld, J.: Small
821 interannual variability of global atmospheric hydroxyl, *Science*, 331, 67-69,
822 doi:10.1126/science.1197640, 2011.

823 Murray, L. T., Logan, J. A., and Jacob, D., J.: Interannual variability in tropical tropospheric
824 ozone and OH: The role of lightning, *J. Geophys. Res. Atmos.*, 118, 11,468-11,480,
825 doi:10.1002/jgrd.50857, 2013.

826 Myhre, G., Shindell, D., Breion, F.-M., Collins, W., Fuglestedt, J., Huang, J., Koch, D.,
827 Lamarque, J.-F., Lee, D., 5 Mendoza, B., Nakajima, T., Robock, A., Stephens, G.,
828 Takemura, T., and Zhang, H.: Anthropogenic and natural radiative forcing, in: Climate
829 Change 2013: The Physical Science Basis. Contribution of Working Group I to the Fifth
830 Assessment Report of the Intergovernmental Panel on Climate Change, edited by: Stocker,
831 T. F., Qin, D., Plattner, G.-K., Tignor, M., Allen, S. K., Boschung, J., Nauels, A., Xia, Y.,
832 Bex, V., and Midgley, P. M., available at:
833 http://www.climatechange2013.org/images/report/WG1AR5_ALL_FINAL.pdf (last
834 access: October 27, 2015), 2013.

835 Naik, V., Voulgarakis, A., Fiore, A. M., Horowitz, L. W., Lamarque, J.-F., Lin, M.,
836 Prather, M. J., Young, P. J., Bergmann, D., Cameron-Smith, P. J., Cionni, I.,
837 Collins, W. J., Dalsøren, S. B., Doherty, R., Eyring, V., Faluvegi, G., Folberth, G. A.,
838 Josse, B., Lee, Y. H., MacKenzie, I. A., Nagashima, T., van Noije, T. P. C.,
839 Plummer, D. A., Righi, M., Rumbold, S. T., Skeie, R., Shindell, D. T., Stevenson, D. S.,
840 Strode, S., Sudo, K., Szopa, S., and Zeng, G.: Preindustrial to present-day changes in
841 tropospheric hydroxyl radical and methane lifetime from the Atmospheric Chemistry and
842 Climate Model Intercomparison Project (ACCMIP), *Atmos. Chem. Phys.*, 13, 5277-5298,
843 doi:10.5194/acp-13-5277-2013, 2013.

844 Novelli, P., Steele, P., Tans, P. P.: Mixing ratios of carbon monoxide in the troposphere, *J.*
845 *Geophys. Res.*, 102, 12,855-12,861, doi: 10.1029/92JD02010, 1992.

846 Novelli, P., Masarie, K., A., Lang, P. M.: Distributions and recent changes in carbon
847 monoxide in the lower troposphere, *J. Geophys. Res.*, 103, 19,015-19,033, 1998.

848 Oman, L. D., J. R. Ziemke, A. R. Douglass, D. W. Waugh, C. Lang, J. M. Rodriguez, and J.
849 E. Nielsen (2011), The response of tropical tropospheric ozone to ENSO, *Geophys. Res.*
850 *Let.*, 38, L13706, doi:10.1029/2011GL047865, 2011.

851 Ott, L., Duncan, B., Pawson, S., Colarco, P., Chin, M., Randles, C., Diehl, T., and Nielsen,
852 E.: Influence of the 2006 Indonesian biomass burning aerosols on tropical dynamics

Yasin Elshorbany, ..., 10/27/2015 2:00 PM

Deleted: M.

Yasin Elshorbany, ..., 10/27/2015 1:59 PM

Deleted: Editor

Yasin Elshorbany, ..., 10/27/2015 1:37 PM

Formatted: Font:Not Bold

Yasin Elshorbany, ..., 10/27/2015 1:44 PM

Deleted: Myhre, G., Shindell, D., Bréon, F.-M., Collins, W., Fuglestedt, J., Huang, J., Koch, D., Lamarque, J.-F., Lee, D., Mendoza, B., Nakajima, T., Robock, A., Stephens, G., Takemura, T. and Zhang, H.: Anthropogenic and Natural Radiative Forcing. In: Climate Change 2013: The Physical Science Basis. Contribution of Working Group I to the Fifth Assessment Report of the Intergovernmental Panel on Climate Change [Stocker, T.F., D. Qin, G.-K. Plattner, M. Tignor, S.K. Allen, J. Boschung, A. Nauels, Y. Xia, V. Bex and P.M. Midgley (eds.)]. Cambridge University Press, Cambridge, United Kingdom and New York, NY, USA, 2013,

Yasin Elshorbany, ..., 10/27/2015 1:43 PM

Formatted: Font:Not Italic

Unknown

Field Code Changed

Yasin Elshorbany, ..., 10/27/2015 1:41 PM

Deleted: http://www.climatechange2013.org/images/report/-WG1AR5_Chapter08_FINAL.pdf

873 studied with the GEOS5 AGCM, *J. Geophys. Res.*, 115, D14121,
874 doi:10.1029/2009JD013181, 2010.

875 Patra, P. K., Houweling, S., Krol, M., Bousquet, P., Belikov, D., Bergmann, D., Bian, H.,
876 Cameron-Smith, P., Chipperfield, M. P., Corbin, K., Fortems-Cheiney, A., Fraser, A.,
877 Gloor, E., Hess, P., Ito, A., Kawa, S. R., Law, R. M., Loh, Z., Maksyutov, S., Meng, L.,
878 Palmer, P. I., Prinn, R. G., Rigby, M., Saito, R., and Wilson, C.: TransCom model
879 simulations of CH₄ and related species: linking transport, surface flux and chemical loss
880 with CH₄ variability in the troposphere and lower stratosphere, *Atmos. Chem. Phys.*, 11,
881 12813-12837, doi:10.5194/acp-11-12813-2011, 2011.

882 [Patra, P. K., Krol, M. C., Montzka, S. A., Arnold, T., Atlas, E. L., Lintner, B. R., Xiang B.,
883 Elkins J. W., Fraser P. J., Ghosh A., Hints E.J., Hurst D. F., Ishijima K., Krummel P. B.,
884 Miller B. R., Miyazaki K., Moore F. L., Mühle J., O'Doherty S., Prinn R. G., Steele L. P.,
885 Takigawa M., Wang H. J., Weiss R. F., Wofsy S. C., Young, D.: Observational evidence
886 for interhemispheric hydroxyl-radical parity. *Nature*, 513\(7517\), 219-23, doi:
887 10.1038/nature13721, 2014.](#)

888 Pawson, S., R., Stolarski, S., Douglass, A. R., Newman, P. A., Nielsen, J. E., Frith, S. M.,
889 and Gupta, M. L.: Goddard Earth Observing System chemistry-climate model simulations
890 of stratospheric ozone-temperature coupling between 1950 and 2005, *J. Geophys. Res.*,
891 113, D12103, doi:10.1029/2007JD009511, 2008.

892 [Prather, M., and Spivakovsky, C. M.: Tropospheric OH and the lifetimes of
893 hydrochlorofluorocarbons, *J. Geophys. Res.*, 95\(D11\), 18723–18729,
894 doi:10.1029/JD095iD11p18723, 1990.](#)

895 Prather, M.: Lifetimes and Eigen states in atmospheric chemistry, *Geophys. Res. Lett.*, 21, 9,
896 801-804, 1994.

897 Prather, M.: Time scales in atmospheric chemistry: Theory, GWPs for CH₄ and CO, and
898 runaway growth, *Geophys. Res. Lett.*, 23, 19, 2597–2600, DOI: 10.1029/96GL02371,
899 1996.

900 Prather, M. J., C. D. Holmes, and J. Hsu.: Reactive greenhouse gas scenarios: Systematic
901 exploration of uncertainties and the role of atmospheric chemistry, *Geophys. Res. Lett.*,
902 39, L09803, doi:10.1029/2012GL051440, 2012.

903 Prinn, R. G., Huang, J., Weiss, R. F., Cunnold, D. M., Fraser, P. J., Simmonds, P. G.,
904 McCulloch, A., Harth, C., Reimann, S., Salameh, P., O'Doherty, S., Wang, R. H. J.,
905 Porter, L. W., Miller, B. R., and Krummel, P. B.: Evidence for variability of atmospheric
906 hydroxyl radicals over the past quarter century, *Geophys. Res. Lett.*, 32, L07809,
907 doi:10.1029/2004GL022228, 2005.

908 Randerson, J.T., G.R. van der Werf, L. Giglio, G.J. Collatz, and P.S. Kasibhatla.. Global Fire
909 Emissions Database, Version 3 (GFEDv3.1). Data set. Available at: <http://daac.ornl.gov>
910 (last access: October 27, 2015) from Oak Ridge National Laboratory Distributed Active
911 Archive Center, Oak Ridge, Tennessee, USA. doi:10.3334/ORNLDAAC/1191, 2013.

912 [Rienecker, M. M., Suarez, M. J., Todling, R., Bacmeister, J., Takacs, L., Liu, H.-C., Gu, W.,
913 Sienkiewicz, M., Koster, R. D., Gelaro, R., Stajner, I., and Nielsen, J. E.: The GEOS-5
914 data assimilation system – Documentation of Versions 5.0.1, 5.1.0, and 5.2.0, Technical
915 Report Series on Global Modeling and Data Assimilation, Vol. 27, available at:](#)

Yasin Elshorbany, G..., 1/4/2016 11:15 AM
Deleted: .

Yasin Elshorbany, G..., 1/20/2016 4:48 PM
Formatted: Subscript

Yasin Elshorbany, ..., 10/27/2015 1:58 PM
Deleted: on-line

Yasin Elshorbany, ..., 10/27/2015 1:46 PM
Deleted: [

Yasin Elshorbany, ..., 10/27/2015 1:46 PM
Deleted: /

Yasin Elshorbany, ..., 10/27/2015 1:46 PM
Deleted:]

Yasin Elshorbany, ..., 10/27/2015 1:53 PM
Deleted: Rienecker, M., et al.,

922 | http://gmao.gsfc.nasa.gov/pubs/docs/GEOS5_104606-Vol27.pdf (last access: October 27,
923 | 2015), 2008.

924 | Rohrer, F., and Berresheim, H.: Strong correlations between levels of tropospheric hydroxyl
925 | radicals and solar ultraviolet radiation, *Nature*, 442, 184-187, doi:10.1038/nature04924,
926 | 2006.

927 | Rohrer, F., Lu, K., Hofzumahaus, A., Bohn, B., Brauers, T., Chang, C.-C., Fuchs, H.,
928 | Häsel, R., Holland, F., Hu, M., Kita, K., Kondo, Y., Li, X., Lou, S., Oebel, A., Shao, M.,
929 | Zeng, L., Zhu, T., Zhang, Y., and Wahner, A.: Maximum efficiency in the hydroxyl-
930 | radical-based self-cleansing of the troposphere, *Nature Geoscience* 7, 559–563,
931 | doi:10.1038/ngeo2199, 2014.

932 | Sander, S. P., Abbatt, J., Barker, J. R., Burkholder, J. B., Friedl, R. R., Golden, D. M., Huie,
933 | R. E., Kolb, C. E., Kurylo, M. J., Moortgat, G. K., Orkin, V. L. and Wine, P. H.: Chemical
934 | Kinetics and Photochemical Data for Use in Atmospheric Studies, Evaluation No. 17, JPL
935 | Publication 10-6, Jet Propulsion Laboratory, Pasadena, available at:
936 | <http://jpldataeval.jpl.nasa.gov> (last access: October 27, 2015), 2011.

937 | Schneising, O., Buchwitz, M., Burrows, J. P., Bovensmann, H., Bergamaschi, P., and Peters,
938 | W.: Three years of greenhouse gas column-averaged dry air mole fractions retrieved from
939 | satel- lite – Part 2: Methane, *Atmos. Chem. Phys.*, 9, 443–465, doi:10.5194/acp-9-443-
940 | 2009, 2009.

941 | Schneising, O., Buchwitz, M., Reuter, M., Heymann, J., Bovens- mann, H., and Burrows, J.
942 | P.: Long-term analysis of car- bon dioxide and methane column-averaged mole fractions
943 | re- trieved from SCIAMACHY, *Atmos. Chem. Phys.*, 11, 2863– 2880, doi:10.5194/acp-
944 | 11-2863-2011, 2011.

945 | Schultz, M., S. Rast, M. van het Bolscher, T. Pulles, R. Brand, J. Pereira, B. Mota, A.
946 | Spessa, S. Dalsøren, T. van Noije, S. Szopa, Emission data sets and methodologies for
947 | estimating emissions, RETRO project report D1-6, Hamburg, 26 Feb 2007, available at:
948 | http://gcmd.gsfc.nasa.gov/records/GCMD_GEIA_RETRO.html (last access: October 27,
949 | 2015), 2007.

950 | Shindell, D. T., Faluvegi, G., Stevenson, D. S., Krol, M. C., Emmons, L. K., Lamarque, J.-F.,
951 | Petron, G., Dentener, F. J., Ellingsne, K., Schultz, M. G., Wild, O., Amann, M., Atherton,
952 | C. S., Bergmann, D. J., Bey, I., Butler, T., Cofala, J., Collins, W. J., Derwent, R. G.,
953 | Doherty, R. M., Drevet, J., Eskes, H. J., Fiore, A. M., Gauss, M., Hauglustaine, D. A.,
954 | Horowitz, L.W., Isaksen, I. S. A., Lawrence, M. G., Montanaro, V., Müller, J.-F., Pitari,
955 | G., Prather, M. J., Pyle, J. A., Rast, S., Rodriguez, J. M., Sanderson, M. G., Savage, N. H.,
956 | Strahan, S. E., Sudo, K., Szopa, S., Unger, N., van Noije, T. P. C., and Zeng, G.:
957 | Multimodel simulations of carbon monoxide: Comparison with observations and projected
958 | near-future changes, *J. Geophys. Res.*, 111, D19306, doi:10.1029/2006JD007100, 2006.

959 | [Spivakovsky, C., Wofsy, S., and Prather, M.: A numerical method for the parameterization of
960 | atmospheric chemistry: Computation of tropospheric OH, *J. Geophys. Res.*, 95, 18,433-
961 | 18,439, 1990a.](#)

962 | Spivakovsky, C.M., Yevich, R., Logan, J.A., Wofsy, S.C., McElroy, M.B., and Prather, M.J.,
963 | Tropospheric OH in a three-dimensional chemical tracer model: An assessment based
964 | on observations of CH₃CCl₃, *J. Geophys. Res.*, 95, 18,441-18,471,
965 | doi:10.1029/JD095iD11p18441, 1990b.

Yasin Elshorbany, ..., 10/27/2015 1:58 PM
Deleted: ,

Yasin Elshorbany, ..., 10/27/2015 1:57 PM
Deleted: (

Yasin Elshorbany, ..., 10/27/2015 1:57 PM
Deleted:)

969 Spivakovsky, C M., Logan, J A., Montzka, S A., Balkanski, Y J. Foreman-Fowler, M.,
 970 Jones, D B A., Horowitz, L W., Fusco, A C., Brenninkmeijer, C A M., Prather, M J.,
 971 Wofsy, S C., and McElroy, M B.: Three-dimensional climatological distribution of
 972 tropospheric OH: Update and evaluation, *J. Geophys. Res.*, 105, D7, 8931–8980,
 973 doi:10.1029/1999JD901006, 2000.

974 Stone, D., L.K. Whalley, D.E. Heard.: Tropospheric OH and HO₂ radicals: field
 975 measurements and model comparisons. *Chemical Society Reviews*, 41:19, 6348,
 976 doi:10.1039/c2cs35140d, 2012.

977 Strahan, S.E., B.N. Duncan and P. Hoor, Observationally-derived diagnostics of transport in
 978 the lowermost stratosphere and their application to the GMI chemistry transport model,
 979 Atmos. Chem. Phys., 7, 2435-2445, 2007.

980 Strode, S. A., Duncan, B. N., Yegorova, E. A., Kouatchou, J., Ziemke, J. R., and
 981 Douglass, A. R.: Implications of model bias in carbon monoxide for methane lifetime,
 982 *Atmos. Chem. Phys. Discuss.*, 15, 20305-20348, doi:10.5194/acpd-15-20305-2015, 2015.

983 Voulgarakis, A., Naik, V., Lamarque, J.-F., Shindell, D. T., Young, P. J., Prather, M. J.,
 984 Wild, O., Field, R. D., Bergmann, D., Cameron-Smith, P., Cionni, I., Collins, W. J.,
 985 Dalsøren, S. B., Doherty, R. M., Eyring, V., Faluvegi, G., Folberth, G. A.,
 986 Horowitz, L. W., Josse, B., MacKenzie, I. A., Nagashima, T., Plummer, D. A., Righi, M.,
 987 Rumbold, S. T., Stevenson, D. S., Strode, S. A., Sudo, K., Szopa, S., and Zeng, G.:
 988 Analysis of present day and future OH and methane lifetime in the ACCMIP simulations,
 989 Atmos. Chem. Phys., 13, 2563-2587, doi:10.5194/acp-13-2563-2013, 2013.

990 Voulgarakis, A., M. E. Marlier, G. Faluvegi, D. T. Shindell, K. Tsigaridis, and S. Mangeon,
 991 Interannual variability of tropospheric trace gases and aerosols: The role of biomass
 992 burning emissions, *J. Geophys. Res. Atmos.*, 120, 7157–7173,
 993 doi:10.1002/2014JD022926, 2015.

994 Wang, J. S., Logan, J. A., McElroy, M. B., Duncan, B. N., Megretskaja, I. A., Yantosca, R.
 995 M.: A 3-D model analysis of the slowdown and interannual variability in the methane
 996 growth rate from 1988 to 1997, Global Biogeochemical Cycles, 18, GB3011,
 997 doi:10.1029/2003GB002180, 2004.

998 Wang, J. S., McElroy, M. B., Logan, J. A., Palmer, P. I., Chameides, W. L., Wang, Y., and
 999 Megretskaja, I. A.: A quantitative assessment of uncertainties affecting estimates of global
 1000 mean OH derived from methyl chloroform observations, *J. Geophys. Res.*, 113, D12302,
 1001 doi:10.1029/2007JD008496, 2008.

1002 Wainwright, C. D., Pierce, J. R., Liggio, J., Strawbridge, K. B., Macdonald, A. M., and
 1003 Leaitch, R. W.: The effect of model spatial resolution on Secondary Organic Aerosol
 1004 predictions: a case study at Whistler, BC, Canada, *Atmos. Chem. Phys.*, 12, 10911-10923,
 1005 doi:10.5194/acp-12-10911-2012, 2012.

1006 Wild, O., and Palmer, P. I.: How sensitive is tropospheric oxidation to anthropogenic
 1007 emissions?, *Geophys. Res. Lett.*, 35, L22802, doi:10.1029/2008GL035718, 2008.

1008 Wolter, K., and M. S. Timlin, El Niño/Southern Oscillation behaviour since 1871 as
 1009 diagnosed in an extended multivariate ENSO index (MEI.ext). *Intl. J. Climatology*, 31,
 1010 1074-1087, DOI: 10.1002/joc.2336, 2011.

1011 Worden, H. M., Deeter, M. N., Edwards, D. P., Gille, J. C., Drummond, J. R., and Nédélec,
 1012 P.: Observations of near-surface carbon monoxide from space using MOPITT

Yasin Elshorbany, G..., 1/20/2016 4:48 PM
 Deleted: DOI

Yasin Elshorbany, G..., 1/19/2016 3:26 PM
 Deleted: Strahan, S.E., B.N. Duncan and P. Hoor, Observationally-derived diagnostics of transport in the lowermost stratosphere and their application to the GMI chemistry transport model, *Atmos. Chem. Phys.*, 7, 2435-2445, 2007. .

Yasin Elshorbany, ..., 10/27/2015 2:02 PM
 Deleted: Wang, J., et al.,

1021 multispectral retrievals, J. Geophys. Res., 115, D18314, doi:10.1029/2010JD014242,
1022 2010.
1023

1024 Table 1: Reference Scenario (*Base*) Description

| AGCM Input | Description ^a |
|-------------------------------------|---|
| Dynamics | Model dynamics are constrained by sea surface temperatures and sea ice concentrations from the Community Climate System Model (http://www.cesm.ucar.edu/models/ccsm4.0/ , CCSM-4) through 2005 and from 2006 to 2007 from CCSM-4 with Representative Concentration Pathways (RCP 6.0, Fujino et al. (2006); Hijioka et al. (2008)). The methane tracer is radiatively inactive <u>and archived annually-varying methane fields used in the radiation code</u> ; our aim is reproduce the same meteorology in all simulations so as to more cleanly isolate the impact of the causal factors on methane, CO, and OH trends and variations. |
| <i>Parameterization of OH Input</i> | |
| Chemical Variables | Nitrogen oxides (as a family), ozone, overhead ozone column, and various VOCs are monthly, archived fields for 2000 and are repeated for each year of the <i>Base</i> simulation; these fields were taken from a one year (2000) GEOS-5 AGCM simulation, which was part of the ACCMIP study (Lamarque et al., 2013), with a full-representation of ozone-NO _x -VOC photochemistry (Duncan et al., 2007b; Strahan et al., 2007) and emissions of NO _x , VOCs, and species important to the stratospheric ozone layer (e.g., N ₂ O, HFCs, CFCs). |
| Meteorological Variables | Pressure, temperature, cloud albedo and water vapor are taken from the AGCM as the simulation progresses. |
| <i>Emissions^b</i> | |
| Methane | Annually-repeating natural (e.g., wetlands, biomass burning) and annually-varying anthropogenic emissions (EDGAR 3.2 , TransCom CTL scenario) are described in Patra et al. (2011). |
| CO | Annually-repeating emissions representative for year 2000 time slice of the ACCMIP _v (Lamarque et al., 2013; Strode et al., 2015). |
| <i>Methane Oxidation</i> | |
| Troposphere | CH ₄ + OH → αCO: tropospheric OH calculated by parameterization of OH. CO yield (α) = 1 (Duncan et al., 2007a). |
| Stratosphere | Calculated based on its reaction with OH, Cl and O ¹ D from archived monthly fields from one year of an AGCM simulation. |
| <i>VOC Oxidation^b</i> | VOC + OH → αCO; CO yield (α) varies with VOC (Duncan et al., 2007b). Isoprene + OH → αCO, where CO yield (α) varies with [NO _x] (Duncan et al., 2007a). |

1025 ^aAll scenarios are for 1988-2007. We use the methane initial condition of 1655 ppb by January 1988 at the GMD South Pole (SPO) station,
 1026 (Patra et al., 2011, TransCom protocolv7), which was reached after a 12-year model spin up; results are thus considered valid from January 1,
 1027 1988.

1028 ^bOnly methane and CO are treated as emission fluxes. The source of CO via VOC oxidation is calculated using archived, 3d fields from a GEOS-5 AGCM full chemistry
 1029 simulation. Figures S1 and S2 show the methane and CO fluxes, respectively, used in all scenarios,

1030

Yasin Elshorbany, G..., 1/20/2016 4:49 PM
 Deleted: intercomparison

Yasin Elshorbany, ..., 10/27/2015 1:12 PM
 Deleted: - ... [1]

Yasin Elshorbany, ..., 10/27/2015 1:15 PM
 Deleted: s

Yasin Elshorbany, ..., 10/27/2015 1:15 PM
 Deleted: fluxes from the "CTL" and "EXTRA" scenarios of the TransCOM exercise (Patra et al., 2011)

1038 Table 2: Description of Simulation Scenarios

| Model Scenario | Relation to Other Scenarios | Purpose of Scenario |
|---|---|--|
| 1. <i>Base</i> | Table 1. | Reference scenario |
| 2. <i>E_{CH₄}</i> Vary <i>Base</i> + all methane source types varying annually | Same as <i>Base</i> , except that the “EXTRA” methane emission scenario is used (Patra et al., 2011). The primary difference between the CTL and EXTRA scenarios is that the CTL emissions are composed of repeating annual cycles of all source types, except for anthropogenic emissions which varies from year-to-year, while the EXTRA emission scenario has all source types (e.g., biomass burning, wetlands, rice paddies, etc.) varying annually (Fig. S 1). | To understand the influence of interannual variations in natural sources of methane on the trends and variations of model OH and observed methane and CO distributions. Wetlands are the largest single source of methane and the largest source of interannual variations (e.g., Patra et al., 2011; Voulgarakis et al., 2015). |
| 3. <i>BBE_{CO}</i> Vary <i>Base</i> + BB CO emissions varying annually | Same as <i>Base</i> , except CO emissions from biomass burning (BB) annually vary. Emissions are from the REanalysis of the TROpospheric chemical composition (RETRO v2.0, Schultz et al., 2007) emission inventory for 1988-1996 and the Global Fire Emissions Database (GFEDv3.1, Giglio et al., 2010; Randerson et al., 2013) for years 1997-2007. | To understand the influence of interannual variations in the biomass burning source of CO (Fig. S 2). From 1988-2007, there were several large events, such as in Indonesia in 1997 [Duncan et al., 2003a] and 2006 and worldwide in 1998 [Duncan et al., 2003b]. |
| 4. <i>FFBBE_{CO}</i> Vary <i>Base</i> + FF and BB CO emissions varying annually | Same as <i>BBE_{CO}</i> Vary, except CO emissions from fossil fuels annually vary. Anthropogenic emissions are from the Emission Database for Global Atmospheric Research (EDGARv4.2) for 1988-2007. | To understand the combined influence of interannual variations in the anthropogenic and biomass burning sources of CO. |
| 5. <i>OH_{Input}</i> Vary <i>Base</i> + parameterization of OH chemical variables varying annually | Same as <i>Base</i> , except the monthly, archived chemical variables used as input to the parameterization of OH are annually varying. Taken from the same GEOS-5 AGCM simulation as in <i>Base</i> scenario with a full-representation of ozone-NO _x -VOC photochemistry and annually varying anthropogenic and biogenic emissions of NO _x , VOCs, and species important to the stratospheric ozone layer (e.g., N ₂ O, HFCs, CFCs) (Strahan et al., 2007; Duncan et al., 2007b; Oman et al., 2011). | To understand the influence of interannual variations in other factors that affect OH. These factors include the overhead ozone column, NO _x and anthropogenic VOCs. |
| 6. <i>AllVary</i> <i>Base</i> + <i>E_{CH₄}</i> Vary + <i>FFBBE_{CO}</i> Vary + <i>OH_{Input}</i> Vary | Annually varying methane and CO emissions from all sources and annually-varying factors that influence OH. | To understand the combined influence of annually-varying 1) CO emissions from fossil fuel and biomass burning, 2) effects of NO _x and VOCs on OH, and 3) methane emissions from all sources. |

Yasin Elshorbany, G..., 1/20/2016 5:35 PM

Formatted: Font:10 pt

Yasin Elshorbany, ..., 12/28/2015 4:09 PM

Deleted: Fig. S 1

1039

1041 Table 3: Data Used In Model Evaluation of Methane, CO, and OH

| Data | Species | Quantity | Time Range | Reference |
|--|-------------|---|----------------|---|
| NOAA ESRL Global Monitoring Division (GMD) surface data | CO, methane | mixing ratio (ppbv) | 1980-present | Novelli et al., 1992, 1998; Dlugokencky et al., 2010, 2014. |
| Envisat SCanning Imaging Absorption spectroMeter for Atmospheric CHartographY (SCIAMACHY) ^a | methane | atmospheric column (molec/cm ²) | 2003-2005 | Bovensmann et al., 1999; Schneising et al., 2009; Schneising et al., 2011; Frankenberg et al., 2011 |
| Terra Measurement of Pollution In The Troposphere (MOPITT) Instrument ^b | CO | atmospheric column (molec/cm ²) | 1999-present | Worden, 2010; Deeter et al., 2012; Deeter, 2013. |
| Aura Tropospheric Emission Spectrometer (TES)/Microwave Limb Sounder (MLS) Joint Product | CO | mixing ratio (ppbv) | 8/2004-10/2012 | Luo et al., 2013 |
| NOAA surface network | MCF | OH interannual variability (IAV) ^c | 1997-2007 | Montzka et al., 2011 |

1042 ^aWe use version 3.7 gridded product of the column-averaged methane dry mole fraction (Schneising et al., 2009; [http://www.iup.uni-](http://www.iup.uni-bremen.de/sciamachy/NIR_NADIR_WFM_DOAS/products)
 1043 [bremen.de/sciamachy/NIR_NADIR_WFM_DOAS/products](http://www.iup.uni-bremen.de/sciamachy/NIR_NADIR_WFM_DOAS/products)). The methane data since November 2005 are considered to be of reduced quality (in comparison to data from
 1044 2003-October 2005) due to detector degradation in the spectral range used for the methane column retrieval (Schneising et al., 2011; Frankenberg et al., 2011).

1045 ^bWe use the gridded monthly CO retrievals (thermal infrared radiances) V006 L3 product (<http://eosweb.larc.nasa.gov>)

1046 ^cThere are only very sparse and uncertain direct observations (e.g., Stone et al., 2012).

1047

1048 Table 4: list of the correlation parameters of the different model scenarios and the monthly
 1049 GMD measurements for the simulation period (1988-2007)

| Scenario | ALT ^a | | BRW | | NWR | | MLO | | RPB | | SPO | |
|---------------------------------------|------------------|------------------|------|----------------|------|----------------|------|----------------|------|----------------|------|----------------|
| | S* | R ^{2**} | S | R ² |
| CH₄ data | | | | | | | | | | | | |
| <i>Base</i> | 0.56 | 0.66 | 0.57 | 0.60 | 0.76 | 0.64 | 0.76 | 0.58 | 0.68 | 0.82 | 0.79 | 0.91 |
| <i>E_{CH₄}Vary</i> | 0.74 | 0.68 | 0.74 | 0.56 | 0.74 | 0.63 | 0.79 | 0.57 | 0.71 | 0.72 | 0.82 | 0.89 |
| <i>BBE_{CO}Vary</i> | 0.82 | 0.68 | 0.84 | 0.66 | 1.03 | 0.76 | 1.07 | 0.72 | 1.00 | 0.84 | 1.07 | 0.93 |
| <i>FFBBE_{CO}Vary</i> | 0.58 | 0.54 | 0.56 | 0.46 | 0.74 | 0.54 | 0.77 | 0.52 | 0.66 | 0.64 | 0.79 | 0.81 |
| <i>OH_{input}Vary</i> | 0.53 | 0.63 | 0.53 | 0.56 | 0.71 | 0.60 | 0.70 | 0.56 | 0.62 | 0.78 | 0.74 | 0.90 |
| <i>AllVary</i> | 0.69 | 0.49 | 0.68 | 0.40 | 0.64 | 0.45 | 0.70 | 0.43 | 0.62 | 0.47 | 0.76 | 0.73 |
| | | | | | | | | | | | | |
| CO data | | | | | | | | | | | | |
| <i>Base</i> | 0.74 | 0.79 | 0.70 | 0.75 | 0.83 | 0.57 | 0.98 | 0.71 | 0.74 | 0.68 | 0.88 | 0.82 |
| <i>E_{CH₄}Vary</i> | 0.74 | 0.79 | 0.70 | 0.75 | 0.82 | 0.57 | 0.98 | 0.71 | 0.73 | 0.68 | 0.87 | 0.82 |
| <i>BBE_{CO}Vary</i> | 0.81 | 0.86 | 0.74 | 0.73 | 0.84 | 0.57 | 1.01 | 0.74 | 0.82 | 0.68 | 0.79 | 0.64 |
| <i>FFBBE_{CO}Vary</i> | 0.92 | 0.88 | 0.97 | 0.87 | 0.84 | 0.42 | 0.89 | 0.70 | 0.83 | 0.70 | 0.81 | 0.63 |
| <i>OH_{input}Vary</i> | 0.74 | 0.81 | 0.71 | 0.77 | 0.81 | 0.56 | 0.93 | 0.71 | 0.67 | 0.66 | 0.92 | 0.85 |
| <i>AllVary</i> | 0.90 | 0.88 | 0.96 | 0.85 | 0.80 | 0.37 | 0.82 | 0.68 | 0.77 | 0.67 | 0.84 | 0.68 |

1050 ^aGMD stations shown include Alert, Canada (ALT, 82°N, 62°W), Point Barrow, USA (BRW, 71°N, 156°W), Niwot Ridge, USA (NWR, 40°N, 105°W),
 1051 Mauna Loa, Hawaii, USA (MLO, 20°N, 155°W), Ragged Point, Barbados (RPB, 13°N, 59°W), and South Pole,
 1052 Antarctica (SPO, 90°S, 25°W).
 1053 *: "S" refers to the correlation slope (dy/dx) of the simulation/measurement comparison.
 1054 **: "R²" refers to the correlation coefficient.
 1055

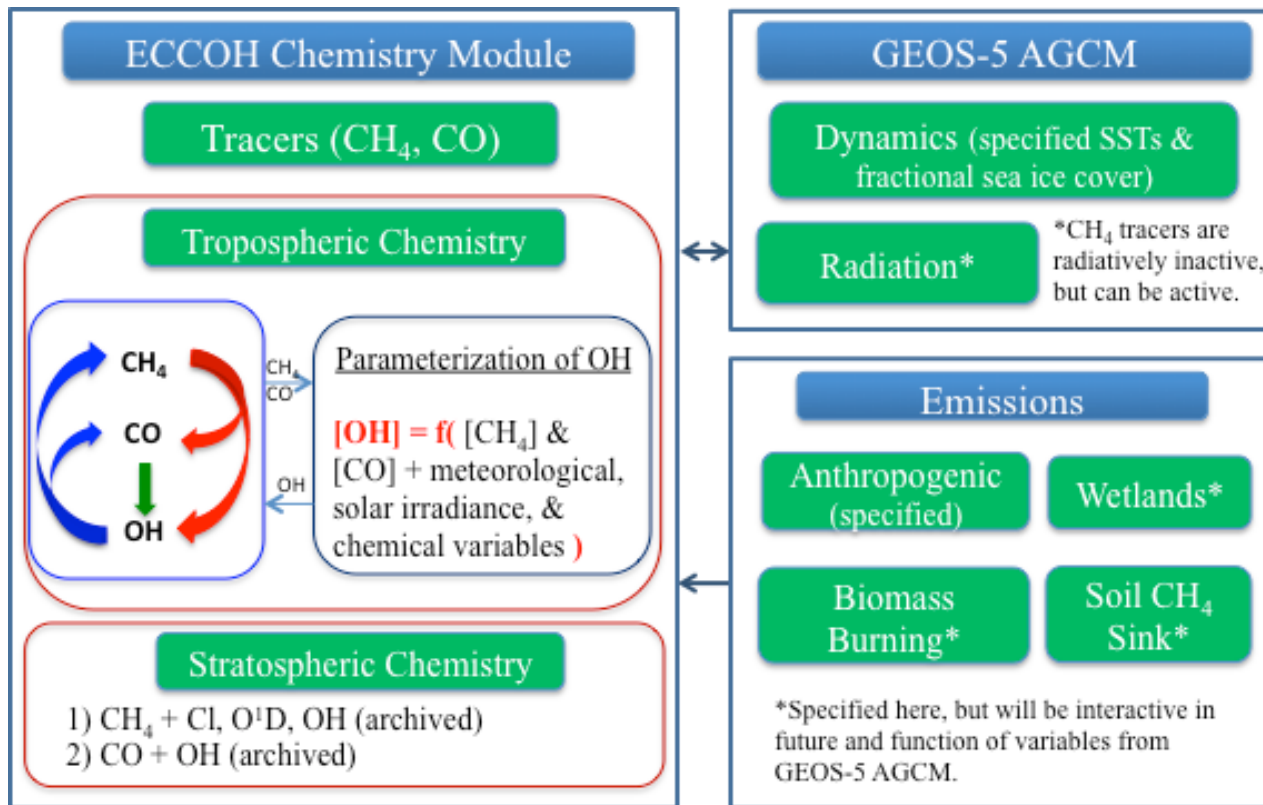


Fig. 1: Schematic representation of the implementation of the ECCOH module within the GEOS-5 AGCM.

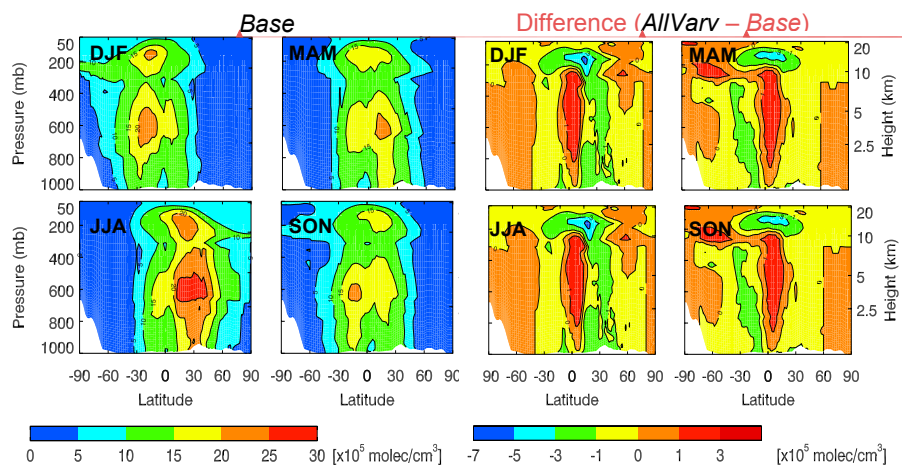


Fig. 2: Seasonal zonal mean (1988-2007) of OH ($\times 10^5$ molecules/cm³) for the *Base* scenario (left 4 panels) and the difference (*AllVarv-Base*, right 4 panels) for December-February (DJF), March-May (MAM), June-August (JJA) and September-November (SON).

Yasin t
Forma
Yasin t
Forma
Yasin t
Forma

Yasin t
Delete
Yasin t
Forma
Yasin t
Delete
Yasin t
Delete
Yasin t
Delete
Yasin t
Forma

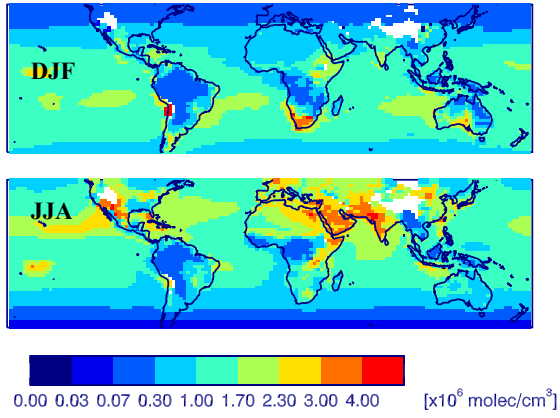


Fig. 3: Seasonal mean (1988-2007) OH ($\times 10^6 \text{ molecules/cm}^3$) for the *Base* scenario for December- February (DJF) and June-August (JJA) at 850 mb.

Yasin Elshorbany, G..., 1/20/2016 4:06 PM
Deleted: ar

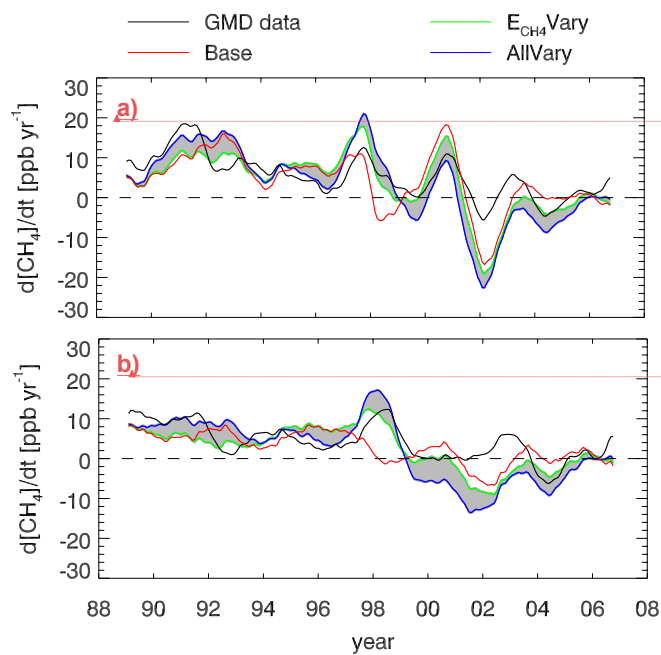


Fig. 4: a) 12-month running mean atmospheric growth rate of methane (ppbv yr^{-1}) for the average of 92 GMD stations and from model output for several scenarios averaged for those station locations. The shaded area is the difference between the $E_{\text{CH}_4}\text{Vary}$ and $All\text{Vary}$ scenarios, which indicates the total contribution of nonlinear feedbacks (i.e., from variations of CO emissions and variables input to the parameterization of OH) of the $\text{CH}_4\text{-CO-OH}$ system to methane's growth rate. b) Same as a) but for the average of 17 GMD stations, which covers 100% of the simulation period. Refer to Fig. S 4 to Fig. S 7 for methane's growth rate from other scenarios.

Yasin Elshorbany, ..., 1/11/2016 12:01 PM
Formatted: Font:(Default) Arial, Bold

Yasin Elshorbany, ..., 1/11/2016 12:01 PM
Formatted: Font:(Default) Arial, Bold

Yasin Elshorbany, ..., 1/11/2016 12:04 PM
Deleted: .

Yasin Elshorbany, GS..., 1/4/2016 2:42 PM
Deleted: Atmospheric methane growth rate (ppbv/yr , average of 92 GMD stations) from several scenarios. The shaded area is the difference between the $E_{\text{CH}_4}\text{Vary}$ and $All\text{Vary}$ scenarios.

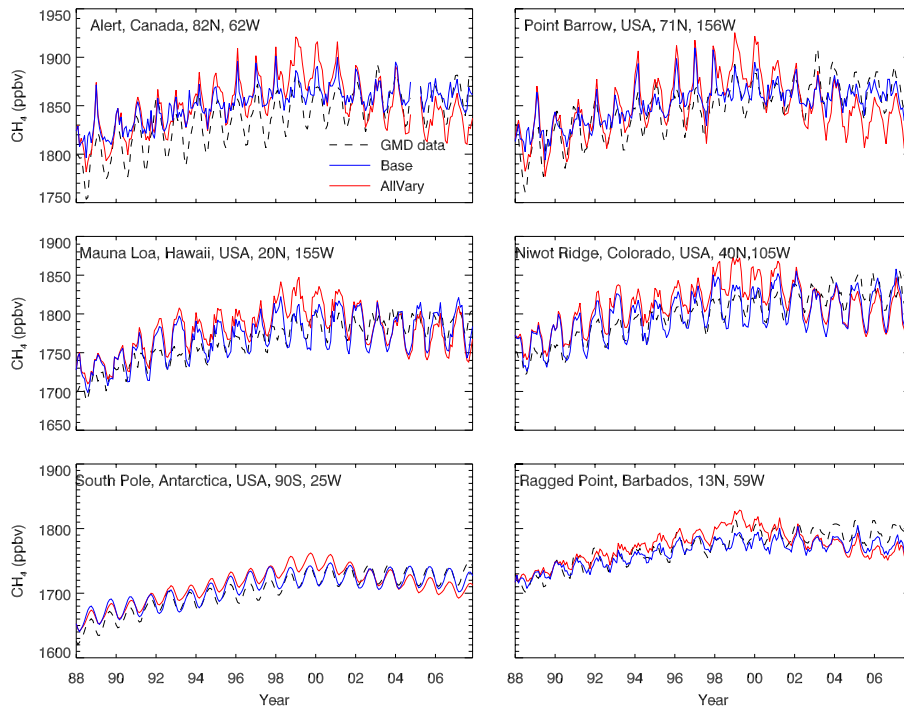


Fig. 5: Monthly methane (ppbv) from the *Base* and *AllVary* scenarios and observations from six GMD stations. Similar plots for the other scenarios are given in Fig. S 8 to Fig. S

11.

- Yasin Elshorbany, G..., 1/20/2016 8:43 AM
Deleted: ures
- Yasin Elshorbany, G..., 1/20/2016 8:42 AM
Deleted: 3
- Yasin Elshorbany, G..., 1/20/2016 8:42 AM
Deleted: -
- Yasin Elshorbany, G..., 1/20/2016 8:42 AM
Deleted: 6

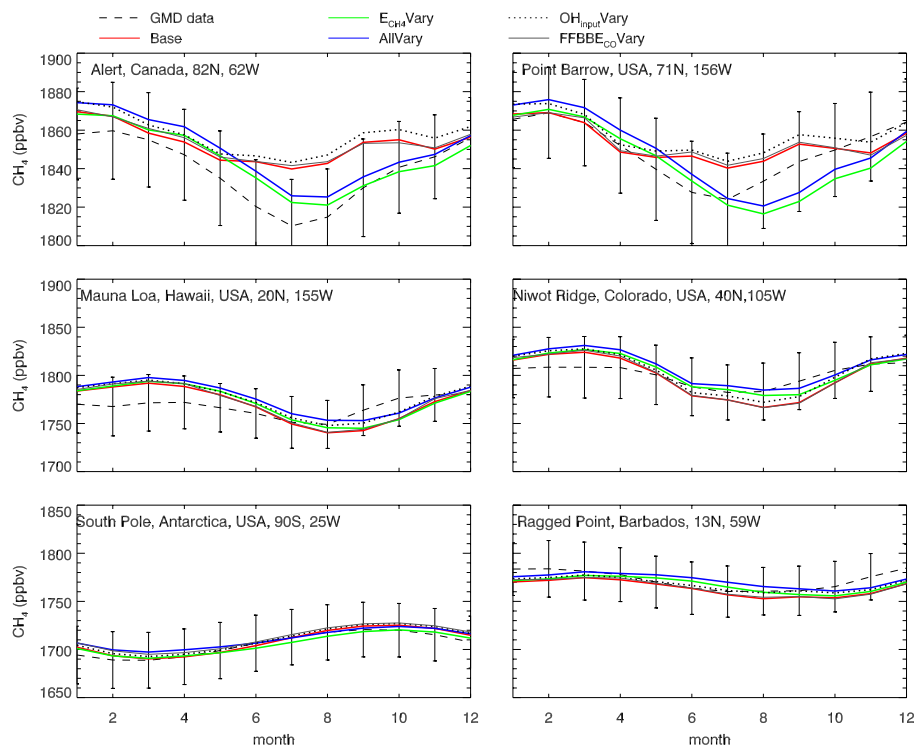


Fig. 6: Monthly methane (ppbv) averaged over 1988-2007 for several scenarios and observations at six GMD stations. Vertical lines represent the standard deviation of the observed annual mean.

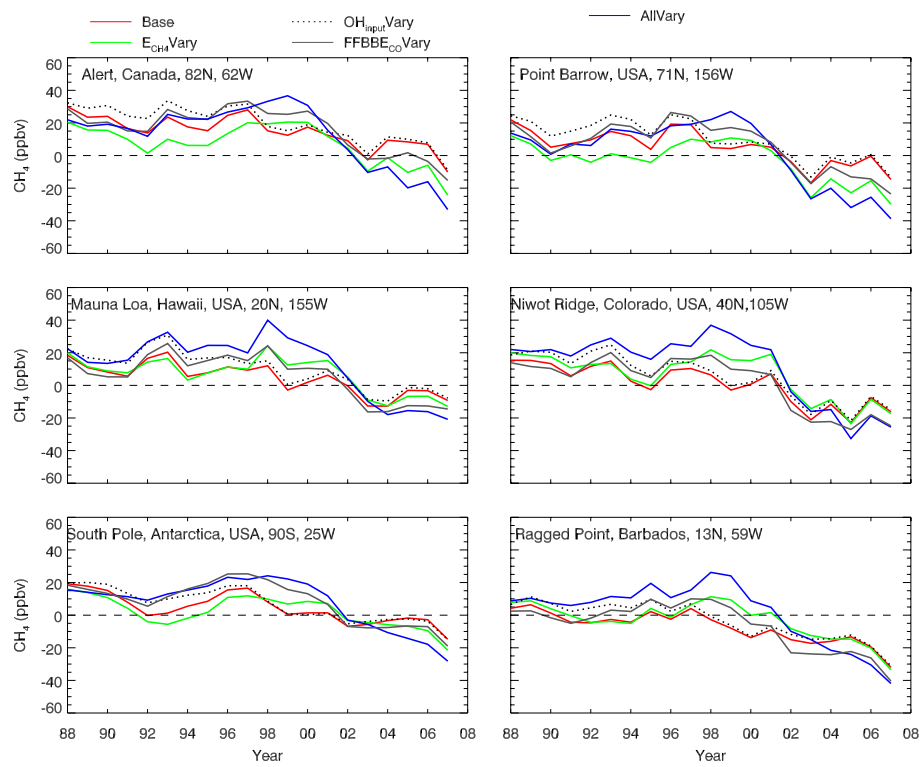


Fig. 7: Annual methane deviation (ppbv; simulated-measured) for several scenarios and observations at six GMD stations.

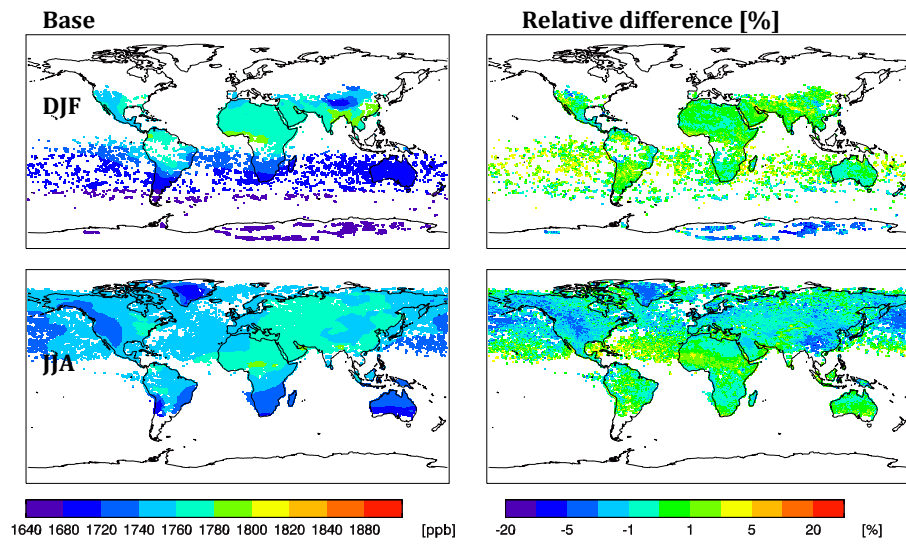


Fig. 8: Seasonal mean (2004) methane dry column (ppbv; left column) from the *Base* scenario and the relative difference (%; $(Base-observations)/observations$; right column) with SCIAMACHY data. Simulated methane levels are gridded to the spatial resolution of the SCIAMACHY data.

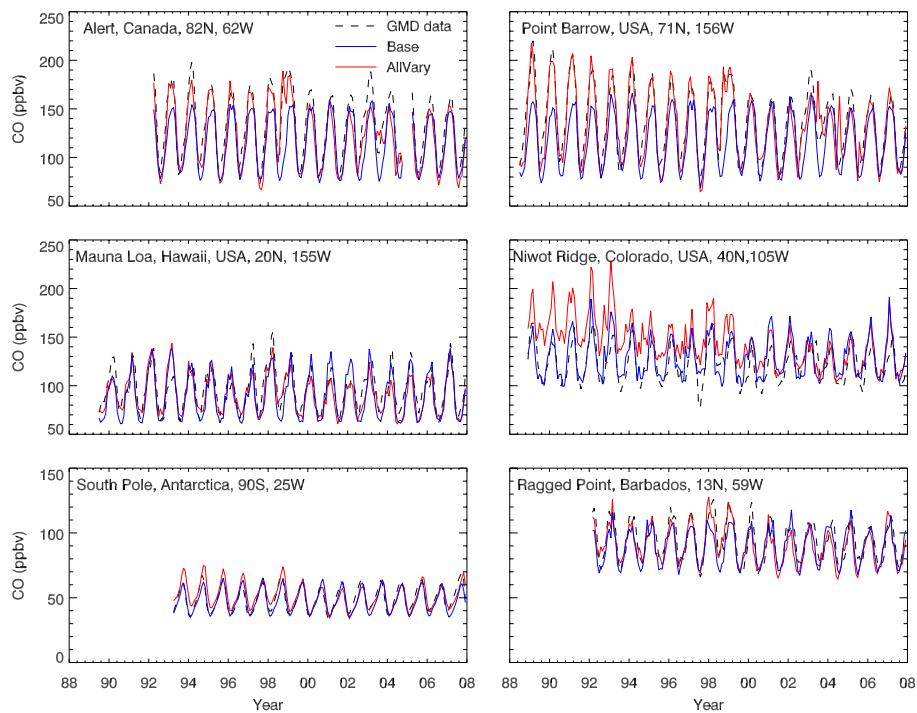


Fig. 9: Monthly CO (ppbv) from the *Base* and *AllVary* scenarios and observations from six GMD stations. Similar plots for the other scenarios are given in Fig. S13 to Fig. S16.

- Yasin Elshorbany, G..., 1/20/2016 8:43 AM
Deleted: ures
- Yasin Elshorbany, G..., 1/20/2016 8:43 AM
Deleted: 9
- Yasin Elshorbany, G..., 1/20/2016 8:43 AM
Deleted: -
- Yasin Elshorbany, G..., 1/20/2016 8:43 AM
Deleted: 2

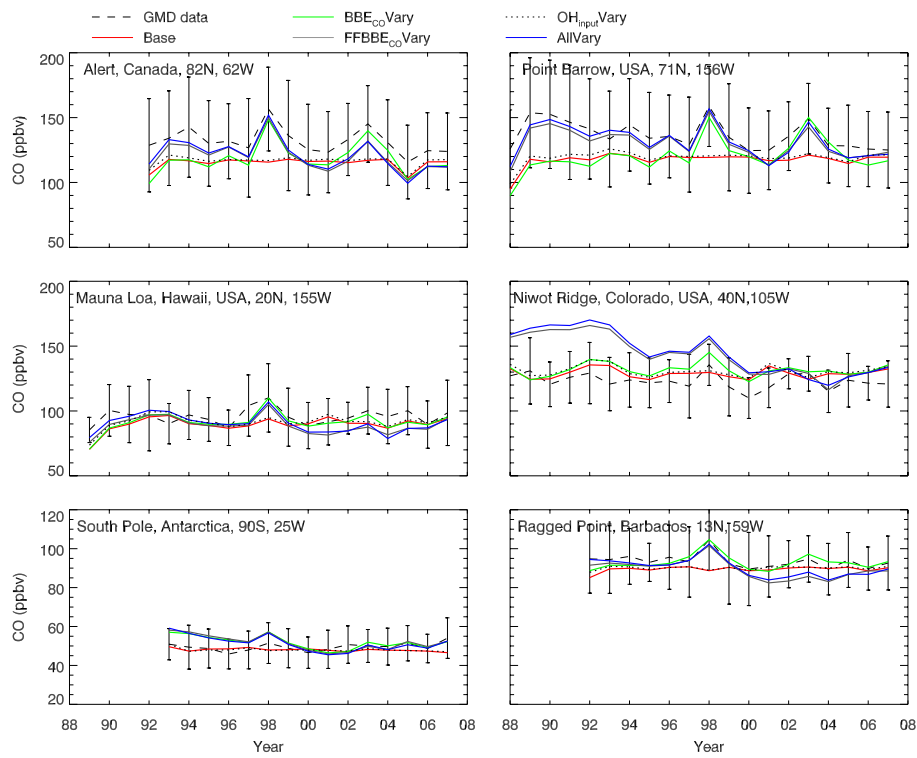


Fig. 10: Annual mean CO (ppbv) from several scenarios and observations at six GMD stations. Vertical lines represent the standard deviation of the observed annual mean.

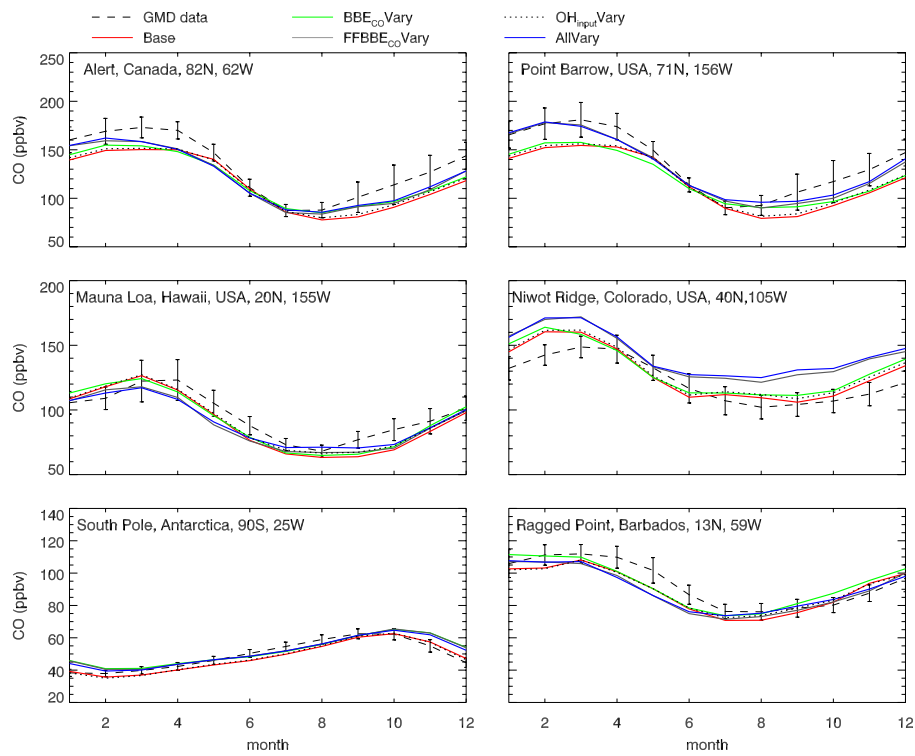


Fig. 11: Monthly CO (ppbv) averaged over 1998-2007 for several scenarios and observations at six GMD stations. Vertical lines represent the standard deviation of the observed monthly mean.

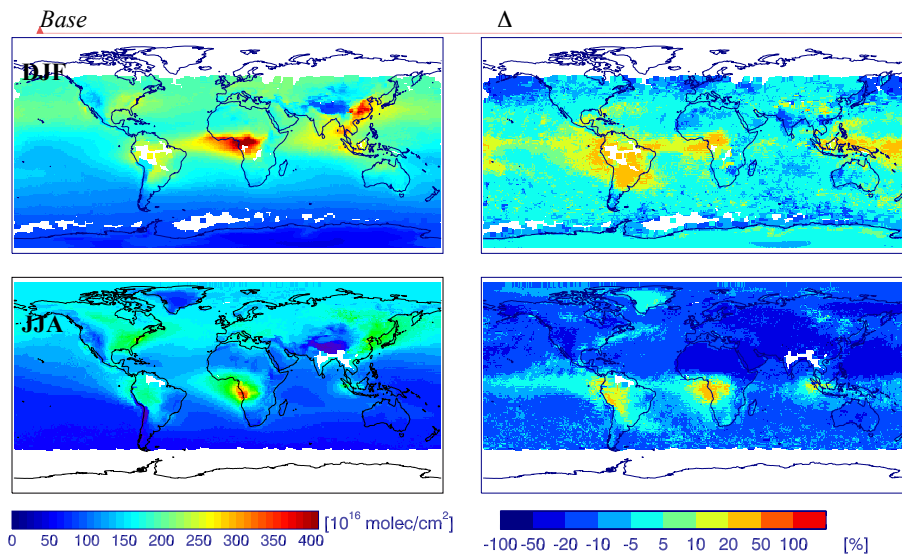


Fig. 12: Seasonal mean (2006-2007) CO columns ($\times 10^{16}$ molecules/cm²) from the *Base* scenario (left column) and the relative difference (%; (*Base*-observations)/observations; right column) with MOPITT data.

Yasin Elshorbany, G..., 1/20/2016 4:07 PM
Formatted: Font:Italic

Yasin Elshorbany, G..., 12/8/2015 3:30 PM
Deleted: Vertical lines represent the standard deviation of the observed annual mean.

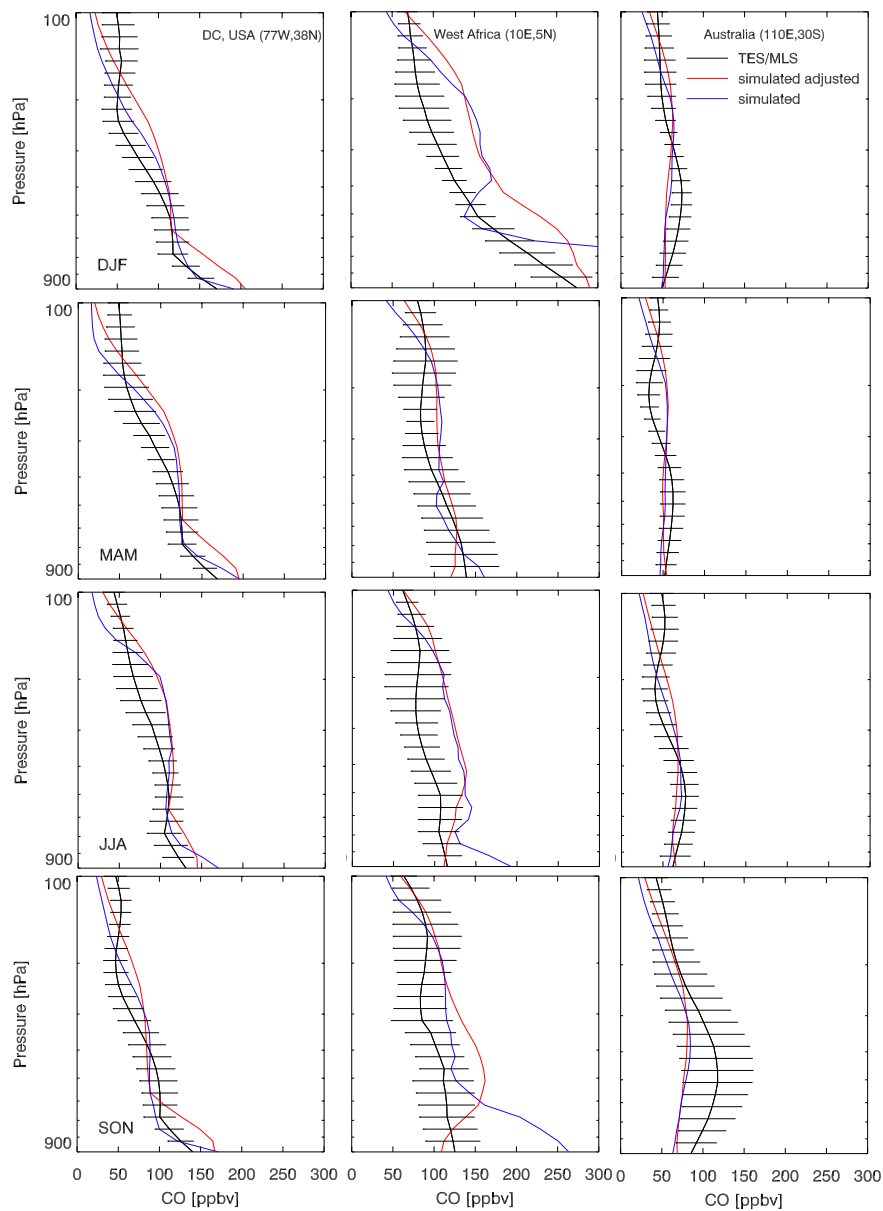


Fig. 13: Seasonal mean (2006-2007) CO vertical profiles (ppbv) over select locations of TES/MLS data, the *Base* scenario ('simulated'), and the *Base* scenario adjusted with averaging kernels ('simulated adjusted'). The horizontal bars represent the standard deviation of the individual overpasses used to create the seasonal mean.

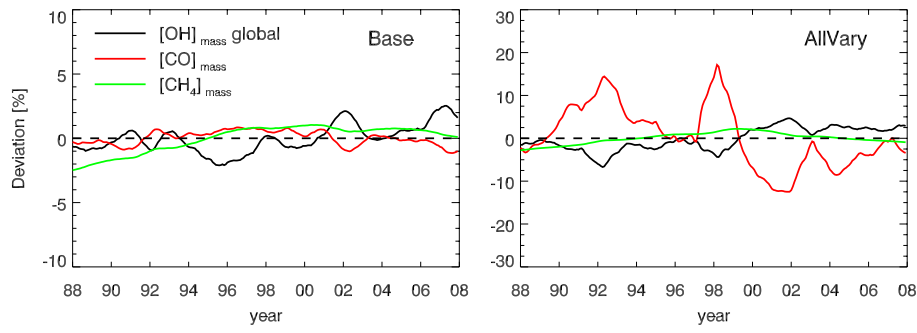


Fig. 14: Deviations of tropospheric, mass-weighted OH, CO and methane (12 month running mean) from the *Base* (left) and *AllVary* (right) scenarios. Note the different scales of the y-axes.

Yasin Elshorbany, G..., 12/3/2015 5:20 PM

Deleted: top

Yasin Elshorbany, G..., 12/3/2015 5:20 PM

Deleted: bottom

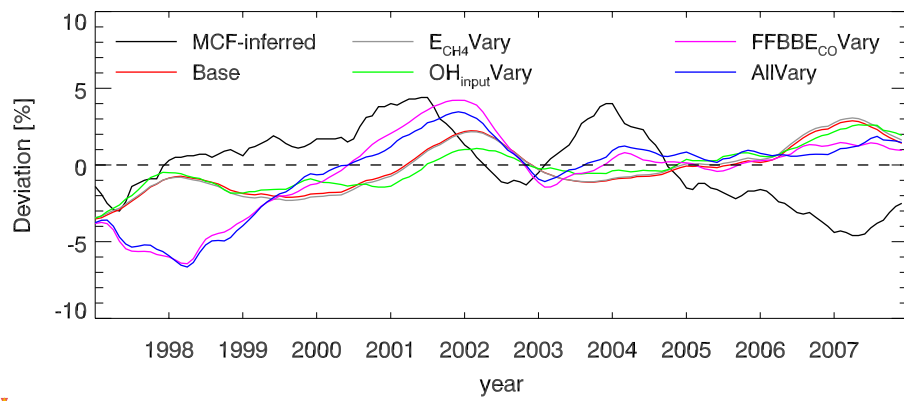


Fig. 15: Deviations (%) of the global, mass-weighted, pseudo first order rate constant (k') of the reaction of OH with MCF-inferred from MCF measurements (black; adapted from Montzka et al., 2011) and from several scenarios.

Yasin Elshorbany, G..., 12/8/2015 5:55 PM

Deleted: <sp>

Unknown

Formatted: Font:Times New Roman, Font color: Text 1

Yasin Elshorbany, G..., 1/20/2016 4:08 PM

Deleted:

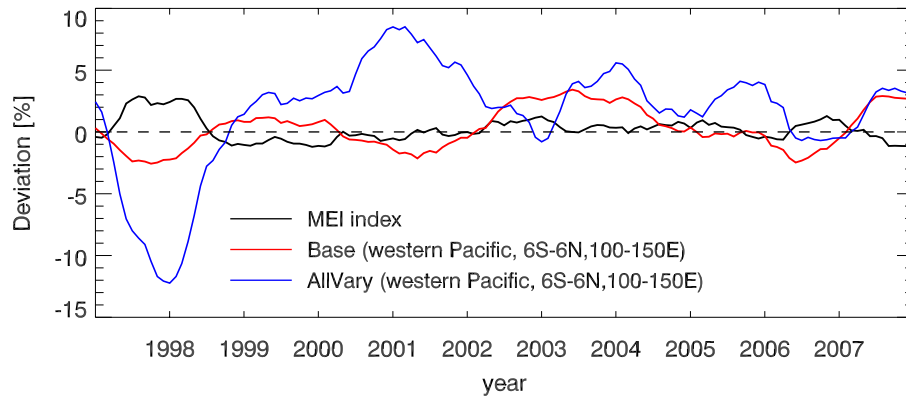


Fig. 16: Deviation (%) of global, mass-weighted OH from various scenarios and the Multivariant ENSO Index (MEI). The lines are 12-month running means. Positive values of MEI indicate El Niño conditions and negative values indicate La Niña conditions. The correlation coefficient (R^2) for the *Base* scenario vs the MEI index is 0.20 while for the *AllVary* scenario is 0.59.

- Yasin Elshorbany, ..., 12/29/2015 5:32 PM
Formatted: Superscript
- Yasin Elshorbany, GS..., 1/4/2016 2:50 PM
Formatted: Font:Italic
- Yasin Elshorbany, GS..., 1/4/2016 2:50 PM
Formatted: Font:Italic

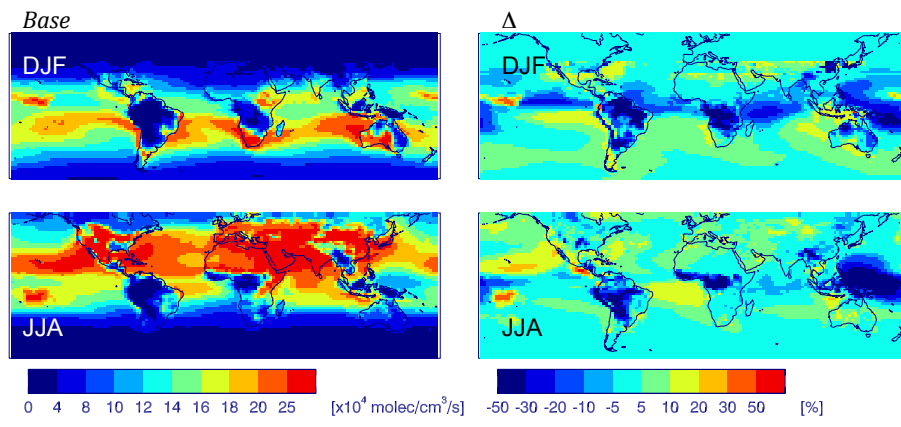


Fig. 17: Seasonal mean (1988-2007), mass-weighted tropospheric methane loss rate (left column; $\times 10^4$ molecules/cm³/s) with relative difference with the *AllVary* scenario ($(Base - AllVary)/Base$; right column).

Yasin Elshorbany, G..., 12/7/2015 5:20 PM
 Formatted: Font:Italic

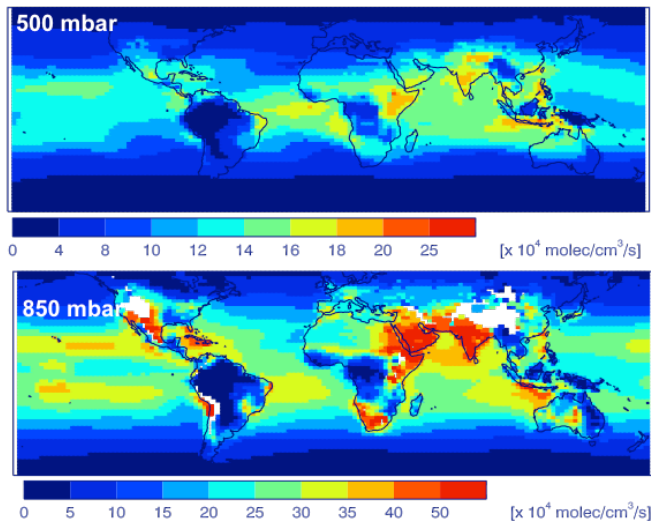


Fig. 18: Mean methane loss rate (1988-2007; $\times 10^4$ molecules/cm³/s) at 500 mb (top) and 850 mb (bottom) for the *Base* scenario.

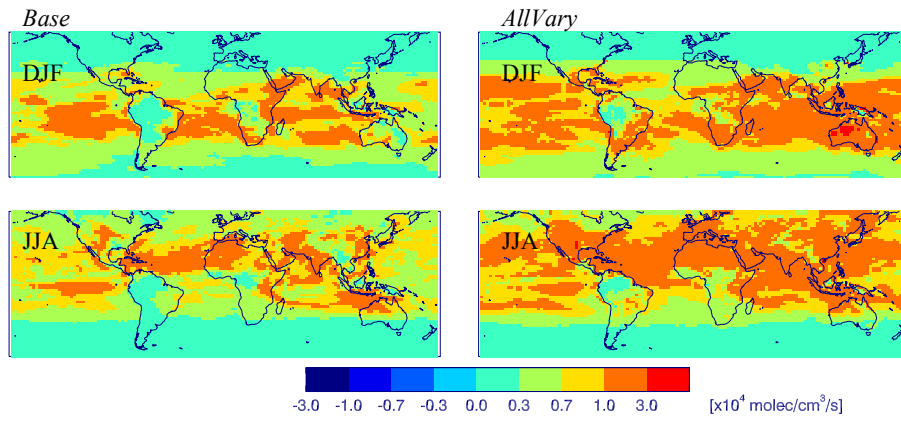


Fig. 19: Seasonal mean (1988-2007) standard deviation of tropospheric methane loss rates ($\times 10^4$ molecules/cm³/s) from the *Base* (left column) and *AllVary* (right column) scenarios.

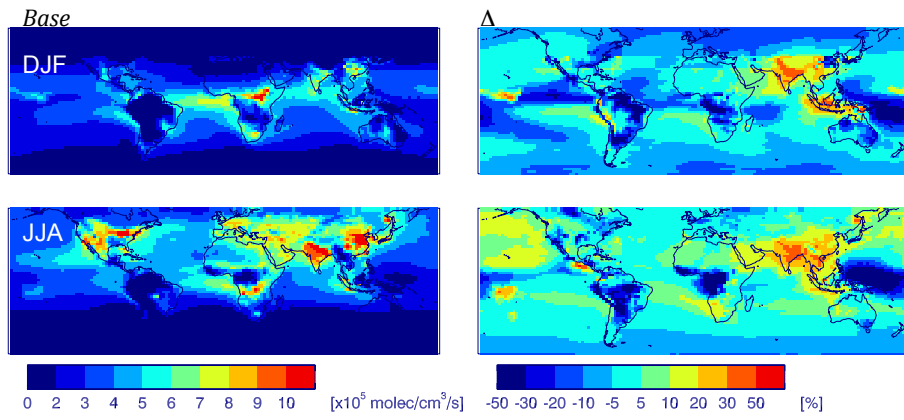


Fig. 20: Seasonal mean (1988-2007), mass-weighted tropospheric CO loss rates (left column; $\times 10^5 \text{ molecules/cm}^3/\text{s}$) from the *Base* scenario and relative difference (%) between the *Base* and *AllVary* scenarios ($(\text{Base}-\text{AllVary})/\text{Base}$; right column).

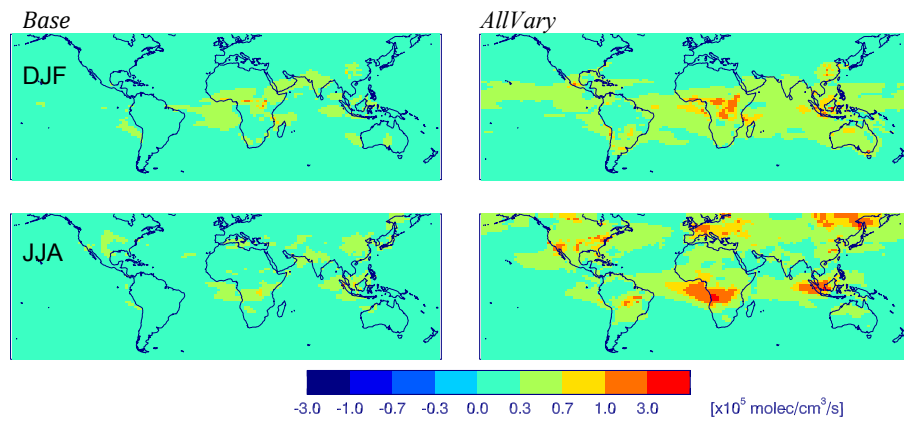


Fig. 21: Seasonal mean (1988-2007) standard deviation of tropospheric CO loss rates ($\times 10^5$ molecules/cm³/s) from the *Base* (left column) and *AllVary* (right column) scenarios.

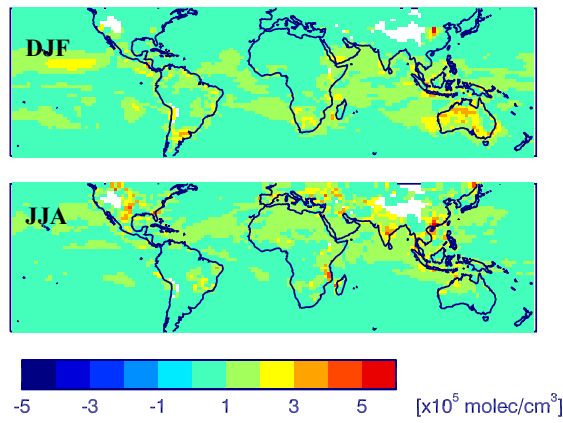


Fig. 22: Seasonal mean (1988-2007) standard deviations of OH ($\times 10^5$ molecules/cm³) at 850 mb, for the *AllVary* scenario.

Yasin Elshorbany, G..., 12/8/2015 3:55 PM

Deleted: OH

Yasin Elshorbany, G..., 1/20/2016 8:45 AM

Deleted: ar

1. Emissions

In this section, we show the various emissions used in the simulation scenarios (Table 1 and Table 2).

1.1 Methane

As shown below, CTL total emissions (annually-repeating natural sources (i.e., wetlands and biomass burning) and annually-varying anthropogenic sources) are higher in the northern hemisphere by about 20% while EXTRA emissions (all emissions vary) are higher by about 20% in the tropics (Patra et al., 2011).

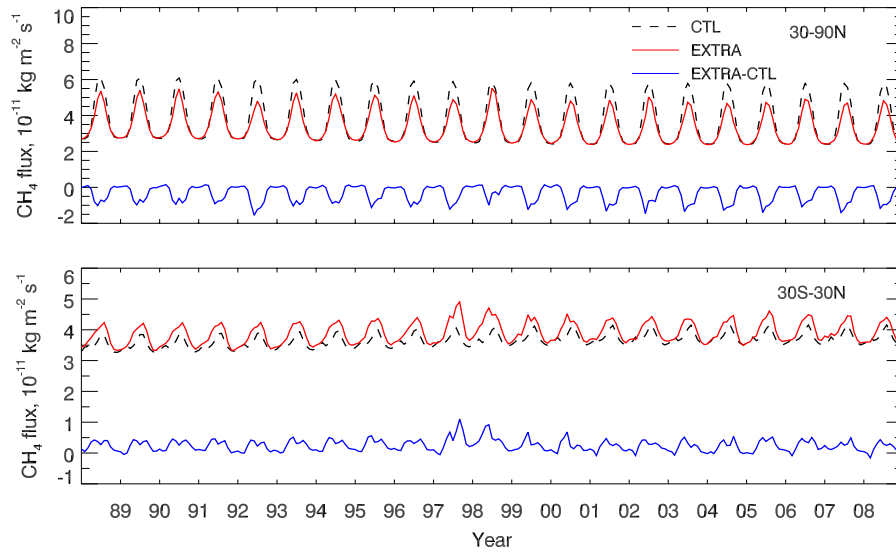


Figure S 1: Monthly methane CTL (dashed) and EXTRA (red) emissions ($\times 10^{-11}$ kg/m²/s) used in the *Base* and *E_{CH4}Vary* scenarios, respectively. The difference between them is shown in blue (EXTRA-CTL).

Yasin Elshorbary, G..., 1/20/2016 8:51 AM

Style Definition: Normal: Indent: First line: 0 cm

Yasin Elshorbary, ..., 1/11/2016 12:08 PM

Style Definition: Heading 2

Yasin Elshorbary, G..., 1/20/2016 8:55 AM

Style Definition: Caption

Yasin Elshorbary, G..., 1/20/2016 4:10 PM

Formatted: Indent: First line: 0 cm

Yasin Elshorbary, G..., 1/20/2016 8:09 AM

Deleted: see

Yasin Elshorbary, GS..., 1/4/2016 2:23 PM

Formatted: Indent: Left: 0 cm, Tabs: 0 cm, Left + Not at -1 cm

1.2 CO

Here, we show the biomass burning (BB) and fossil fuel (FF) CO emissions used in the *Base* and *AllVary* scenarios.

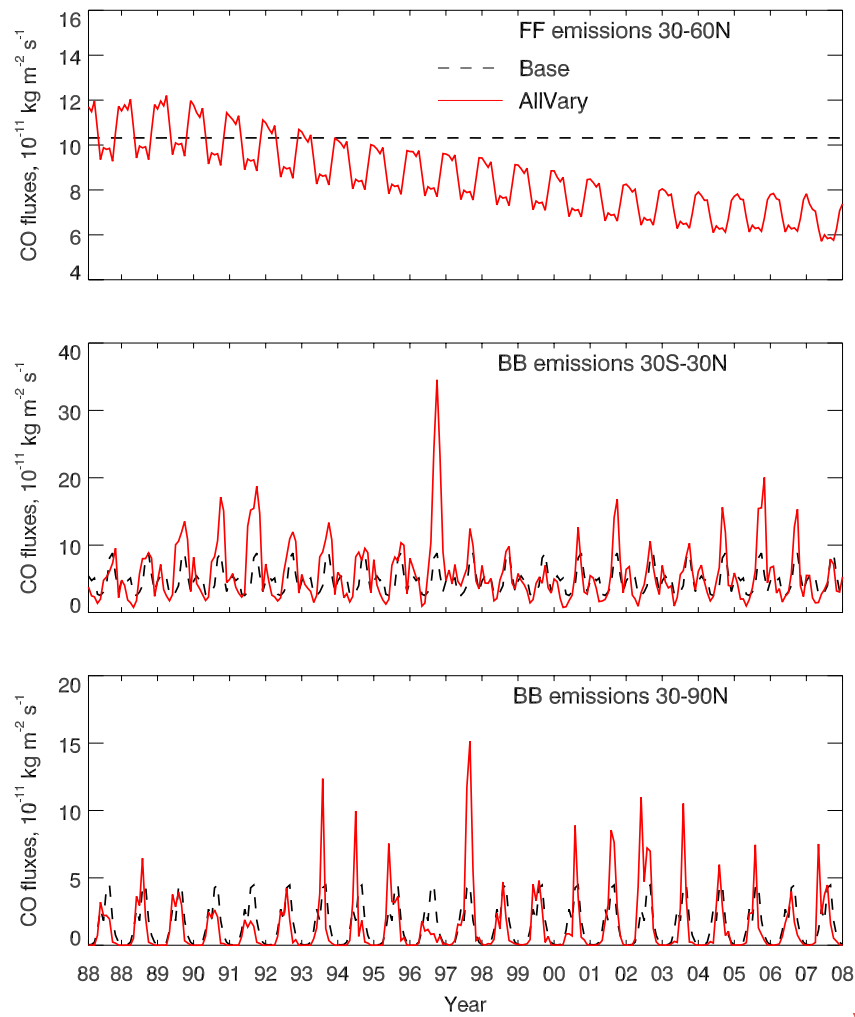


Figure S 2: Monthly CO emissions ($\times 10^{-11} \text{ kg/m}^2/\text{s}$) used in the *Base* and *AllVary* scenarios.

Yasin Elshorbany, GS..., 1/4/2016 2:22 PM

Formatted: Normal, No bullets or numbering

Yasin Elshorbany, GS..., 1/4/2016 2:22 PM

Deleted: Here, we show the biomass burning (BB) and fossil fuel (FF) CO emissions used in the *Base* and *AllVary* scenario.

The figure below shows the sensitivity of the global burdens of methane, CO, and OH to emissions. For instance, the simulated larger burdens of CO levels in the *BBE_{CO}Vary* scenario lead to decreased OH levels and thus higher methane burdens compared to the *E_{CH₄Vary}* scenario.

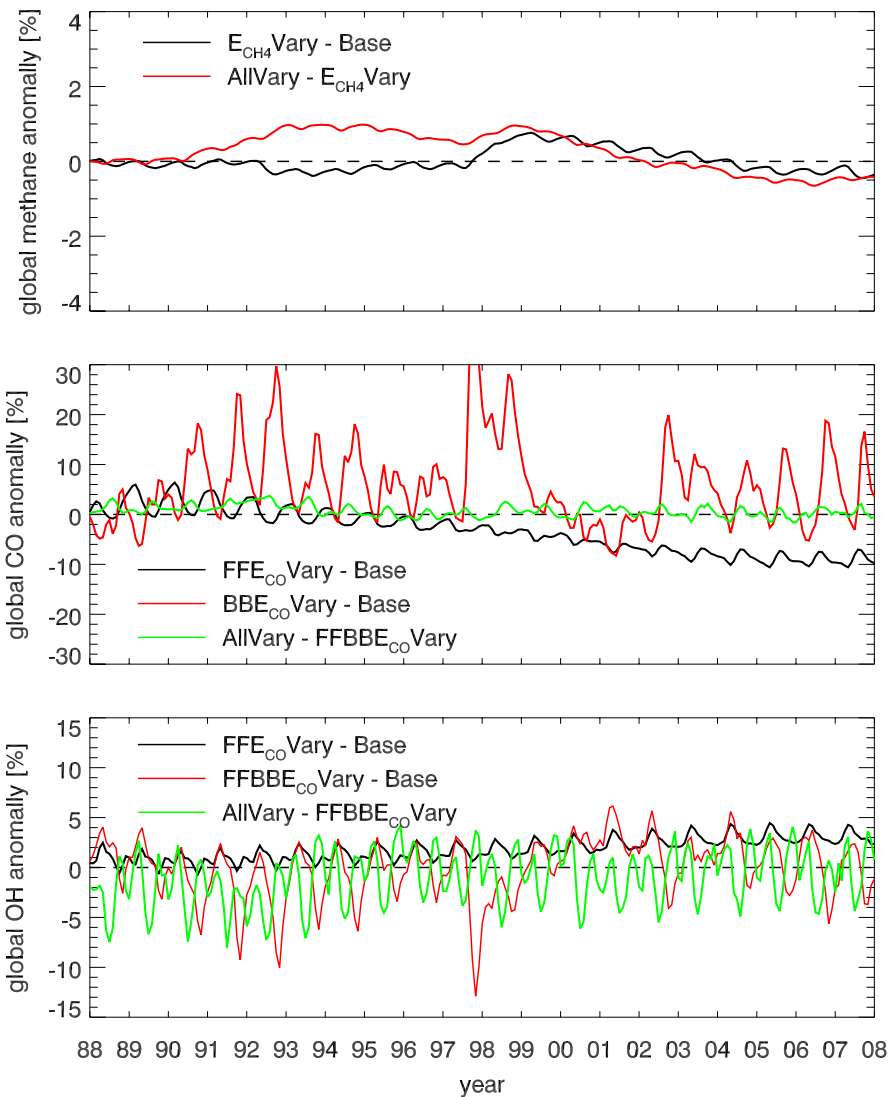


Figure S 3: Relative difference (%) of globally mass-weighted tropospheric methane, CO, and OH (from up to bottom) between the different scenarios.

Unknown

Formatted: Font color: Text 1

2. Comparison to measurements

2.1 Methane

Global Methane Growth Rate

We reproduce Figure 4a in the manuscript but show the difference between the *Base* and *OH_{input}Vary* (Figure S 4) and *FFBBE_{CO}Vary* (Figure S 5) scenarios. These figures incorporate the results concluded in Sect. 4.3 demonstrating the non-linear feedbacks on methane's growth rate. It further demonstrates that non-linear feedbacks on growth rates in 1994-1997 are mainly due to interannual variability in OH constraints (Figure S 4) while the other non-linear feedbacks are related to interannual variability in CO emissions (Figure S 5).

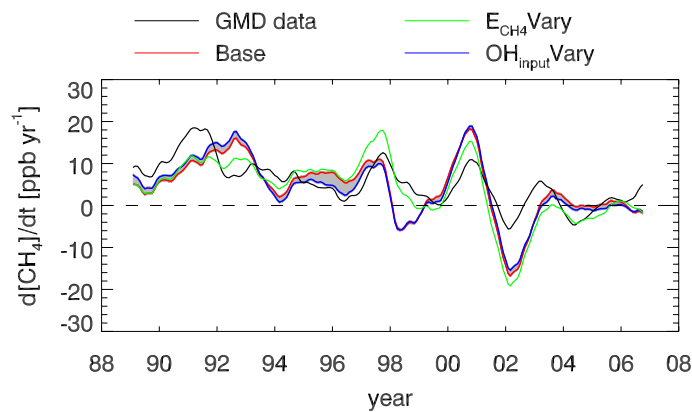


Figure S 4: 12-month running mean atmospheric growth rate of methane (ppbv yr⁻¹) for the average of 92 GMD stations and from model output averaged for those station locations for several scenarios. The shaded area is the difference between the *OH_{input}Vary* and *Base* scenarios.

Yasin Elshorbany, G..., 1/19/2016 6:29 PM

Deleted: .

... [1]

Yasin Elshorbany, G..., 1/20/2016 4:12 PM

Formatted: Indent: First line: 0 cm

Yasin Elshorbany, ..., 1/12/2016 12:43 PM

Formatted: Font:Italic

Unknown

Formatted: Font color: Blue

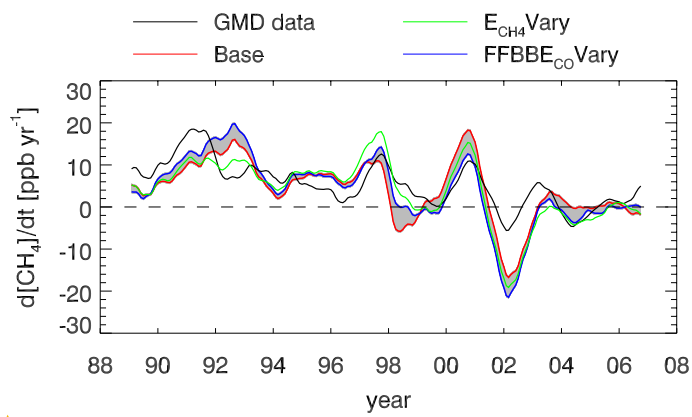


Figure S 5; Same as Figure S 4 but the shaded area is the difference between the *FFBBE_{CO}Vary* and *Base* scenarios.

Yasin Elshorbary, G..., 1/20/2016 8:55 AM
Formatted: Caption, Line spacing: single

Unknown
Formatted: Font color: Blue

Yasin Elshorbary, ..., 1/12/2016 12:30 PM
Deleted: 4

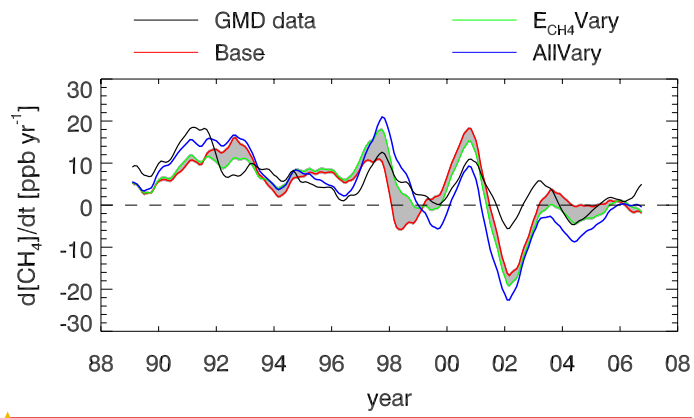


Figure S 6: Same as Figure S 4 but the shaded area is the difference between the E_{CH_4} Vary and Base scenarios.

Unknown

Formatted: Font color: Blue

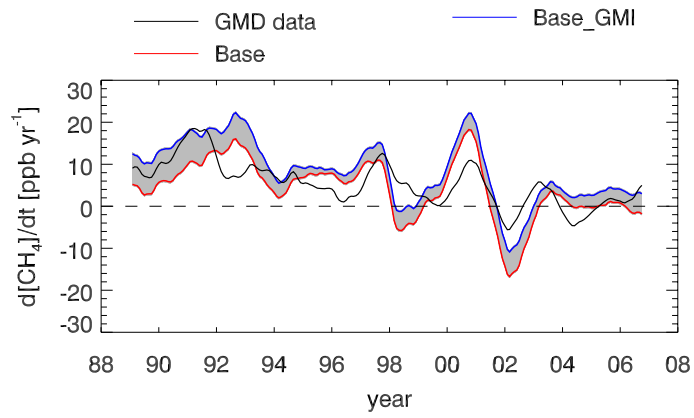


Figure S 7: Same as Figure S 4 but the shaded area is the difference between the *Base_GMI* and *Base* scenarios. The *Base_GMI* scenario is similar to the *Base* scenario, except that OH concentrations are from a full chemistry simulation of the NASA Global Modeling Initiative (GMI) model.

Yasin Elshorbany, G..., 1/19/2016 1:45 PM
Deleted: 7

GMD Measurements

Here, we show the comparison of simulated methane by different scenarios (that are not shown in the manuscript) as compared to GMD measurements.

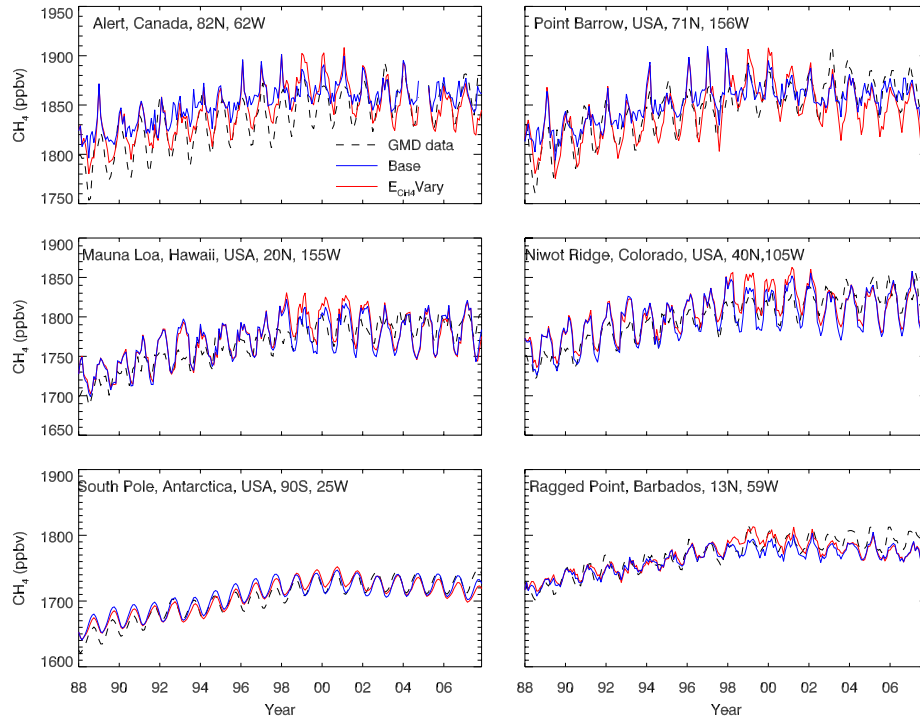


Figure S 8: Monthly methane (ppbv) from the *Base* and *E_{CH_4} Vary* scenarios and observations from six GMD stations.

Yasin Elshorbany, ..., 1/12/2016 12:44 PM

Deleted: -

Yasin Elshorbany, G..., 1/20/2016 8:52 AM

Deleted: :

Yasin Elshorbany, ..., 12/28/2015 4:10 PM

Deleted: 3

Yasin Elshorbany, G..., 1/20/2016 8:55 AM

Formatted: Indent: First line: 0 cm

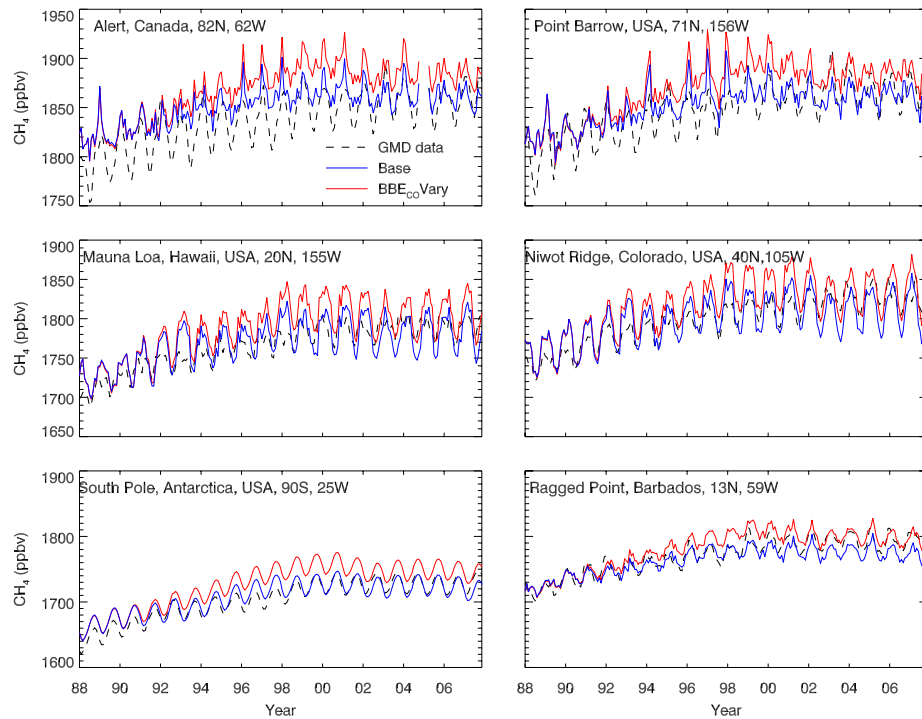


Figure S 9: Monthly methane (ppbv) from the *Base* and *BBECOVary* scenarios and observations from six GMD stations.

Yasin Elshorbany, G..., 1/20/2016 8:55 AM

Formatted: Indent: First line: 0 cm

Yasin Elshorbany, ..., 12/28/2015 4:10 PM

Deleted: 4

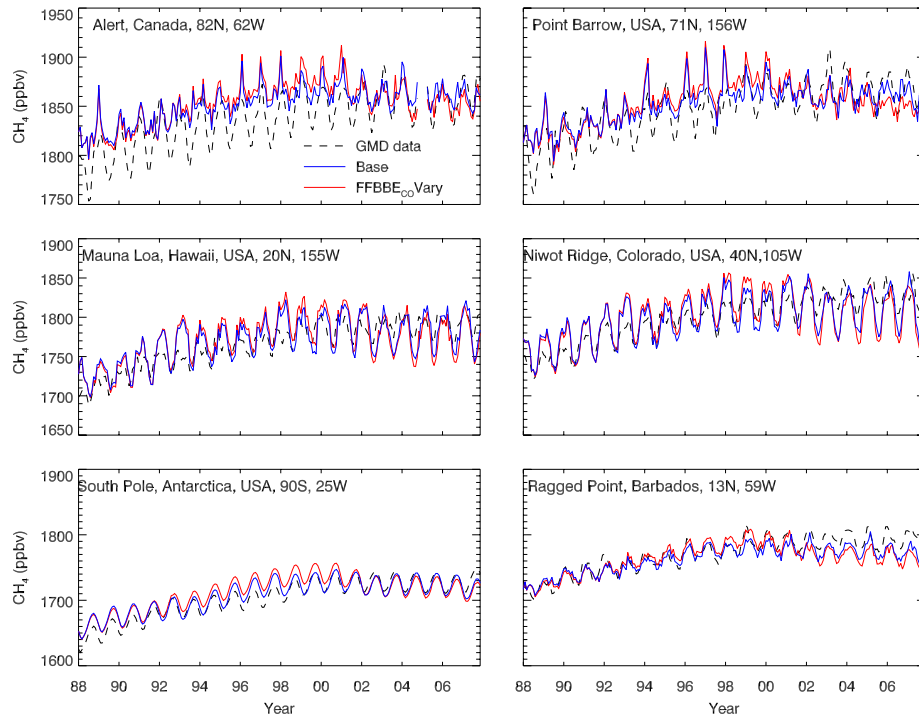


Figure S 10: Monthly methane (ppbv) from the *Base* and *FFBBE_{co}Vary* scenarios and observations from six GMD stations.

Yasin Elshorbany, ..., 12/28/2015 4:10 PM
Deleted: 5

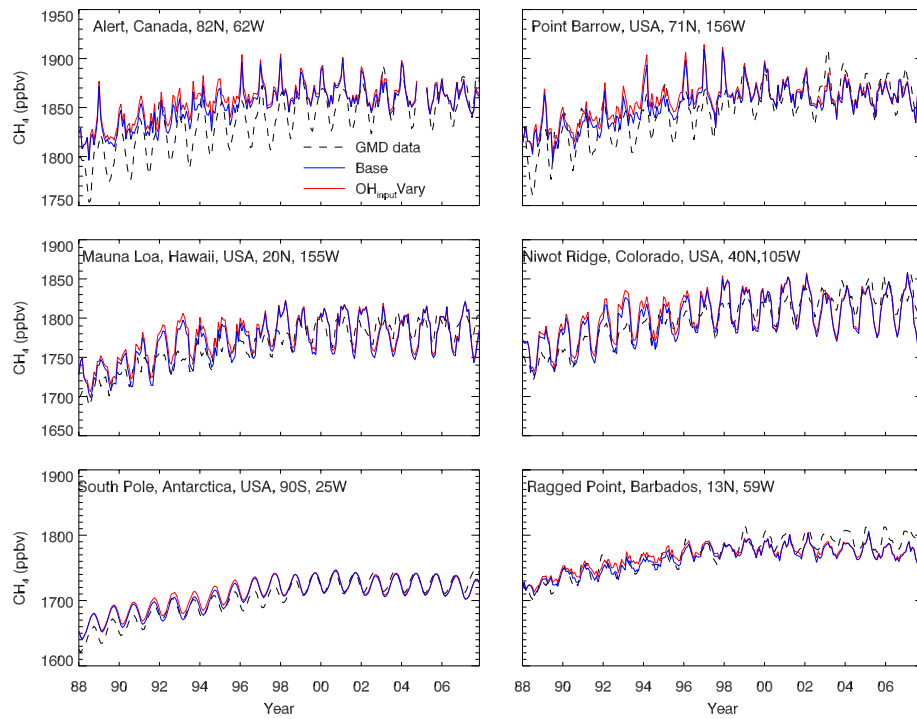


Figure S 11: Monthly methane (ppbv) from the *Base* and *OH_{input}Vary* scenarios and observations from six GMD stations.

Yasin Elshorbany, G..., 1/20/2016 8:55 AM

Formatted: Indent: First line: 0 cm

Yasin Elshorbany, ..., 12/28/2015 4:10 PM

Deleted: 6

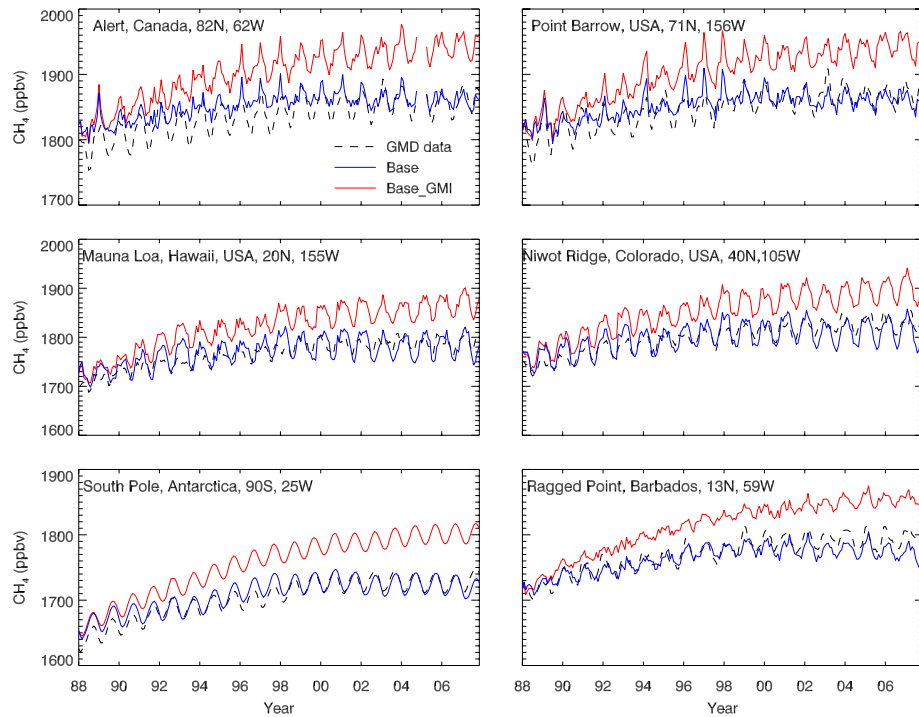


Figure S 12: Monthly methane (ppbv) from the *Base* and *Base GMI* scenarios and observations from six GMD stations. The *Base GMI* scenario is similar to the *Base* scenario, except that OH concentrations are from a full chemistry simulation of the GMI model.

Yasin Elshorbany, ..., 1/19/2016 12:40 PM

Formatted: Normal, Indent: First line: 0 cm

Yasin Elshorbany, G..., 1/19/2016 1:45 PM

Deleted: 12

2.2 CO

Here, we show additional figures for the comparison of simulated CO as compared to measurements.

GMD measurements

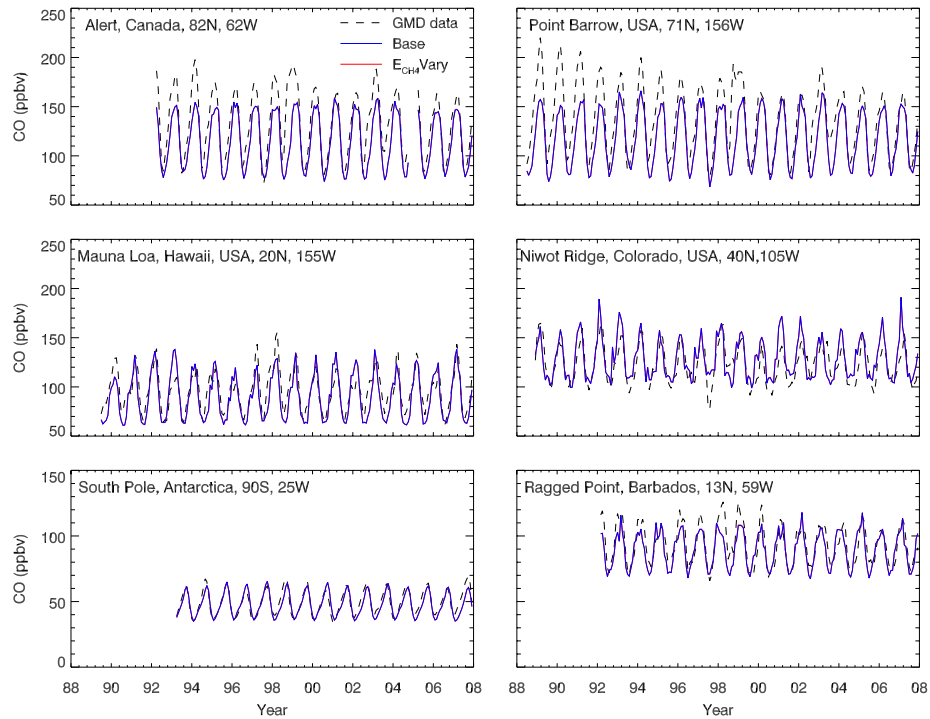
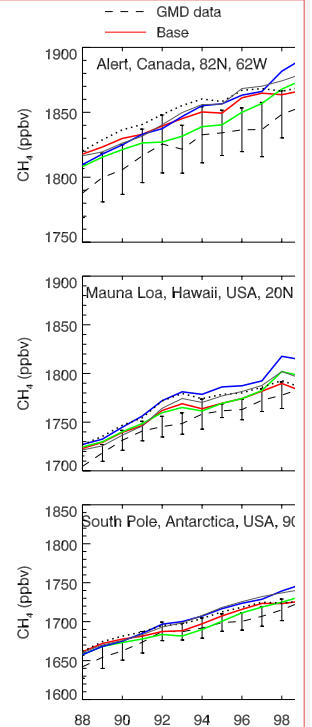


Figure S 13: Measured and simulated monthly near surface CO levels from the Base and $E_{CH_4}Vary$ scenarios.

Yasin Elshorbany, G..., 1/19/2016 2:01 PM



Deleted: ... [2]

Yasin Elshorbany, G..., 1/20/2016 8:13 AM

Deleted: :

Yasin Elshorbany, ..., 12/28/2015 4:10 PM

Deleted: 9

Yasin Elshorbany, G..., 1/20/2016 8:53 AM

Deleted: by

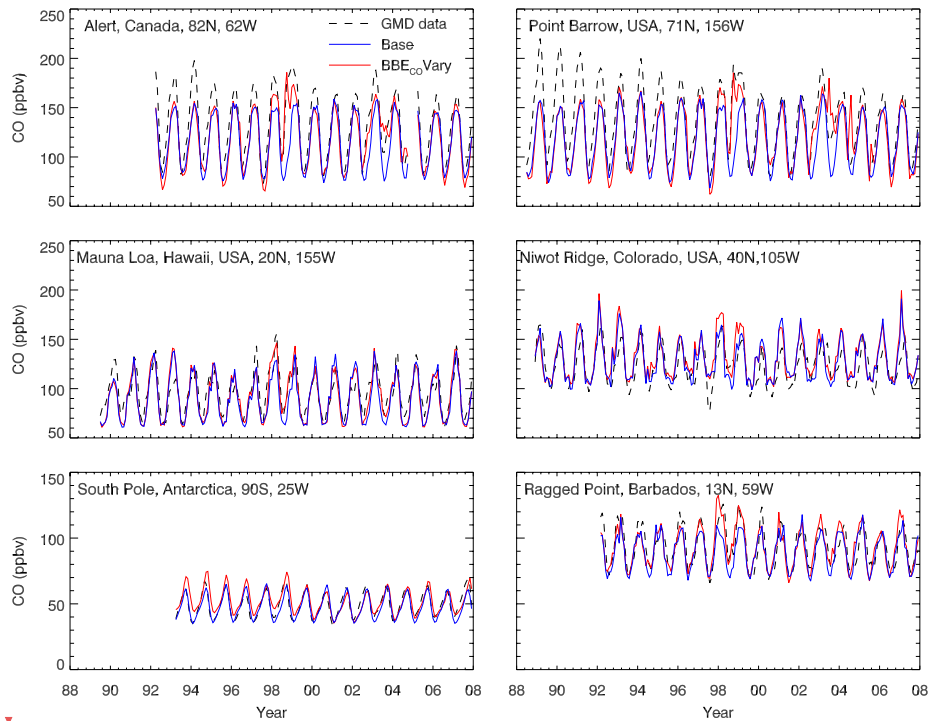


Figure S 14: Measured and simulated monthly near surface CO levels from the *Base* and *BBEcoVary* scenarios.

Yasin Elshorbany, ..., 1/12/2016 11:28 AM

Deleted: -

Yasin Elshorbany, G..., 1/20/2016 8:55 AM

Formatted: Indent: First line: 0 cm

Yasin Elshorbany, ..., 12/28/2015 4:10 PM

Deleted: 10

Yasin Elshorbany, G..., 1/20/2016 8:53 AM

Deleted: by

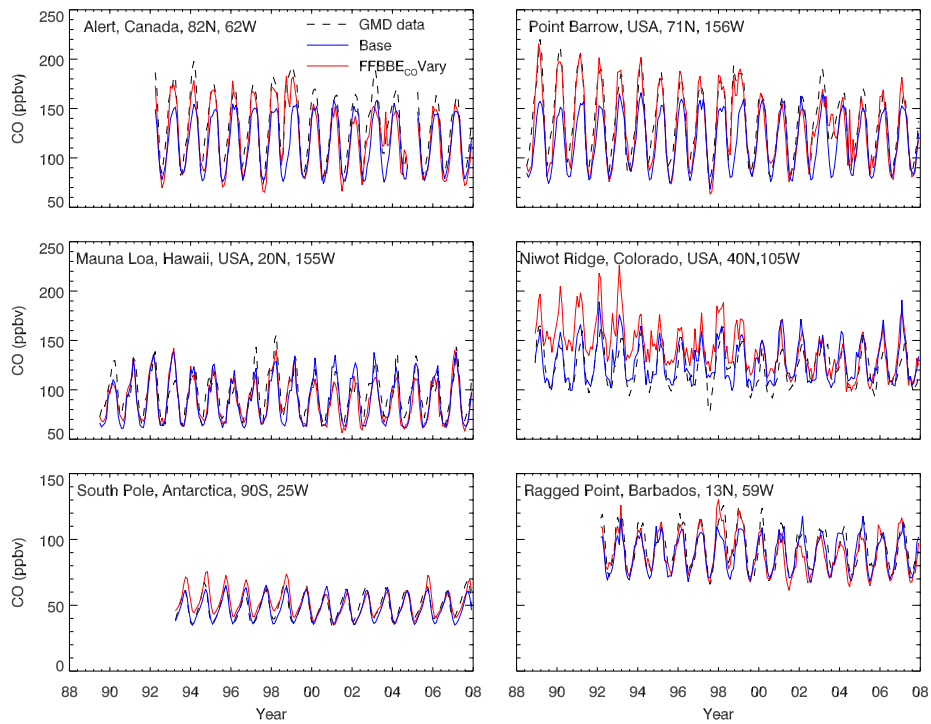


Figure S 15: Measured and simulated monthly near surface CO levels from the Base and *FFBBE_{CO}Vary* scenarios.

- Yasin Elshorbany, G..., 1/20/2016 8:55 AM
- Formatted: Indent: First line: 0 cm
- Yasin Elshorbany, ..., 12/28/2015 4:10 PM
- Deleted: 11
- Yasin Elshorbany, G..., 1/20/2016 8:53 AM
- Deleted: by

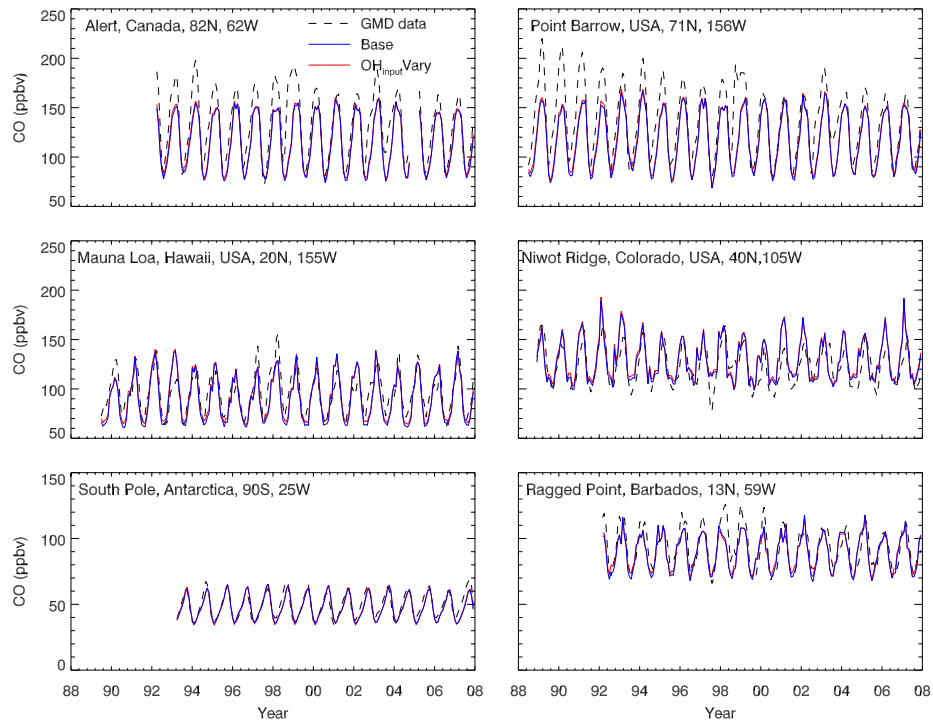


Figure S 16: Measured and simulated monthly near surface CO levels from the Base and OH_{input} Vary scenarios.

Yasin Elshorbany, G..., 1/20/2016 8:55 AM

Formatted: Indent: First line: 0 cm

Yasin Elshorbany, ..., 12/28/2015 4:10 PM

Deleted: 12

Yasin Elshorbany, G..., 1/20/2016 8:53 AM

Deleted: by

3. Comparison of simulated OH to full chemistry simulation.

Here, we compare simulated OH from the *Base* and *AllVary* scenario to that of ACCMIP.

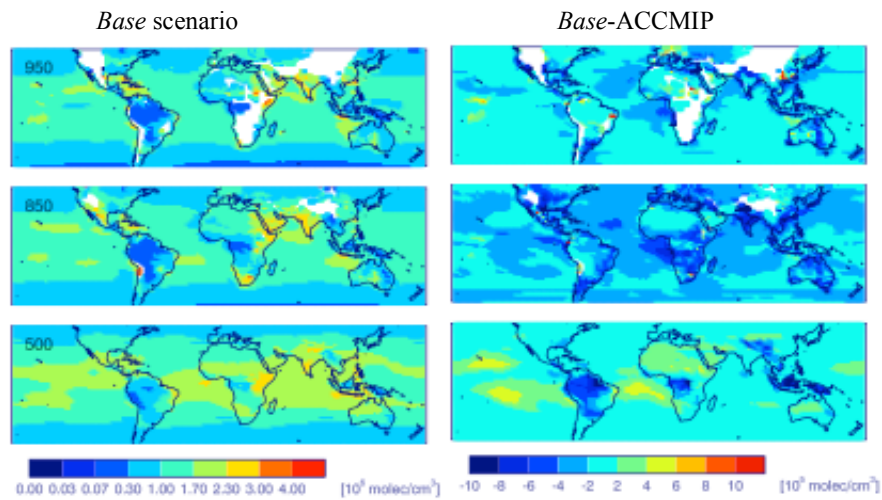
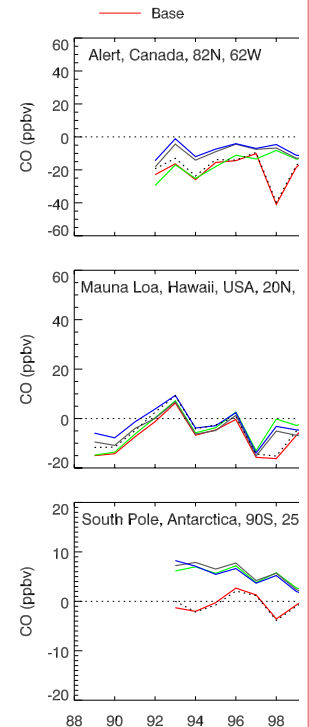


Figure S 17: Annual mean OH (left column; $\times 10^6$ molecules/cm³) from 1999-2007 for the *Base* scenario and their corresponding difference ($\times 10^5$ molecules/cm³) from the full chemistry ACCMIP (GEOS5CCM) simulation (*Base-ACCMIP*, right panels) at 950, 850 and 500 mb (from top to bottom). White gaps indicate no model output at that pressure level.

Yasin Elshorbany, G..., 1/19/2016 2:48 PM



Deleted: ... [3]

Yasin Elshorbany, ..., 12/28/2015 2:40 PM

Formatted: Font:Italic

Unknown

Formatted: Font color: Text 1

Yasin Elshorbany, ..., 12/28/2015 2:43 PM

Formatted: Font:Italic

Unknown

Formatted: Font color: Text 1

Yasin Elshorbany, G..., 1/20/2016 4:17 PM

Deleted: by

Yasin Elshorbany, ..., 12/28/2015 4:10 PM

Deleted: 23

Yasin Elshorbany, G..., 1/20/2016 8:55 AM

Formatted: Indent: First line: 0 cm

Yasin Elshorbany, G..., 1/20/2016 8:54 AM

Deleted: ar

Yasin Elshorbany, G..., 1/20/2016 4:17 PM

Deleted: up

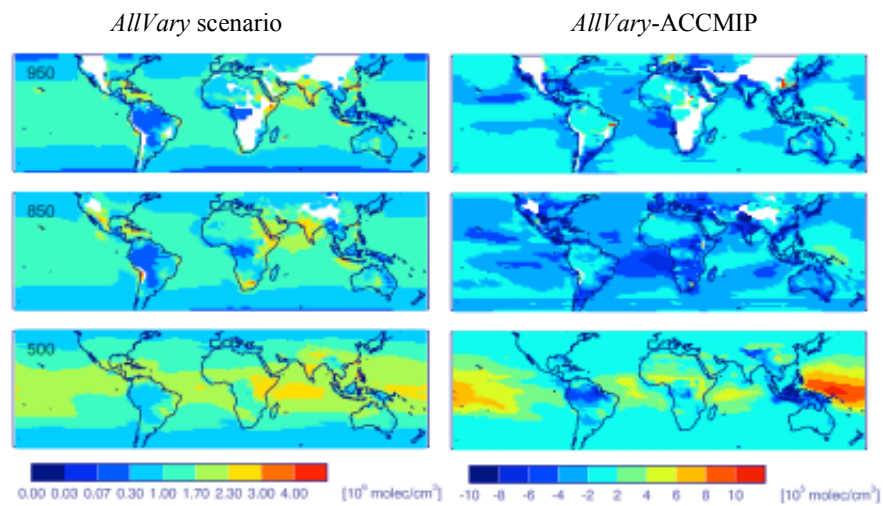


Figure S 18: Annual mean OH (left column, 10^6 molecules/cm³) from 1999-2007 for the *AllVary* scenario and the corresponding difference (10^5 molecules/cm³) from the full chemistry ACCMIP simulations (*AllVary*-ACCMIP, right column) at 950, 850 and 500 mb (from up to bottom).

Yasin Elshorbany, ..., 1/12/2016 11:19 AM

Deleted: -

Yasin Elshorbany, G..., 1/20/2016 8:55 AM

Formatted: Indent: First line: 0 cm

Yasin Elshorbany, ..., 12/28/2015 4:10 PM

Deleted: 24

Yasin Elshorbany, G..., 1/20/2016 8:56 AM

Deleted: ir

Yasin Elshorbany, G..., 1/20/2016 8:56 AM

Deleted: ar

4. Differences in the spatial distribution of methane, CO and OH:

Here, we show the influence of different scenarios on the spatial distribution of tropospheric methane, CO and OH.

Yasin Elshorbany, G..., 1/20/2016 8:56 AM

Formatted: Indent: First line: 0 cm

Yasin Elshorbany, G..., 1/20/2016 4:17 PM

Deleted: emissions

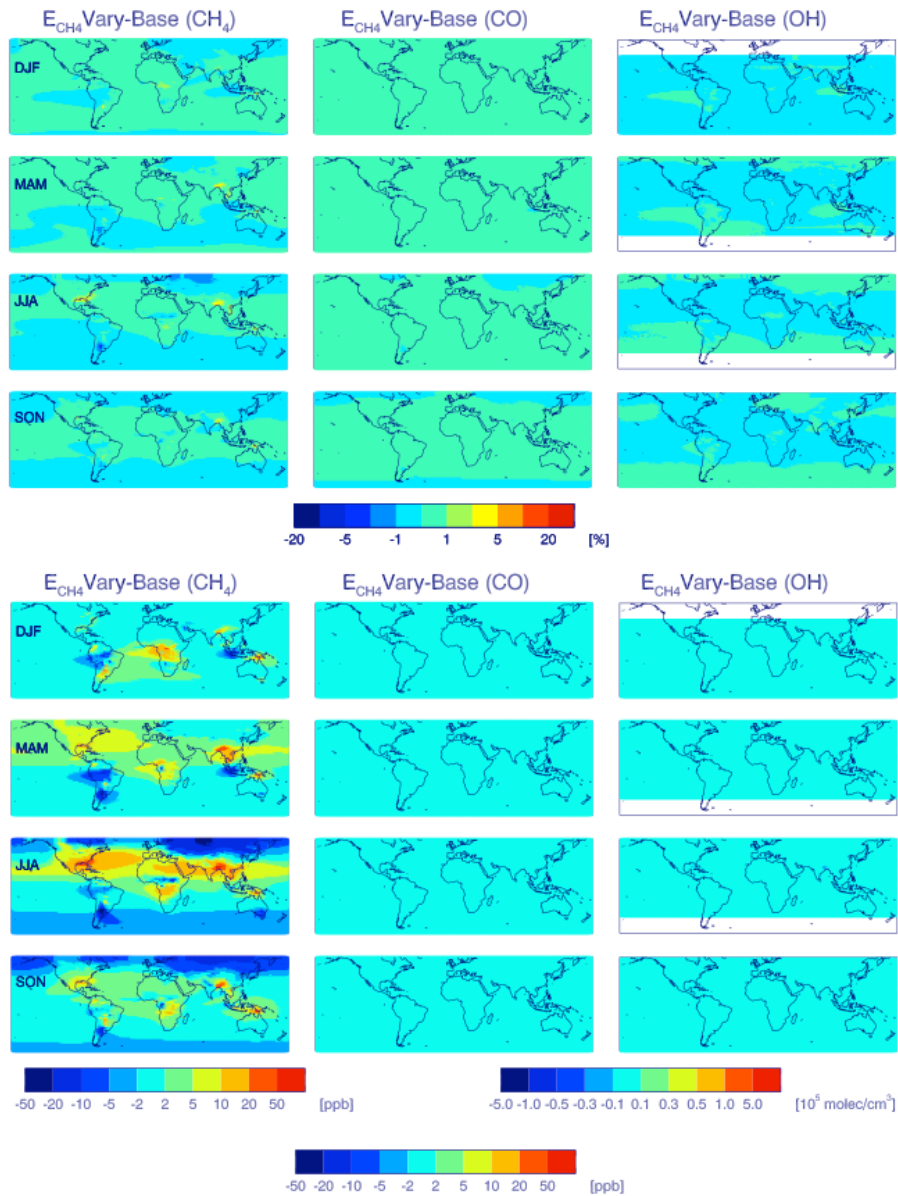


Figure S 19: Relative (%; upper panels) and absolute (lower panels) differences of seasonal, tropospheric methane (ppbv), CO (ppbv), and OH ($\times 10^5$ molecules/ cm^3) between the E_{CH_4} Vary and Base scenarios.

Yasin Elshorbany, G..., 1/20/2016 8:56 AM

Deleted: .

Yasin Elshorbany, ..., 12/28/2015 4:10 PM

Deleted: 25

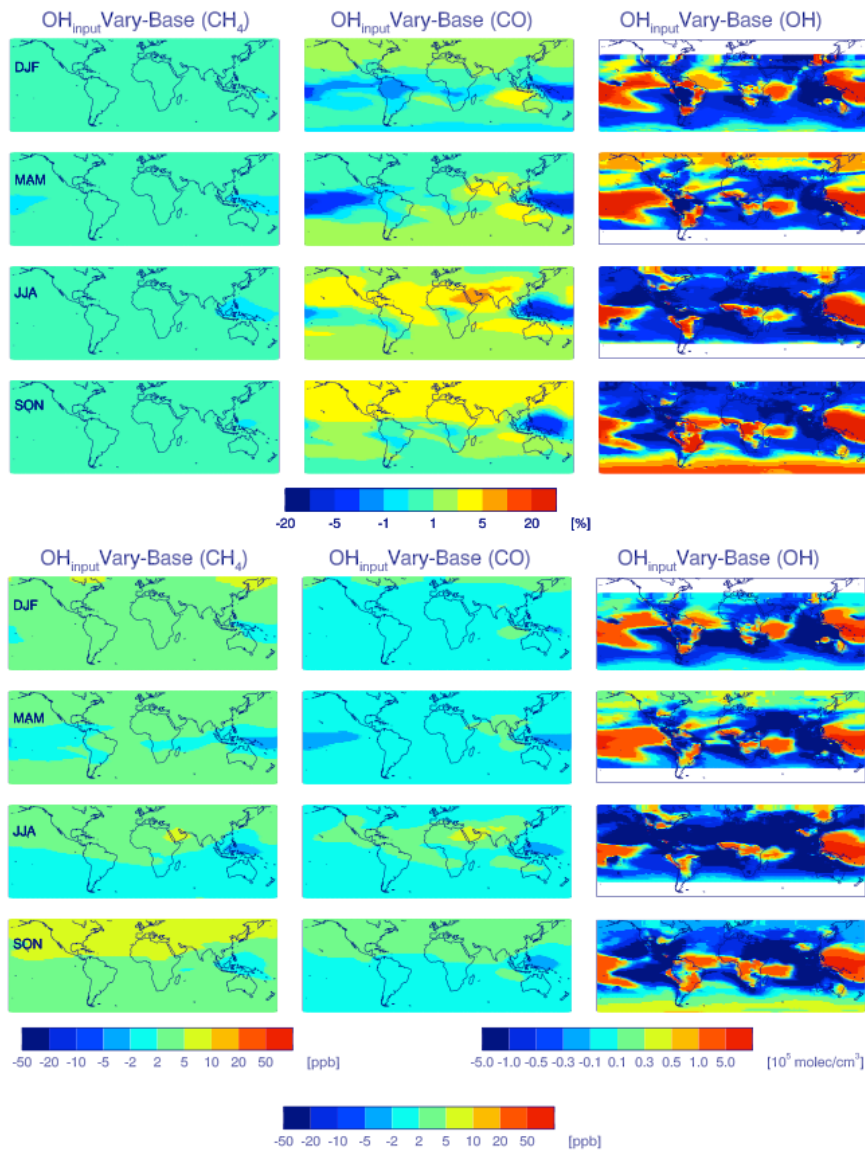


Figure S 20: Relative (%; upper panels) and absolute (lower panels) differences of seasonal, tropospheric methane (ppbv), CO (ppbv), and OH ($\times 10^5$ molecules/cm³) between the $OH_{input}Vary$ and $Base$ scenarios.

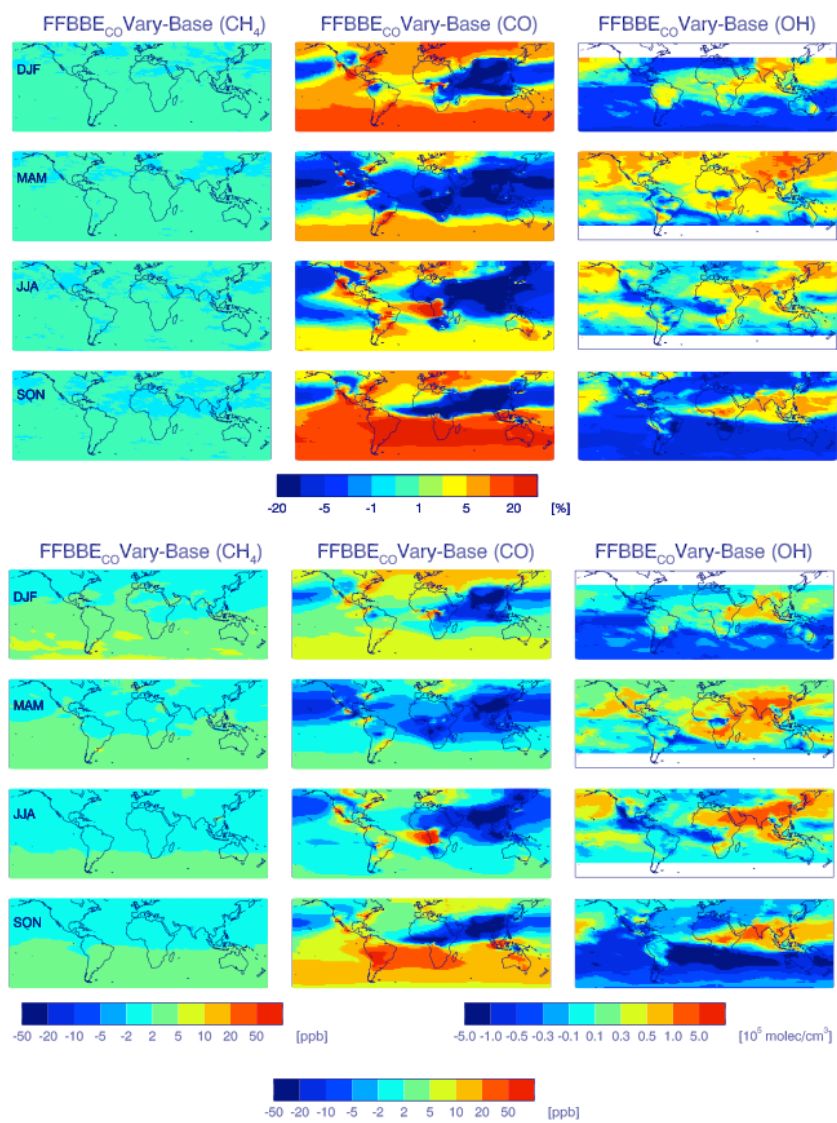


Figure S 21; Relative (%; upper panels) and absolute (lower panels) differences of seasonal, tropospheric methane (ppbv), CO (ppbv), and OH ($\times 10^5$ molecules/cm³) between the *FFBBeCO Vary* and *Base* scenarios.

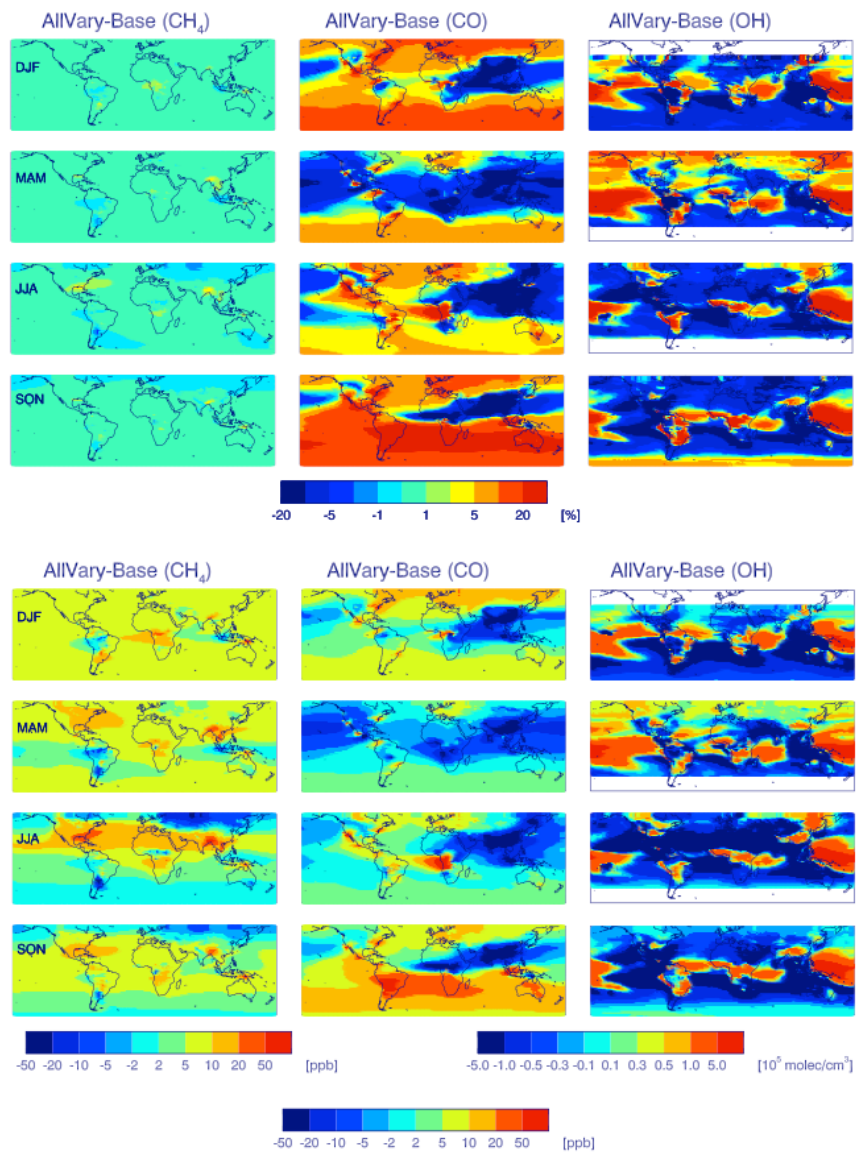


Figure S 22: Relative (%) and absolute differences of seasonal, tropospheric methane (ppbv), CO (ppbv), and OH ($\times 10^5$ molecules/cm³) between the *AllVary* and *Base* scenarios.

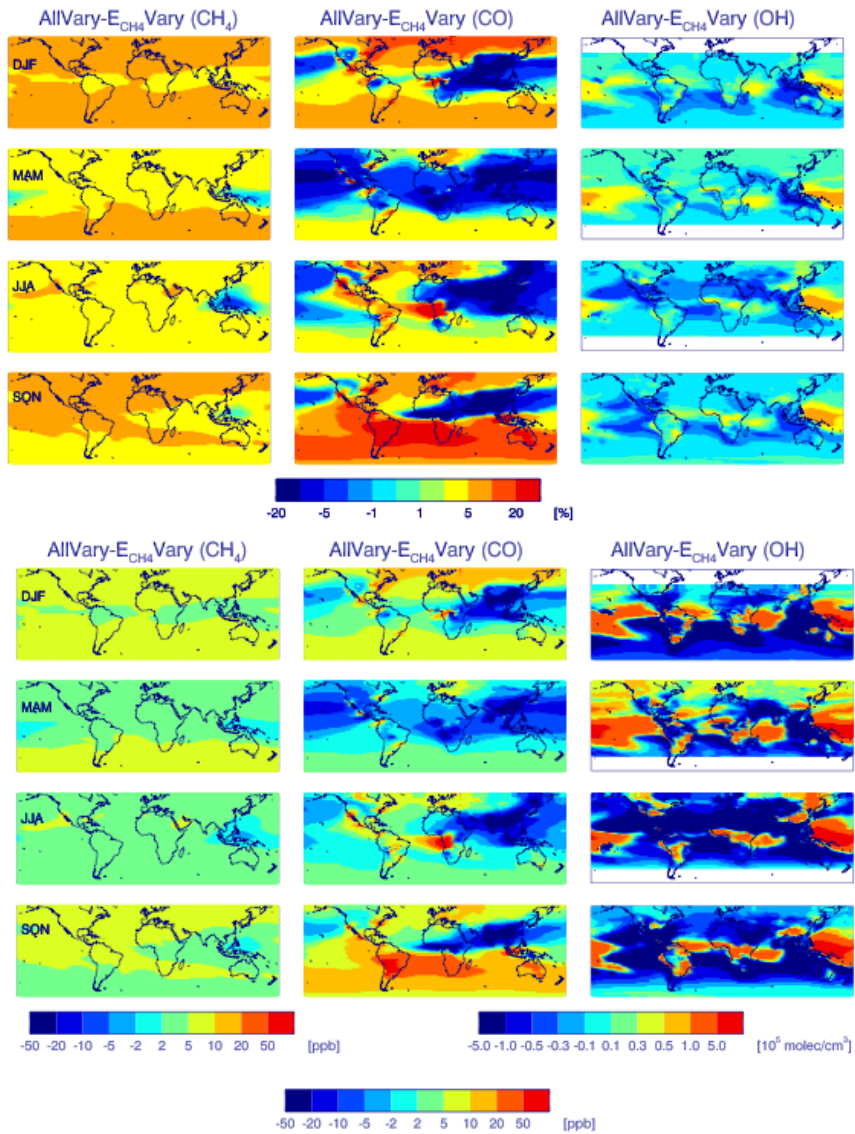


Figure S 23: Relative (%; upper panels) and absolute (lower panels) differences of seasonal, tropospheric methane (ppbv), CO (ppbv), and OH ($\times 10^5$ molecules/cm³) between the *AllVary* and *E_{CH4}Vary* scenarios.

Yasin Elshorbany, G..., 1/19/2016 1:44 PM
Formatted: Justified, Line spacing: single

Yasin Elshorbany, ..., 12/28/2015 4:10 PM

Deleted: 29

Yasin Elshorbany, G..., 1/20/2016 8:14 AM

Deleted: .

Yasin Elshorbany, G..., 1/20/2016 8:14 AM

Deleted: Page Break

... [4]

Unknown

Formatted: Font color: Text 1